The Open University
Milton Keynes, United Kingdom

L'ONCOLOGIA ITALIANA È NATA QUI
Sistema Socio Sanitario
Fondazione IRCCS Istituto Nazionale dei Tumori
via Venezian, 1 20133 Milano
Regione Lombardia

Affiliated Research Centre
Fondazione IRCCS Istituto Nazionale dei Tumori
Milano, Italia

Role of transcription factor *Atf3* in the bone marrow microenvironment during breast cancer development: a response marker or an active player of tumourigenesis?

Thesis submitted to the Open University, Milton Keynes (UK)
For the degree of Doctor of Philosophy
School of Life, Health and Chemical Sciences

Milena Perrone
Personal Identifier: G4632431
Molecular Immunology Unit
Department of Research
Fondazione IRCCS Istituto Nazionale dei Tumori

December 2021

DECLARATION

The data presented in this thesis are original, were not previously used for any other PhD degree and were originated by myself and by the below cited collaborators.

During my PhD I worked in the Molecular Immunology Unit, Department of Research, at the Fondazione IRCCS Istituto Nazionale dei Tumori, under the supervision of Dr. Mario Paolo Colombo.

This work was supported by Grants from Associazione Italiana per la Ricerca sul Cancro (AIRC; Investigator Grant nr. 22205 and nr. 18425).

My director of studies was Dr. Sangaletti Sabina (PhD) and my supervisors were Dr. Claudia Chiodoni (PhD) and Dr. Daniele Lecis (PhD).

Immunofluorescence shown in Figures 28-31, 36, 38, 43 were performed with the help of my director of studies Dr. Sabina Sangaletti.

Immunohistochemistry included in this thesis (Figures 23 A-B and 37) were performed by Prof. Tripodo Claudio (MD, PhD) and Dr. Valeria Cancila (PhD), Tumor Immunology Unit, Department of Health Sciences, University of Palermo.

Bioinformatic analyses (Figures 24 A-B, 39 A-B, 47C and 50C) were performed by Dr. Matteo Milani, bioinformatician of Molecular Immunology Unit.

All in vivo experiments were performed with the support of Laura Botti, the technician specialized in animal manipulation and surgery.

The results reported in Figures 23D, 36-37-38 of this thesis are published in Cancer Research (Chiodoni C, 2020), where I am listed as second author.

The other results collected in this thesis are included in a manuscript under preparation.

ABSTRACT

Cancer is a systemic disease able to reprogram the bone marrow (BM) niche towards a pro-tumorigenic state.

The timing in which BM cells start to sense the development of distant tumours and the molecular players involved in cancer-adapted immune response are largely unknown. In this context, by using the MMTV-NeuT mammary carcinoma mouse model, we have recently described the BM hematopoietic and stromal changes that support the initial steps of mammary transformation and identified the Activating transcription factor 3 (*Atf3*) among the genes significantly up modulated during the transcriptional reprogramming of the BM hematopoietic niche, at both early and late stages of disease. Additionally, *Atf3* expression in the BM perfectly correlated with the pathologic disease score.

These data supported the need to further investigate the role of *Atf3* during the BM emergency haematopoiesis associated with tumour progression.

In order to identify in which specific BM cell populations *Atf3* was more expressed, we checked ATF3 activation in different progenitor and mature immune cell subsets starting from early stages of mammary gland transformation and along tumour progression. Taking advantage of two mouse models of luminal breast cancer, we demonstrated, extending previous observations, that ATF3 induction during cancer progression is a multistep process characterized by its activation in two different subsets of BM myeloid cells.

At early time point we observed high ATF3 expression and nuclear localization in common myeloid progenitor cells (FcγR+) localized in proximity of the vascular niche. This feature was maintained at invasive stage of mammary transformation, when ATF3 became also expressed in mature monocyte/macrophage cells.

Of note, the nuclear localization of ATF3 was associated with the formation of myeloid progenitor clusters in the BM of tumour-bearing mice and its overexpression in progenitor cells drove the expansion and the differentiation of monocyte/macrophage cells. The role of ATF3 in monocyte/macrophage differentiation was supported by *in vivo* data showing a defective recruitment of circulating monocytes and a low number of tumour-associated macrophages in PyMT41c tumours transplanted into $Atf3^{fl/fl}LySMCre^{+/-}$ mice.

Further studies demonstrated that BM-mesenchymal stem cells (BM-MSCs) were the first sensors of peripheral tumours and that ATF3 induction in the BM hematopoietic niche was the consequence of the cross talk between tumour-primed BM-MSCs and hematopoietic stem cells (HSCs), which ultimately leads to a tumour-restricted release of *Atf3*+ cells into the circulation.

Specifically, tumour-educated BM-MSCs, through the release of IL-1β, an inflammatory cytokines that induce HSCs to differentiate towards myeloid progenitor cells, activated *Atf3* expression in naïve HSCs and initiated a specific lineage commitment.

Indeed, *in vivo* inhibition of IL-1β at early stage of disease significantly decreased *Atf3* activation in HSCs and reduced myeloid progenitor clustering, a necessary step towards the establishment of emergency haematopoiesis. Furthermore, the blocking of IL-1β when the tumour was well-established caused a down-regulation of *Atf3* expression in both precursors and mature monocytes and, consequently, decreased myeloid cell expansion.

Overall, this project demonstrated that the biphasic induction of ATF3 in the BM is functionally associated with a key role during emergency haematopoiesis and myeloid cell expansion, also suggesting a possible therapeutic targets.

GRAPHICAL ABSTRACT

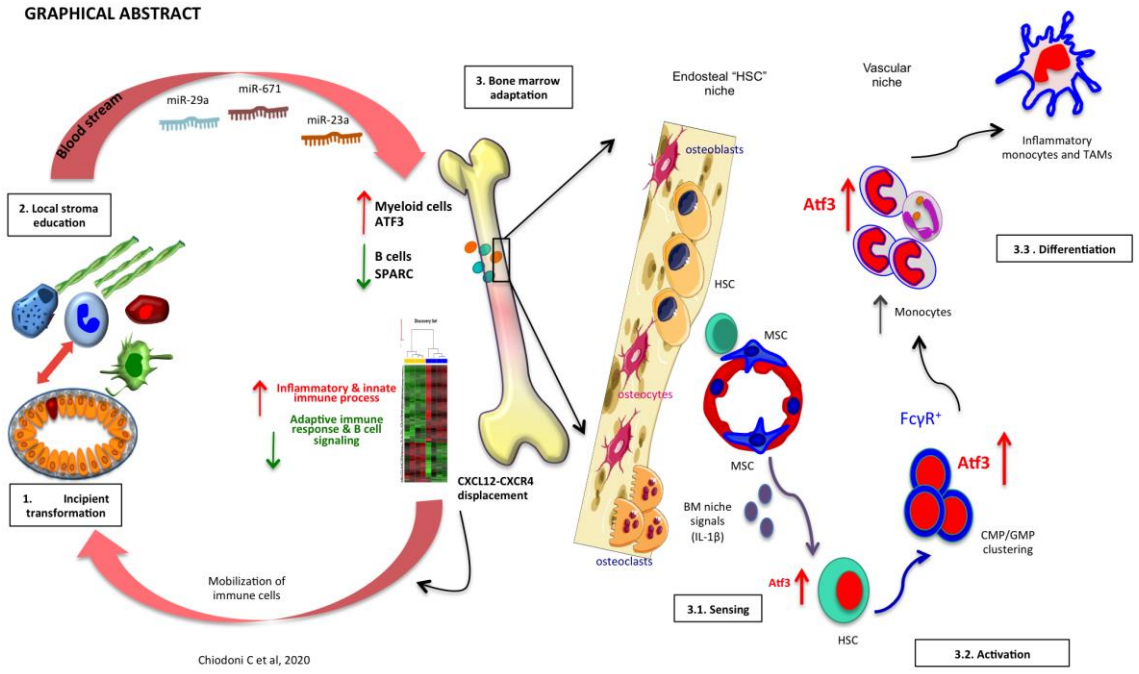

- The cross-talk between tumor and bone marrow starts early, at pre-malignant stages of disease.

- Stromal-derived signals drive ATF3 activation in HSCs and initiate a specific lineage commitment.

- ATF3 activation in immature myeloid cells is a hallmark of tumor-promoting myelopoiesis.

LIST OF ABBREVIATIONS

(ATF3) Activating transcription factor 3;

(BC) breast cancer;

(BM) bone marrow;

(CD) cluster of differentiation;

(CLP) common lymphoid progenitor;

(CMP) common myeloid progenitor;

(CSF) colony stimulating factor;

(ECM) extracellular matrix;

(FACS) fluorescent activated cell sorting;

(FC) flow cytometry;

(GEP) gene expression profile;

(GMPs) granulocyte-monocyte progenitors;

(H&E) hematoxylin & eosin;

(HER-2) human epidermal growth factor receptor-2;

(HSC) hematopoietic stem cell;

(IHC) immunohistochemistry;

(M-CSF) macrophage-colony stimulating factor;

(MDSC) myeloid derived suppressor cell;

(MEP) megakaryocyte/erythroid progenitor;

(MSC) mesenchymal stem cell;

(PB) peripheral blood;

(qPCR) quantitative polymerase chain reaction;

(SCF) stem cell factor;

(SPARC) secreted protein acidic and rich in cysteine;

(TAM) tumour-associated macrophage;

(TLR) toll-like receptor;

(TME) tumour microenvironment;

(WT) wild type.

TABLE OF CONTENTS

1) INTRODUCTION

1.1 Bone marrow

The bone marrow (BM) is the primary lymphoid organ deputed to hematopoietic stem cells (HSCs) maintenance and to the production of all blood and immune cells.
BM is composed by specialized niches in which hematopoietic and non-hematopoietic cells are interconnected by a complex network of blood vessels and sympathetic nerves, that support and guide the balance between the expansion and the differentiation of hematopoietic stem and progenitor cells (HSPCs) into mature immune cells (Fig 1).

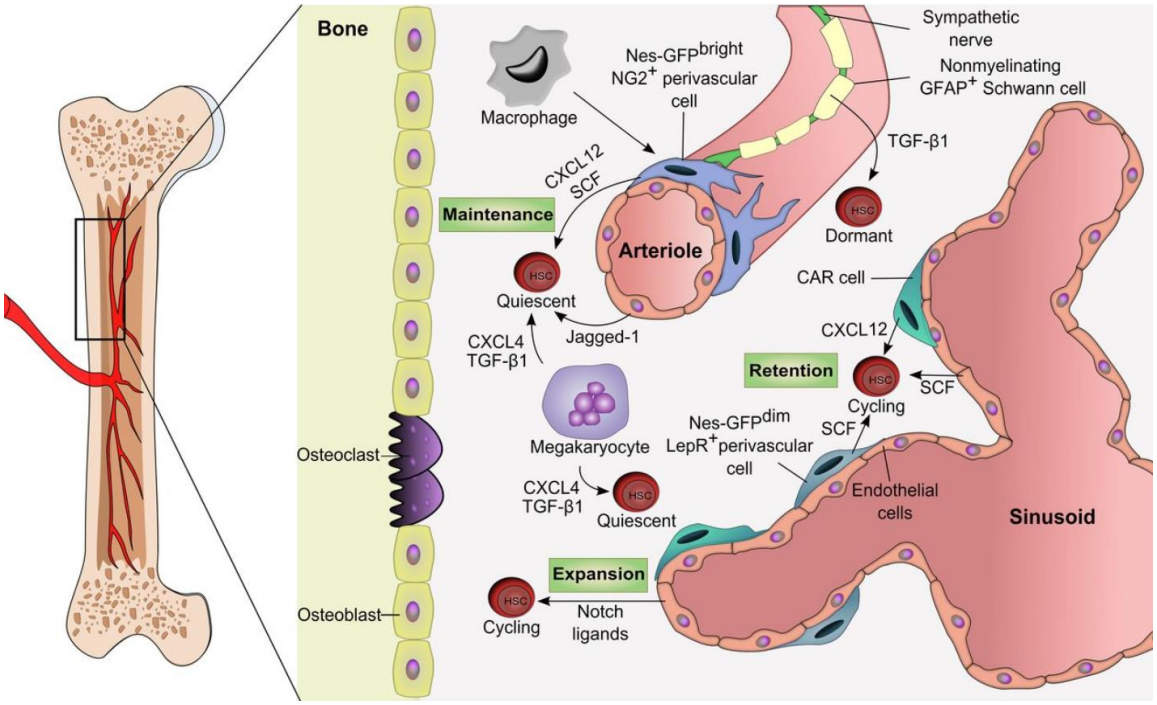

Figure 1. Representation of the BM microenvironment under homeostatic conditions. Quiescent HSCs are in close contact with arterioles where soluble factors such as CXCL-12, SCF and TGF-β1 secreted by perivascular, endothelial and sympathetic neuronal cells promote their dormancy. Proliferation signals induce HSCs to migrate in the sinusoidal region. Mature immune cells (macrophages, megakaryocytes) and stromal cells (CAR cells) in the BM microenvironment actively contribute to HSC regulation. Boulais P.E, 2015.

Two specific niches can be identified in the BM: the endosteal and the vascular niche (Xie Y, 2009).
These specific niches work together in order to regulate the normal haematopoiesis, but are characterized by different extracellular matrix composition and soluble factors. Signals released from cells of the endosteal niche maintain HSC quiescence and self-renewal, while those from vascular niche are involved in HSC activation/differentiation and extravasation (Blank U, 2008) (Wilson A, 2006).

Quiescent HSCs are in close contact with bone lining cells (osteoblasts, osteocytes and osteoclasts) in the endosteal region, while committed progenitors and more differentiated cells are localized, respectively, in the central and perisinusoidal region in close contact with blood vessels and pericytes (Lord BI, 1975) (Lambertsen RH, 1984).
BM niches are not static entities, but rapidly respond to the immune perturbation associated with peripheral adaptation to injury and inflammation (Trumpp A, 2010).

1.1.1) BM stromal cell composition

HSCs fate in the BM is highly regulated by the activity of stromal cell populations, in particular cells of mesenchymal lineage, including pericytes, mesenchymal stem cells (MSCs) and their progenies (osteoblasts, adipocytes, fibroblasts, endothelial and reticular cells).
MSCs produce high levels of stem cell factor (SCF), Flt-3 ligand, thrombopoietin (TPO), TGF-β, IL-6, IL-7, IL-8, IL-11, IL-12, granulocyte-macrophage (GM-) and macrophage (M-) colony stimulating factors (CSFs) (Majumdar M.K, 2000) (Di N.M, 2002) (Kfoury Y, 2015).
SCF is essential for BM niche activity and long-term HSC maintenance (Omatsu Y, 2010). CXCL12-abundant reticular cells (CAR cells), a type of MSCs expressing CXCL12 at high levels, are the major producer of SCF (Méndez-Ferrer, 2010).
IL-7 promotes B lymphocyte differentiation (Cordeiro Gomes A, 2016); IL-15 is crucial for T cell proliferation; IL-21 for natural killer maturation (Parrish-Novak J, 2000); G-CSF and IL-1 induce myeloid progenitor cells differentiation (Pietras E.M, 2016).
The production of vascular cell adhesion molecule-1 (VCAM1), laminin, fibronectin, collagen and proteoglycans from MSCs also contribute to HSCs regulation (Prockop D.J. 1997) (Pittenger M. F, 1999).
Furthermore, MSCs are able to modify the activity of mature immune cells, such as T cell, B cells, NK cells, macrophages, monocytes and neutrophils.
MSCs affect innate and adaptive immunity cells by cell-to-cell contact or through the release of immune regulator factors (cytokines, chemokines and growth factors). The release of immune molecules from MSCs is strictly dependent on the sites and the target cells (Song N, 2020) (Details in Fig 2).

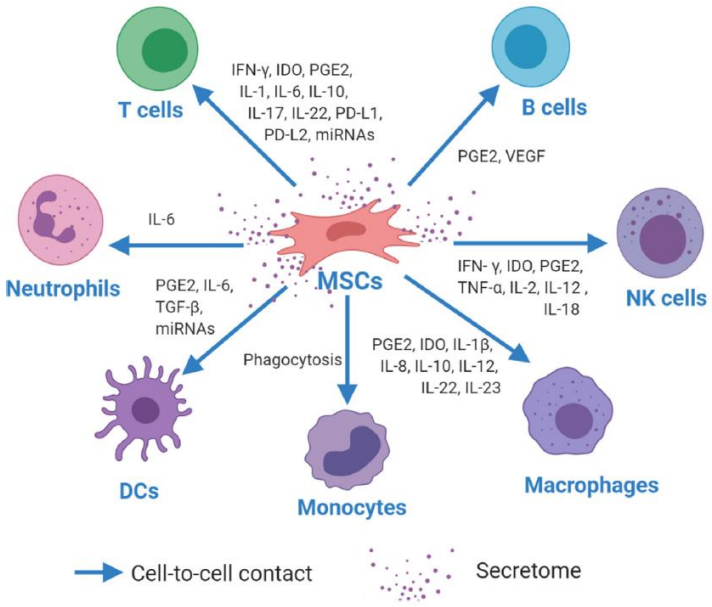

Figure 2. Schematic representation showing immunomodulatory interaction between MSCs and mature immune cells. Song N, 2020.

MSCs are multipotent stem cells that can be isolated from the BM and expanded *in vitro*. Initially, Sacchetti et al. identified a subpopulation of multipotent MSCs, expressing the CD146+ marker, with high self-renewal capacity (Sacchetti B, 2007). Subsequently, Morikawa et al. characterized a subset of MSCs, more specific for the vascular niche, that are negative for the Ter119 and CD45 hematopoietic markers and express the platelet-derived growth factor receptor-α (PDGFR-α) and the stem-cell antigen-1 (Sca-1) (Morikawa S, 2009).

Pericytes and endothelial cells also support the HSC niche through the release of Jagged-1 and DEL-1.

Similarly to MSCs, osteoblasts produce different molecules (CXCL12, SCF, OPN, THPO, ANG1, Jagged-1, RANKL) involved in HSC maintenance ((Taichman R.S, 1998) (Taichman R, 2005). Osteoblasts affect HSC numbers (Calvi LM, 2003) and support lymphoid committed progenitors (Visnjic D, 2004) (Terashima A, 2016).

Adult BM contains adipocytes, which are negative regulators of the hematopoietic microenvironment (Naveiras O, 2009). Indeed, the release of adiponectin inhibits HSC proliferation and prevents HSC expansion.

In addition to BM-stromal derived signals, also extracellular matrix (ECM) interaction and cell-cell communication indicate HSCs to remain quiescente, to self-renew or to differentiate (Balduino A, 2012).

Collagen types I and IV, laminin and fibronectin are the principal components of the BM-ECM composition. The ECM provides the structural scaffold for the BM stromal

niche and represents a reservoir of many growth factors, cytokines and metalloproteinases (Marastoni S, 2008). However, through the delivery of negative signals via LAIR-1, the ECM could also regulate HSC differentiation but also immune cell activation (Sangaletti S, 2014)

1.1.2) BM immune cell composition

The BM is the major site of the haematopoiesis process and plays a crucial role in preserving immune cells homeostasis and in generating mature blood cells.

All mature immune cells are produced in lymphoid organs starting from the differentiation of the HSCs. HSCs have the ability to maintain quiescence, to self-renewal and/or to differentiate into myeloid or lymphoid progenitor cells (Fig 3).

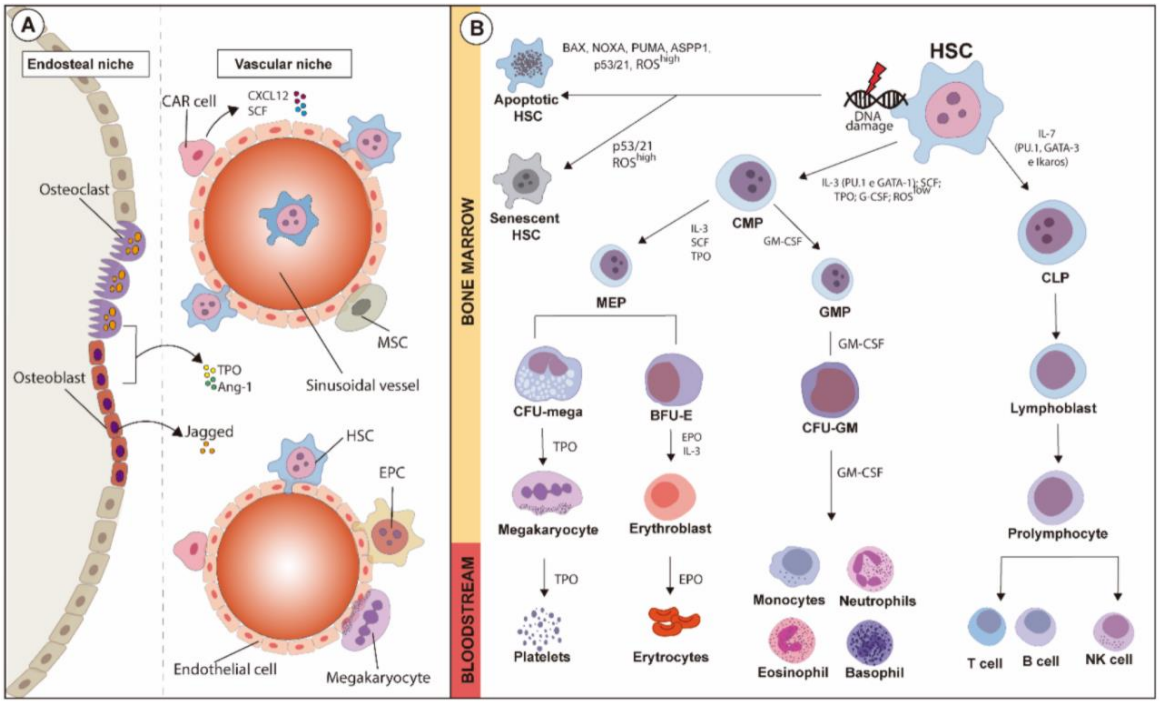

Figure 3. Schematic representation of the BM endosteal and vascular niches and the hierarchy differentiation of the hematopoietic lineage. A) HSC area contains both endosteal and vascular niche. In the endosteal niche, bone lining cells support the vascular niche in order to modulate the balance between the expansion and the differentiation of HSCs. B) The fate-decision of HSCs is modulated by the activation of transcription factors (PU.1, GATA-1, Ikaros) and the release of soluble factors from stromal cell populations (MSCs, endothelial cells, osteoblasts). Adapted from Scharf P, 2020.

HSC are classified in Long-term HSCs (LT-HSCs; c-Kit$^+$Lin$^-$Sca-1$^+$CD34$^-$Flk2$^-$), which maintain stem cell pool or differentiate in Short-term HSCs (ST-HSCs; c-Kit$^+$Lin$^-$Sca-1$^+$CD34$^+$Flk2$^-$) and Multi-Potent Progenitors (MPPs; c-Kit$^+$Lin$^-$Sca-1$^+$CD34$^+$Flk2$^+$), in which self-renewal ability is progressively restricted in favor of their ability to differentiate into mature immune cells.

MPPs progress towards oligo-potent progenitors, common lymphoid progenitors (CLPs) and common myeloid progenitors (CMPs), that have more lineage-restricted capacity (Kondo, 1997) (Akashi, 2000). CLPs generate lymphocytes, while CMPs ($Lin^-c\text{-}Kit^+CD34^+CD16/32^{low}$) give rise to megakaryocyte/erythroid progenitors (MEPs, $Lin^-c\text{-}Kit^+CD34^-CD16/32^-$) and to granulocyte/monocyte progenitors (GMPs, $Lin^-c\text{-}Kit^+CD34^+CD16/32^{high}$) (Nakorn, 2003) (Miyawaki, K, 2015) (Yamamoto R, 2013) (Doulatov S, 2012) (Challen G, 2009).

Multi-, oligo- or uni-potent progenitors receive lineage-instructive signals from the surrounding microenvironment and further proliferate and differentiate in mature cells in the BM or migrate into other lymphoid organs to complete their maturation.

Lymphoid progenitors give rise to B cells, T cells and natural killer (NK) cells. B cells ($B220^+$) and NK ($NK1.1^+$) cells mature in the BM. B cells give rise to plasma cells and memory B cells in secondary lymphoid organs. NK cells lack the antigen specificity and do not require the antigen exposure to mediate their anti-tumour and anti-viral response.

T cells ($CD4^+$ helper T cells and $CD8^+$ cytotoxic T cells) complete their maturation in the thymus.

Myeloid progenitor cells differentiate into granulocytes (neutrophils, eosinophils and basophils) and monocytes, which terminally differentiate into macrophages. Neutrophils and monocytes are both positive for CD11b antigen but can be distinguished by Ly6G marker, expressed only on neutrophil cell membrane and Ly6C marker, more specific for monocytes (Yang J, 2014) (Terry R.L, 2014) (Tamoutounour S, 2013).

Myeloid cells that express at low levels both Ly6G and Ly6C antigens are more immature myeloid cells that can differentiate into neutrophil or monocytic cells (Rose S, 2012).

Lymphocytes are responsible for adaptive immunity, myeloid cells for innate immune response. This hierarchical organization allows rapid adaptation in response to specific hematopoietic demand.

Flow cytometry (FC) is the best method used to identify, quantify and isolate BM immune cells. Fig 4 shows the most common cluster of differentiation (CD) markers used to characterize BM progenitor and mature cells.

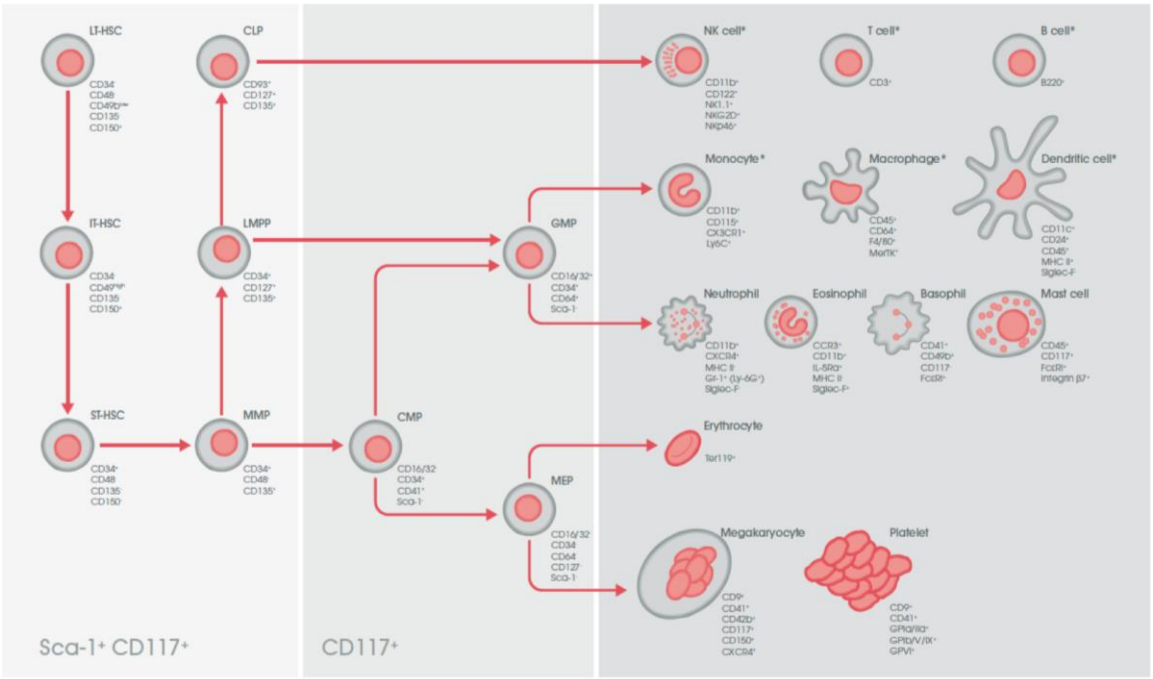

Figure 4. Immunophenotyping of mouse progenitor and mature BM hematopoietic cells by flow cytometry. Adapted from Abcam (https://www.abcam.com/primary-antibodies/immune-cell-markers-poster).

1.1.3) HSCs adaptation during inflammation and pathological disease

Hematopoiesis is a mechanism strictly controlled and balanced by a complex network of interactions between stimulatory and inhibitory factors.

Under stimulation, HSPCs and MSCs activate lineage specific transcription factors and initiate a general pro-inflammatory program that significantly impacts on BM niche fate, HSCs output and egress of immune cells from the BM, ultimately leading to a stress-induced hematopoiesis.

Inflammatory cytokines released during acute and chronic inflammation are the principal mediators of this BM stress-induced response. This cross-talk between distant infection and BM activation is reflected in the serum, where soluble factors (colony-stimulating factors, interleukins, interferons and chemokines) are rapidly released and reach the BM, where they bind their respective receptors, expressed on hematopoietic and non-hematopoietic cells residing in specialized BM niches.

Acute inflammatory signals (interferon (IFN), tumour necrosis factor (TNF), toll-like receptor (TLR), lipopolysaccharide (LPS)) and pathogen or danger associated ligands destroy stem cell homeostasis and stimulate HSC proliferation and differentiation. Initially, these signals provide a BM rapid response that activates both myeloid and lymphoid progenitors in order to coordinate and mediate a prompt immune-activation.

Persistent HSC activation during chronic inflammatory processes (systemic immune activation and tumour-development) contributes to HSC exhaustion, BM failure and hematopoietic malignancies.

During the initial response to acute inflammation, ligation of pattern-recognition receptors (PRRs) and toll-like receptors (TLRs) induces the release of chemokines and cytokines at the site of infection. Chemokines favor extravasation of immune cells from the blood into the afflicted tissue; cytokines stimulate locally activation of the immune system. However, persistent sensing of pathogen associated molecular patterns (PAMPs) results in the loss of control of the local infection and increased demand of BM immune cells.

Adaptive immune cells (T and B cells) proliferate during antigen presentation and are rapidly mobilized from BM to secondary lymphoid organs.

During systemic infection, inflammation or tumor progression, the release of inflammatory factors such as IL-1, IL-3, IL-6, G-CSF and GM-CSF in the BM alters the expression of growth factors and retention signals for lymphoid cells (Ueda Y, 2009) (Cheers C, 1988) (Basu S, 2000) (Cain DW, 2011). This mechanism generates vacant niches that are replenished by BM myeloid precursors (Ueda J, 2005). As a consequence, myeloid progenitor cells proliferate in these spaces and boost myeloid cell output (Fig 5).

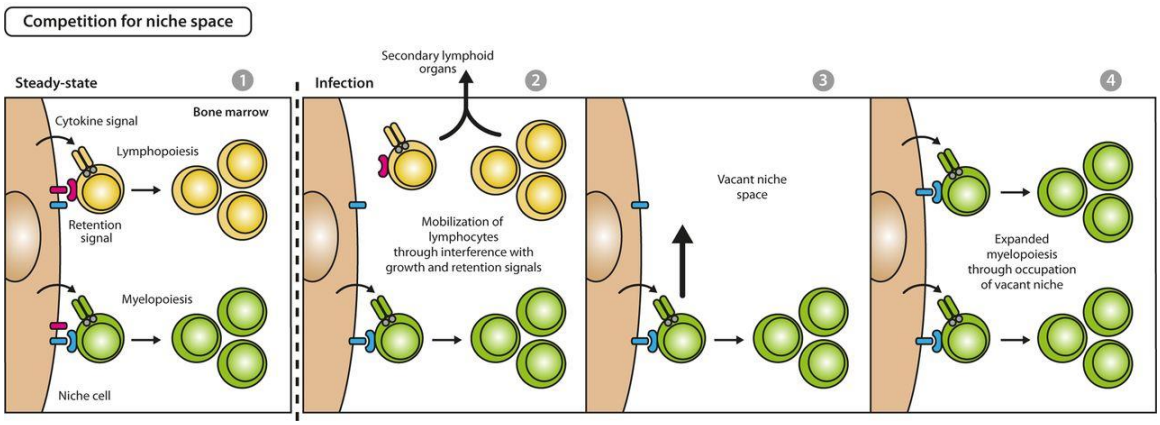

Figure 5. Schematic representation showing the lymphoid and myeloid niches at steady state and during an emergency myelopoiesis. Reduction of growth and retention signals induces lymphocyte mobilization to secondary lymphoid organs and generates vacant niche spaces that are replenished by myeloid cells. Takizawa H, 2012.

Innate immune cells (especially monocytes, macrophages and neutrophils) are replenished from the BM to maintain their number in the site of injury, where they are rapidly consumed. Under normal conditions, immature myeloid cells (CMPs and GMPs) that originate in the BM differentiate into mature myeloid cells. Following

pathological perturbation, activated immature myeloid cells are unable to complete their differentiation and acquire immunosuppressive functions.
This atypical BM hematopoietic response is defined as emergency myelopoiesis.

1.1.4) HSCs and MSCs are key players during an emergency hematopoiesis

The expression of receptors for inflammatory cytokines and growth factors on BM cells is altered during inflammation.
HSCs express TLRs, IL-1R, IL-6R, IFNAR, CSF1R and CSF2RB receptors on HSC membrane surfaces (Fig 6). The engagement of these receptors by the cognate ligands promotes HSC differentiation.

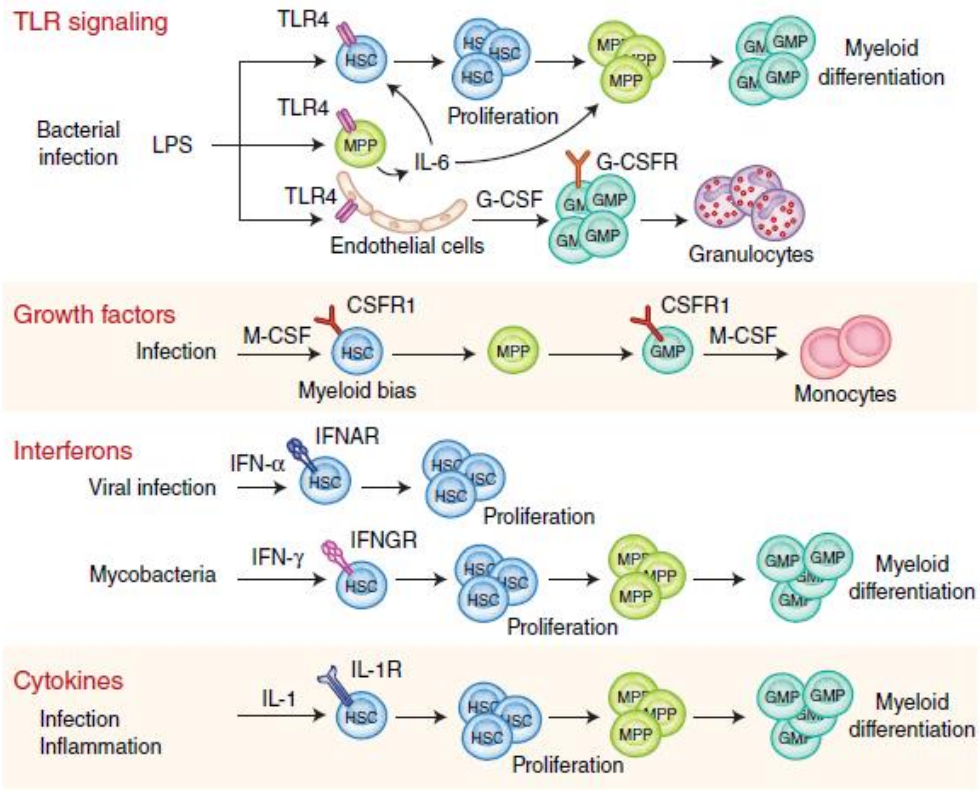

Figure 6. HSCs adaptation to inflammatory stimuli. HSCs and MMPs sense inflammation through the expression of TLRs, IL-1R, IL-6R, IFNAR, CSF1R and CSF2RB receptors on their membrane surface. Adapted from Chavakis T, 2019.

The activation of TLR4 by LPS on HSCs stimulates GMP differentiation towards neutrophils; the stimulation of TLR9 by CpG activates monocyte-dendritic cell progenitors (Yáñez A, 2017). HSPCs have functional TLR/NF-kB signaling axes responsible for a wide range of cytokines upon stimulation, especially IL-6 (Zhao J.L, 2014).
Furthermore, chronic IFN-γ and G-CSF exposure activates quiescent HSCs (Baldridge MT, 2010) (Schuettpelz LG, 2014). IL-6, IL-1 and IL-17 regulate myeloid and

lymphoid output in normal condition, but during inflammation reprogram hematopoietic progenitor lineage and contribute to blood dysfunction (Reynaud D, 2011) (Pietras EM, 2016). Persistent activation of IL-1 specifically acts on CMPs, promoting myeloid proliferation and differentiation (Nagareddy PR, 2014).

Colony-stimulating factors (granulocyte G- and GM-CSF) are key signals during emergency myelopoiesis, indeed they are able to promote the monocytic (M-) and granulocytic (G-) myeloid-derived suppressor cell (MDSC) (Gabrilovich DI, 2009) differentiation from CMPs (Gabrilovich DI, 2012). The differentiation and the function of these cells are discussed in detail in chapter 1.4.3.

Single-cell transcriptomic analysis and specific conditional knockout mice contributed in detecting stromal cell factors that released during stress-induced hematopoiesis have selective effects on BM HSCs and their progenies (Tikhonova, 2019) (Ding L, 2013). These data illustrate a dynamic and heterogeneous BM microenvironment that is extremely vulnerable to danger signals and rapidly responds to perturbation (Fig 7).

For example, S100 calcium binding protein A8/A9 (S100A8/A9) released by endothelial cells and MSCs activates inflammasome complexes in the hematopoietic progenitors (Zambetti NA, 2016) and induces DNA damage and cell cycle arrest.

Endothelial cells are the major producers of G-CSF during inflammation (Boettcher S, 2014). Activated BM-MSCs, releasing IL-6, GM-CSF and indoleamine 2,3-dioxygenase (IDO1), are also able to support the expansion of tumour-promoting myeloid cells.

Matricellular protein such as Osteopontin (OPN) and secreted protein acidic and rich in cysteine (SPARC) are often dysregulated during stress-hematopoiesis and hematopoietic malignancies. OPN, produced by osteoblasts, favors lymphopoiesis at the expense of granulopoiesis (Kanayama, 2017). SPARC, expressed by stromal cells, induces fibrotic changes during myeloproliferation (Tripodo C, 2012) but also contributes to lymphoid malignancies (Sangaletti S, 2014).

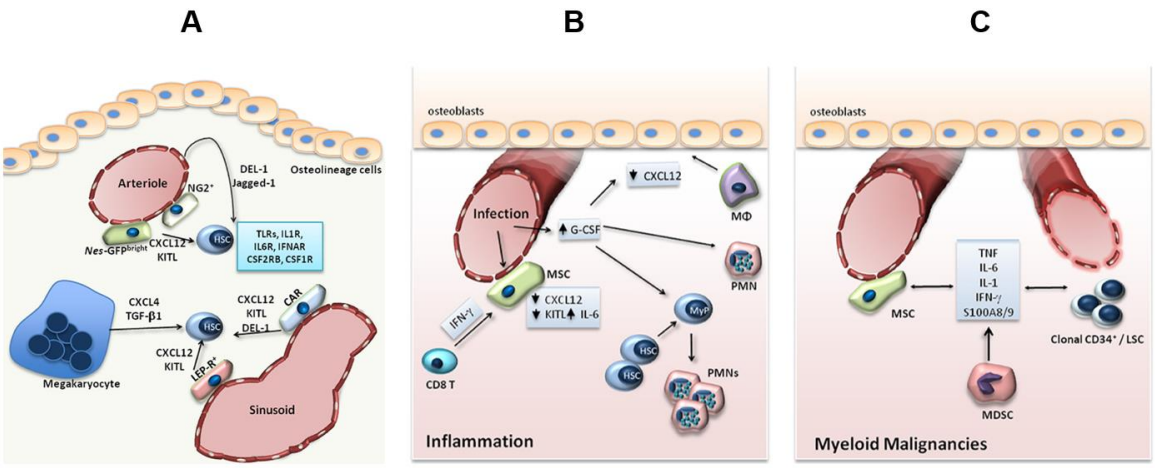

Figure 7. HSC niche in steady state condition (A), upon infection (B) and (C) during myeloid malignancies. During normal conditions, MSCs promote HSCs maintenance through the release of CXCL-12, KITL, Jagged-1 and DEL-1. BM adaptation to inflammation leads to an increased production of G-CSF and IL-6 from MSCs, at the expense of CXCL-12 and KITL. The production of IL-6, TNF, IL-1 by MSCs may also support clonal expansion of myeloid progenitor cells (CD34+) and leukemic stem cells (LSCs). Adapted from Mitroulis I, 2020.

Furthermore, not only BM stromal cells, but also mature cells, including macrophages and T cells control BM niche activity. $CD169^+$ macrophages, in close contact with osteoblasts and MSCs in the BM, called "osteomacs", regulate the expression of ANG1, CXCL12 and KITL and their depletion mobilize HSPCs. Cytotoxic T cells release IFN-γ, which in turn promotes IL-6 secretion by MSCs and HSC activation (Schürch CM, 2014).

1.1.5) HSCs mobilization

The recruitment of HSCs from the BM into the peripheral blood is a finely regulated process involving chemokines and cognate receptors, growth factors and adhesion molecules (Levesque J.P, 2007).

Loss of contact between BM hematopoietic and non-hematopoietic cells or down-regulation of adhesion molecules and chemokines receptors induces mobilization of these cells in the blood. For example, inactivation of either very late antigen-4 (VLA-4) expressed by HSCs, or vascular cell-adhesion molecule-1 (VCAM-1), expressed by endothelial cells, drives HSC rolling on the vascular system (Scott LM, 2003) (Ulyanova T, 2005).

These events are paralleled by changes promoting an increased vascular permeability such a local production of VEGF-A in the BM sinusoids (Lévesque J.P, 2007).

CXCL12-CXCR4 signaling is one of the most relevant pathways driving BM cell mobilization. This axis mediates the interaction of hematopoietic progenitors with the

BM microvasculatures and stimulates trans-endothelial migration (Peled A, 2000) (Tzeng Y.S, 2011). HSCs highly express the chemokine receptor CXCR4 and are attracted towards the stromal-cell- derived factor 1 (SDF-1), also known as CXCL12, expressed by osteoblasts, CAR cells and vascular endothelial cells. Under normal conditions, HSCs are retained in the BM niche by high levels of CXCL12, which is preserved by the hypoxic microenvironment.

Under inflammatory conditions, BM niche cells rapidly adapt the BM hematopoietic response to peripheral perturbation, releasing growth factors that promote myelo/granulopoiesis (Boettcher S, 2014).

Among them G-CSF induces neutrophils boost in the BM, which in turn stimulates protease secretion that inactivates CXCL-12, SCF, V-CAM1 and ANG-1 retention signals (Levesque J.P, 2002) (Fig 8).

Particularly the down-modulation of CXCL12 by metalloproteinases (MMP-2 and MMP-9), elastase and cathepsin G promotes HSC mobilization to peripheral tissue (Heissing B, 2002). Elastase, cathepsin G and MMP-9 decrease the anchorage of HSPCs in the osteoblastic niche, acting on the adhesion molecules VLA-4 and V-CAM1.

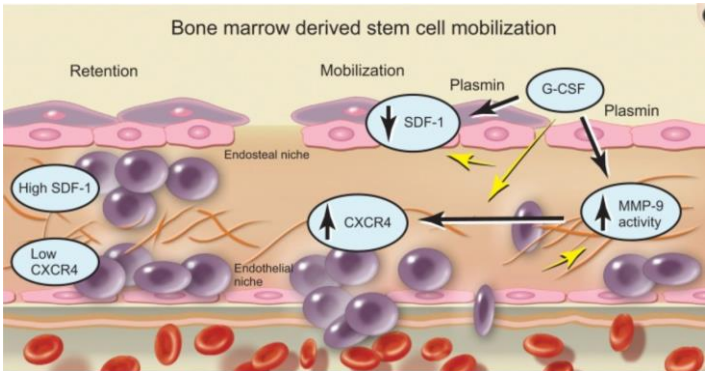

Figure 8. Model illustrating disruption of CXCL12-CXCR4 retention axis in the BM microenvironment after G-CSF stimulation. Hoover-Plow J, 2012.

Disruption of the CXCL12-CXCR4 retention axis has been reported as a key event in the generation of a pathological BM niche that strongly supports myeloproliferation (Colmone A, 2008).

Other than promoting mature myeloid cells and HSPCs mobilization (Greenbaum AM, 2011) (Tay J, 2017), G-CSF also decreases the number and the activity of CD169+ BM macrophages, that in normal condition interact with MSCs to regulate the expression of retention signals in the endosteal niche (Chow A, 2001). Indeed the depletion of CD169+ cells mobilizes HSCs into the sinusoid region (Ehninger A, 2011).

1.1.6) Molecular regulation of quiescent and activated HSCs

In addition to signalling released by BM stromal compartment, transcription factors (TFs) involved in epigenetic, transcriptional and post-transcriptional modifications are important regulators of HSC homeostasis, lineage commitment and cell differentiation.

TFs regulate gene expression when binding the promoter region of their downstream targets. Specific lineage-determining TFs drive HSC differentiation towards mature BM immune cells.

Several critical TFs are activated during haematopoiesis and have been extensively characterized.

PU.1, Runx1/2, IRF1/2, Foxo1, Gata1, Cebp are some of key TFs that dictate stem cell self-renewal and/or lineage commitment differentiation (Figure 9).

Activation of PU.1, one of the earliest TFs in the haematopoietic lineage, induces MMPs to differentiate toward myeloid lineage (Pietras EM, 2016). Acquisition of IRF8, which forms heterodimer with PU.1, is required for monocyte and macrophage differentiation (Friedman AD, 2007) (Tamura T, 2015). Gata-1 drives for erythroid and megakaryocytic cells. Runx regulates CLP fate (Zhu, 2002) (Laslo P, 2006). C/EBP transcription factor regulates monocyte and granulocyte differentiation. C/EBPα is involved in steady-state haematopoiesis (Dahl R, 2003), C/EBPβ is critical during emergency granulopoiesis (Hirai H, 2006) (Hirai H, 2015). RORC1 is a key transcription factor that drives a tumour-promoting BM-myelopoiesis (Strauss L, 2015).

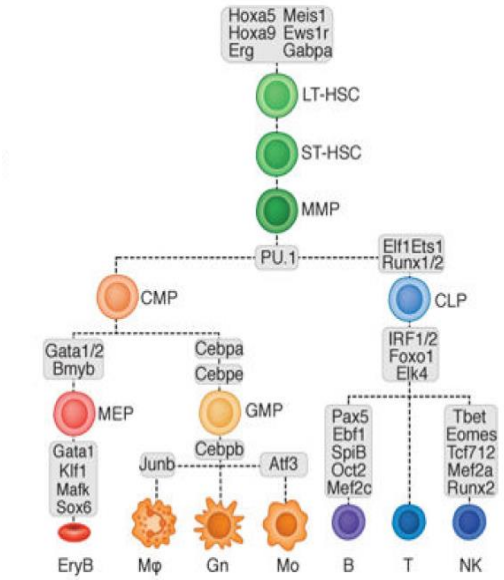

Figure 9. Hematopoietic three display key transcription factors involved during maturation of each cell type. Lara Astiaso D, 2014.

Significant advances in chromatin-immunoprecipitation approach (iChIP) identified ATF3 as a new potential regulator of hematopoietic lineage (Lara-Astiaso D, 2014).

1.2) ATF3

Activating transcription factor 3 (ATF3) is an early adaptive-response gene member of the ATF/cyclic AMP response element-binding (CREB) family of transcription factors. This family also includes ATF1, ATF2, ATF4, ATF5, ATF6, ATF7, B-ATF, CREB and CREM proteins, all induced in response to many stimuli.

ATF/CREB members share the basic-region leucine zipper (bZIP) element: the basic-region is involved in the specific DNA binding, while the leucine zipper motif forms homo- or heterodimers with other bZIP protein, such as AP-1, c/EBP (Hai T, 2006).

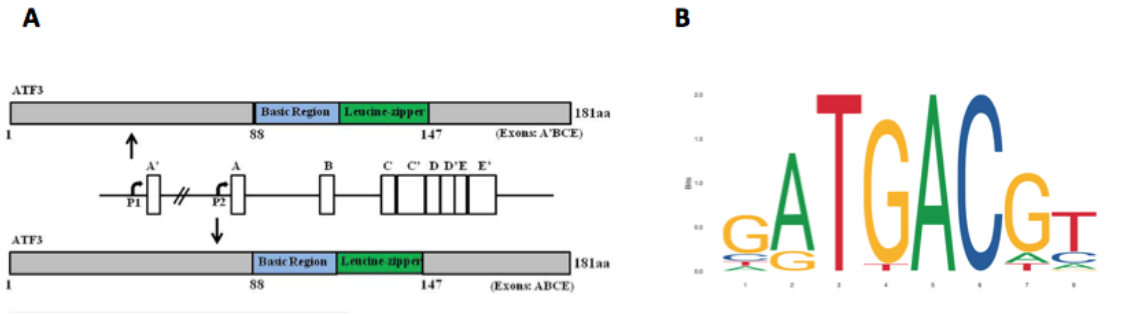

Figure 10. A) ATF3 gene has two promoters (P1 and P2) and comprises four exons. Both promoters (P1 non canonical and P2 canonical) give two full-length proteins that change in their 5' UTR due to the presence of exon A' or A. Rohini M. 2018. B) Sequence motif of ATF3 binding site generated using the JASPAR database.

The *ATF3* gene is located in chromosome 1q32.3 and consists of four exons that encode for a protein composed of 181 amino acids with a molecular weight of 22 kD (Liang G, 1996) (Figure 10A). The alternatively spliced isoform of ATF3 (ATF3ΔZip), lacks the leucine zipper domain (Chen BP, 1994) and although not directly binding the DNA, it retains the ability to stimulate transcription process.

ATF3 protein binds the consensus sequence 5'-TGACGTCA-3', a cycling AMP response element identified in various promoter regions (Deutsch PJ, 1988) or the similar AP-1 site 5'-TGA(C/G)TCA-3' via its bZIP domain (Eferl R, 2003) (Figure 10B).

ATF3 can act as either transcriptional activator or repressor, the regulation of ATF3-target genes depends on the promoter context and by heterodimers formed with other ATF/CREB proteins. ATF3 homodimer acts as a transcriptional repressor (Wolfgang C.D, 1997) (Wolfgang C.D, 2000). When ATF3 forms heterodimers with ATF-2, c-Jun, JunB and JunD can activate or repress their target genes (Hai T, 1999).

1.2.1) ATF3 activation

ATF3 is expressed at low levels under steady-state conditions; nevertheless its expression and nuclear translocation can be quickly promoted by different inflammatory factors, such as those associated with tumor progression.

ATF3 is a key regulator of inflammatory response to stress signals, such as DNA damage, metabolic dysfunction, cellular injury and oxidative stress (Hai T, 1999). The same stimuli induce ATF3 in rats, mice and humans (Fig 11).

ATF3 was initially identified as an immediate early gene, being rapidly activated in case of stress stimuli at the transcriptional level (Hai T, 2001) (Hai T, 1999).

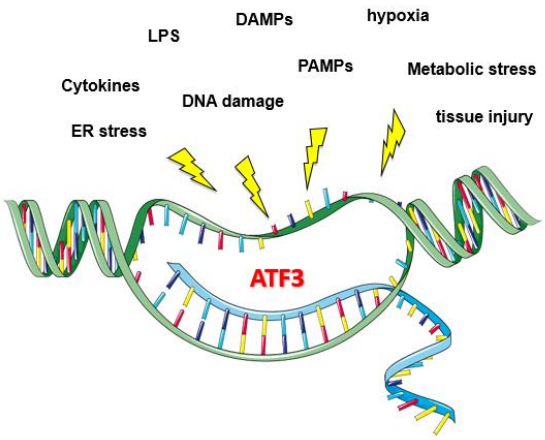

Figure 11. Signals leading to ATF3 activation.

Indeed, the ATF3 promoter region could be bound by ATF/CREB, AP-1 and NF-kB transcription factors.

In addition, the binding sites for Smad, p53 and HIF genes on the ATF3 promoter region, favour the induction of ATF3 expression in response to different stimuli.

The rapid activation of ATF3 is due, in part, to an autoregulatory ATF3 binding site on its own promoter (Wolfgang CD, 2000). In line, the 3' UTR untranslated region (3' UTR) of ATF3 gene contains many AUUUA sequences, a characteristic of several immediate early genes.

Furthermore, ATF3 can be a regulator of cell cycle progression, being its promoter regulated by Myc/Max and E2F transcription factors (Hashimoto Y, 2002).

1.2.2) ATF3 during stress response mechanisms

One common feature between ATF3 and other members of the ATF/CREB family is that they are all involved in stress response mechanisms but at different levels (Hay T, 2006). ATF3, ATF4 and ATF6 have a central role during the endoplasmic reticulum (ER) stress response whereas ATF2 has been associated with transcriptional and DNA damage control (Van Dam H, 1995).

Stressful conditions generated during cancer, infection or inflammation lead to the activation of two pathways: the unfolded protein response (UPR), promoting the activation

of UPR related TFs (ATF4, ATF3, ATF6, CHOP, XBP1s) and the NF-kB signaling axis (RELA, NFKB1, NFKB2, RELB, c-REL), which converge within the nucleus in order to restore cellular homeostasis. UPR and NF-kB signaling cooperate through gene regulatory mechanisms determining the balance between metabolic changes or inflammatory stimuli and the activation of apoptotic/autophagic cell death or repair of cell damage (Schmitz ML, 2018) (Fig 12A).

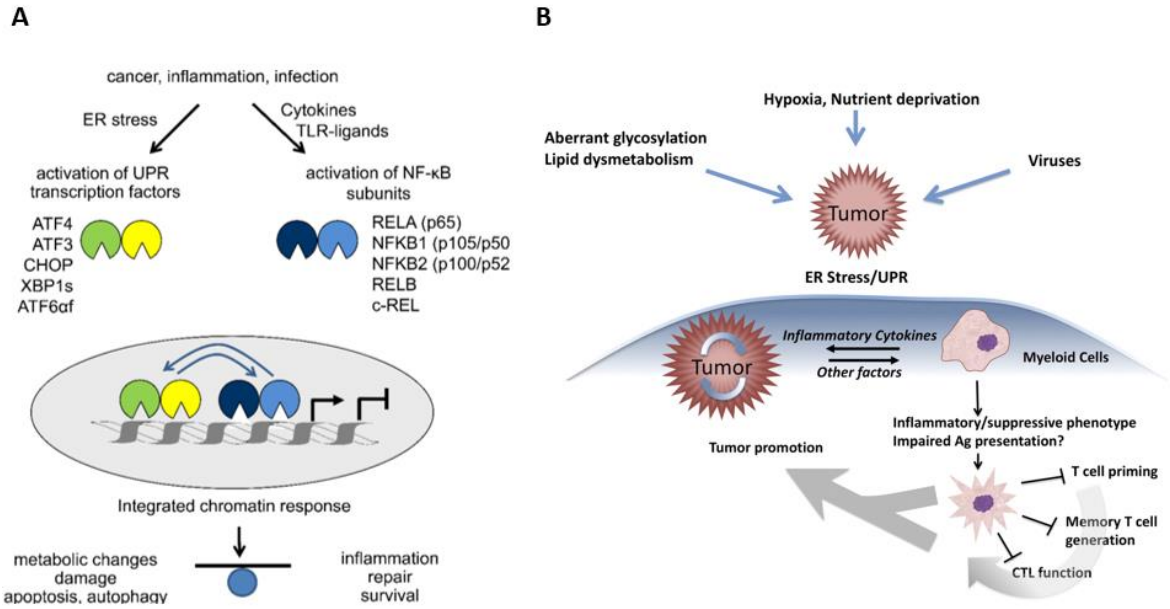

Figure 12 A) Signaling activities during stressful conditions led to ATF3 activation in the nucleus. Cooperation with other TFs (ATF4, ATF6, CHOP, XBP1 and NF-kB) induces apoptosis or stimulates cell repair and survival process (Schmitz ML, 2018). B) Effects of UPR on cancer cells modify the tumor microenvironments. The release of factors from ER-stressed tumour cells generates an inflammatory and immunosuppressive microenvironment that facilitates tumour growth (Mahadevan NR, 2011).

During this transcriptional process ATF3 is a direct target gene of ATF4 (Jiang H.Y, 2004). In turn, ATF3 regulates CHOP (Chen B.P, 1996), suggesting a cascade of transcriptional events finely regulated in response to ER stress.

UPR in tumor cells is associated with genomic instability, angiogenesis and survival. Factors released by tumour cells under UPR mechanism are able to induce ER stress activation in BM-derived myeloid cells and dendritic cells. This mechanism, well known as transmissible ER stress (TERS), is associated with the release of pro-inflammatory cytokines from myeloid cells (Mahadevan NR, 2011) (Cullen SJ, 2013) and activation of immunosuppressive mechanisms, that impact on naïve CD8+ T cells (Mahadevan NR, 2012) (Fig 12B).

1.2.3) Role of ATF3 as immune transcription factor

ATF3 activation has been associated with different human immune diseases such as atherosclerosis, infection and sepsis. Several intracellular signalling has been reported to induce ATF3 under pathological conditions, such as p38 MAPK, JAK/STAT, c-Myc/ERK, JNK/NF-kB.

In response to acute inflammation, ATF3 activation limits the intensity of the inflammatory response and maintains normal host immune response. Recently, it has been shown that ATF3 modulation, during acute stress-induced haematopoiesis (5-fluorouracil or irradiation), prevents stem-cell exhaustion and maintains HSC self-renewal (Liu Y, 2020). However, the consequence of persistent activation of ATF3 during haematopoiesis was not investigated.

More interesting, ATF3 could be a lineage determining transcription factor that can drive differentiation toward a specialized cell type. Indeed, chromatin immunoprecipitation studies performed during hematopoietic differentiation showed a significant enrichment of ATF3 binding motifs in cells of the myeloid lineage (Lara-Astiaso D, 2014). Mechanistically, ATF3 could regulate key genes involved in the generation and in the release of myeloid cells from the BM into the circulation. Maruyama et al. showed that ATF3 can inhibit neutrophil differentiation in the BM and is suppressed by Jun Dimerization Protein 2 *(Jdp2)*, its paralogue gene (Maruyama K, 2012). Furthermore, during airway inflammation ATF3 promotes neutrophils chemotaxis from the BM towards the circulation through the activation of T-cell lymphoma invasion and metastasis 2 (*Tiam2)* gene (Boespflug ND, 2014).

In myeloid cells, ATF3/NF-kB signalling plays an important role during the inflammatory response (Kwon JW, 2015). ATF3 expression is induced in response to a wide range of TLR ligands able to activate the adaptive immune system: pIC (TLR3), LPS (TLR4), zymosan (TLR2/6), pIC/CpG-ODN (TLR3/9) (Whitmore MM, 2007). In this condition ATF3 attenuates the immune response through the inhibition of genes encoding pro-inflammatory mediators, such as IL6, IL-12b and TNFα (Gilchrist M, 2008) (Fig 13). Treatments with IFN-α, IFN-β and IFN-γ also induce ATF3 expression in macrophages, which further regulate IFN-stimulated genes, including CCL12, CCL13, Clec4e (Labzin LI, 2015).

An important role of ATF3 in myeloid cells was identified in the tumour-microenvironment. Signals released from tumour cells (IL-4, TGF-β, TNF-α, hypoxia) activate ATF3 expression in BM-derived macrophages, which in turn regulate target

genes involved in cell invasiveness, trans-endothelial migration and metastasis (MMP9, MMP2, ADAM15). In line, gene expression analysis studies suggest that ATF3 could favour a pro-tumoral skew of myeloid cells, since ATF3 up-regulates *Arg1* but down-regulates *Il-12* in macrophages. Furthermore, in tumour-associated macrophages ATF3 regulates key genes involved in cell growth, chemotaxis, and cell-cell communication (Wolford C, 2013).

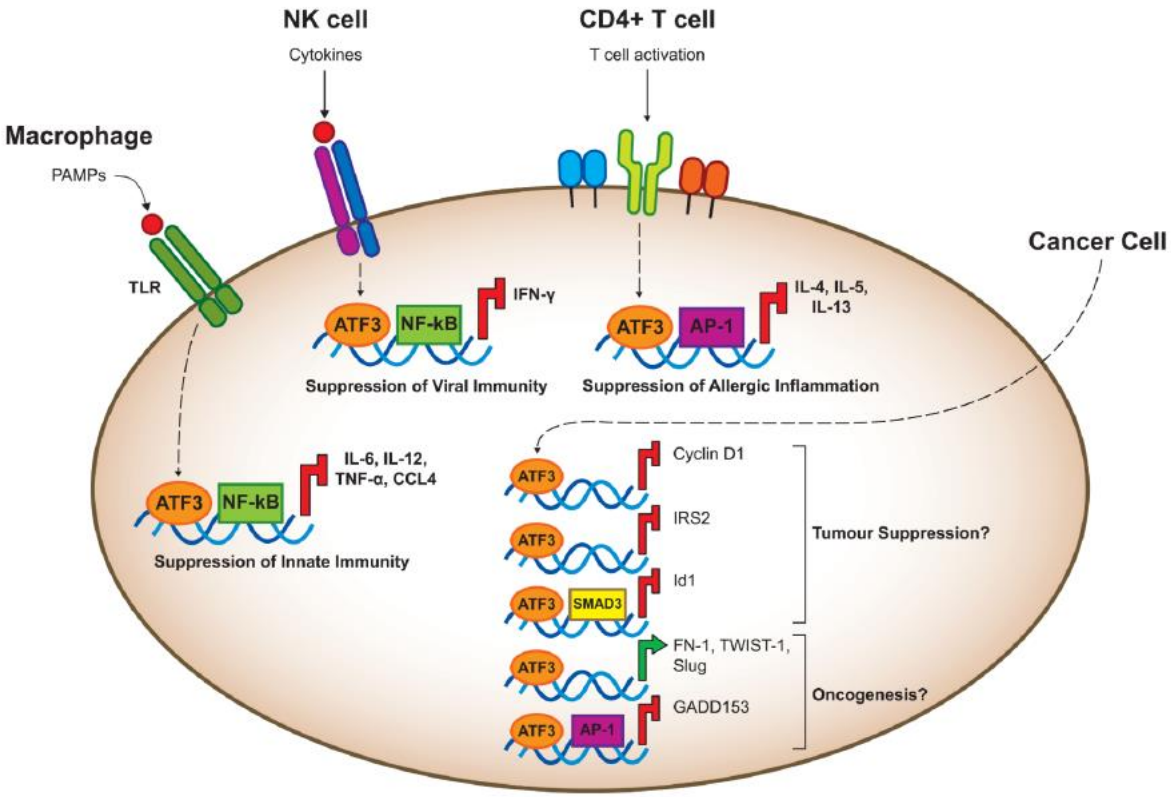

Figure 13. Regulation of immune response and cancer progression after ATF3 activation. ATF3 target genes in immune cells (macrophages, NK and CD4+ T cells) and ATF3 activity as tumour suppressor or oncogene in cancer cells are shown in the figure (Thompson MR, 2009).

Despite the vast majority of studies have characterized the role of ATF3 in myeloid cells, some others have shown that ATF3 is also able to modulate NK and CD4+T cell activity in order to suppress viral immunity and allergic inflammation (Rosenberger CM, 2008) (Gilchrist M, 2008).

Notably, ATF3 is also expressed by tumour cells where it controls the expression of genes involved in cancer progression, such as Slug, TWIST-1, Cyclin D1, GADD153 (Yin X, 2008) (Wolfgang CD, 1997). ATF3 activation is able to regulate the balance between proliferative and apoptotic signals and contribute to cancer progression (Fig 13).

The oncogenic up-regulation of ATF3 has been identified in human breast and prostate cancer or Hodgkin lymphoma, conversely other studies showed a pro-apoptotic function

of ATF3, for example in colorectal and lung cancer cells. Therefore, whether ATF3 acts as tumour suppressor or oncogene is closely related to cell type and tissue microenvironment (Thompson MR, 2009).

1.3) Breast cancer

Breast cancer (BC), one of the most common tumours among women worldwide, is a heterogeneous disease with different pathological features and response to treatments that led to a high mortality rate.

After lung cancer, BC represents the second leading cause of cancer death.

Germline mutation (BRCA1, BRCA2, TP53), genetic variation (SNPs), genomic instabilities (amplification, translocation, deletion) and epigenetic regulation (DNA methylation and histone acetylation), significantly contribute to higher risk of breast cancer development (Coughlin SS, 2019) (Wendt C, 2019) (Mavaddat N, 2015).

The incidence of BC is also influenced by some risk factors including age, gender, race/ethnicity, overweight, excessive consumption of alcohol (Barnard ME, 2015).

Recently, epidemiological studies identified other risk factors correlated with BC development such as menstrual history, age at pregnancy, hormonal levels and breastfeeding (Endogenous Hormones and Breast Cancer Collaborative Group, 2013) (Collaborative Group on Hormonal Factors in Breast Cancer, 2002).

1.3.1) Breast cancer development

Breast transformation starts when mutated cells, within the ducts and/or the lobules, proliferate in abnormal ways and originate a condition identified as hyperplasia.

Proliferative cells can acquire mechanisms of self-sufficiency, apoptosis resistance and evasion of anti-growth signals (Hanahan D, 2000).

At this stage, called carcinoma in situ, the proliferation rate is confined in the initial tissue. In breast cancer there are two types of in situ carcinoma: ductal carcinoma in situ (DCIS) and lobular carcinoma in situ (LCIN).

Altered cells, losing their differentiation state and the contact with other cells, induce local invasion, stromal remodelling, angiogenic switch, ultimately leading to invasion and metastasis. During this process, an established tumour invades the basal membrane of the tissues and spreads to distant organs through blood vessels and the lymphatic

system. LCIN is an atypical lobular hyperplasia that generally is not associated with invasive cancer (Simpson P.T, 2003). Colonization and proliferation of breast tumour cells in distant organs is clinically identified as invasive ductal carcinoma (Fig 14).

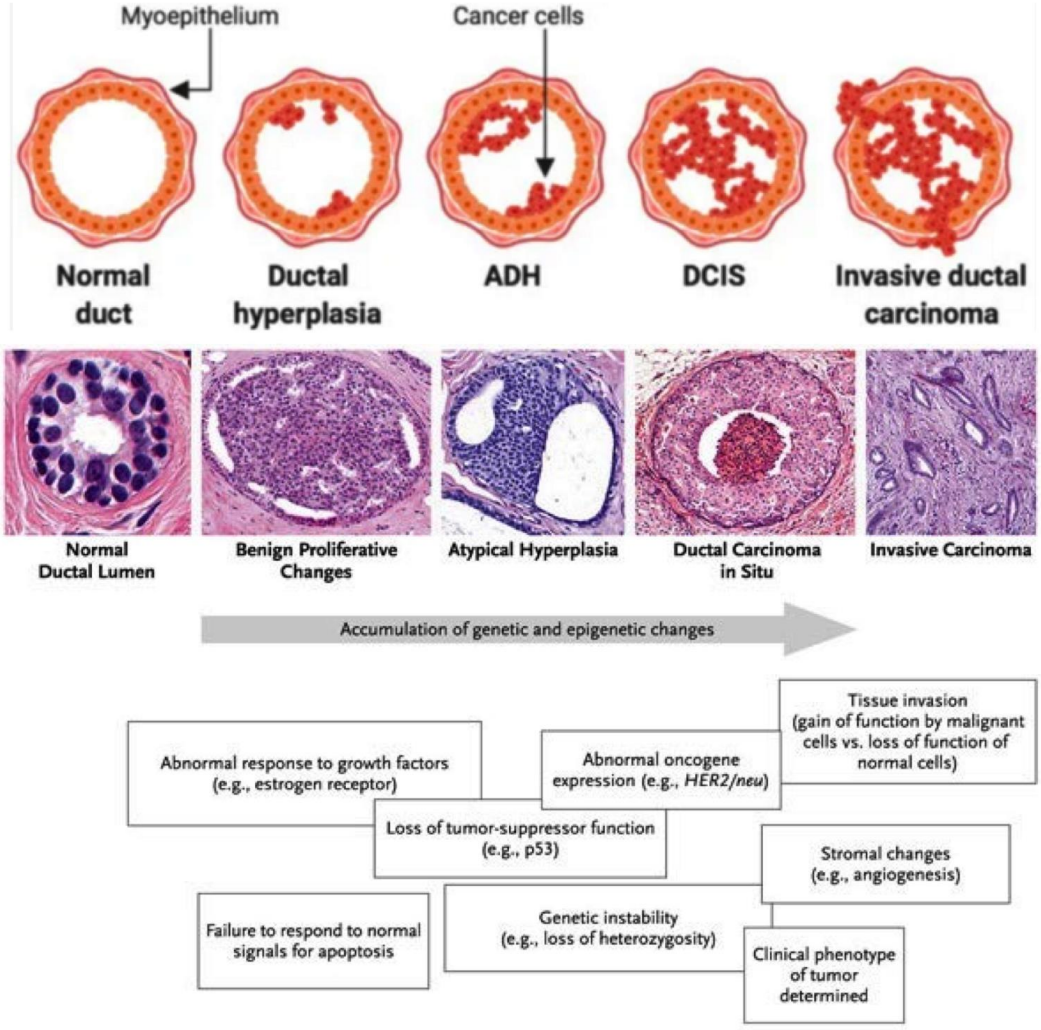

Figure 14. Stages of breast cancer progression. Expansion of tumour cells within the normal duct generates an atypical ductal hyperplasia (ADH) that gradually converges in the ductal carcinoma in situ (DCIS) characterized by the expansion of tumour cells in the mammary ducts. Escape of tumour cells from myoepithelium leds to invasive ductal carcinoma (Tower H, 2019) (Burstein H.J, 2004).

1.3.2) Breast cancer classification

Breast cancer is histologically classified based on the expression of estrogenic receptor (ER), progesterone receptor (PR) and the human epidermal growth factor receptor-2 (HER-2). Histological classification combined with gene expression profiling identified five distinct molecular subtypes: luminal A, luminal B, Her2 positive, normal-like and basal-like (Perou C, 2000). Genomic/transcriptomic analysis of breast cancer studies identified 10 further breast cancer subtypes, with distinct clinical outcomes (Curtis C, 2012).

Breast tumours that do not express ER, PR and HER-2 receptors, identified as triple negative BCs (TNBC), are the most aggressive and with a low overall survival (Molinero L, 2019) (Fig 15). Further characterization performed with molecular studies segregate TNBC in different subtypes (Lehmann B.D, 2011).

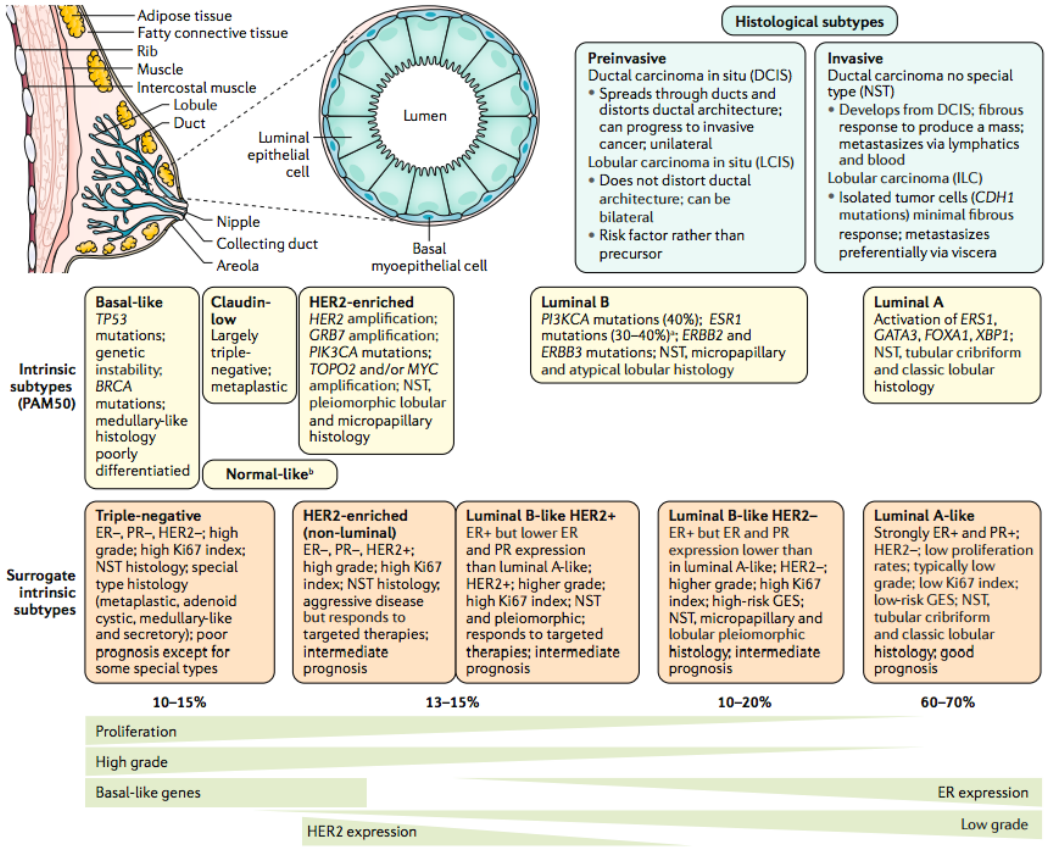

Figure 15. Breast cancer classification based on molecular and histological characteristics (Harbeck N, 2019). PAM50 is a BC classification, based on 50 genes, mostly including hormone receptors and proliferative genes.

Another parameter analysed in clinical practice is the grade: low, intermediate and high when the tumour appears respectively well differentiated, moderately differentiated and poorly differentiated (Elston C, 1991). Finally, the TNM classification, based on the size of the tumour (T), dissemination in the lymph nodes (N) and the presence of metastasis (M) is used to determine breast cancer staging.

1.4) Tumour microenvironment

The tumor microenvironment (TME) is composed by cells, soluble mediators, signaling molecules, extracellular matrix, and mechanical cues that contribute to malignant transformation, supporting tumour growth and metastasis but also protecting the tumour

from host immunity. The TME can also promote therapeutic resistance and provide niches for dormant stem cells (Swartz MA, 2012).

There are some key properties characterizing the TME such as its constant evolution, being the result of tissue remodeling and metabolic alterations occurring in tumour cells as well as of changes in the recruitment of stromal and immune cells, and its educatability.

The TME is composed by stromal cells of mesenchymal origin but also by adaptive and innate immune cells. The polarization of these cells toward a pro-tumoral phenotype might rely on different factors including hypoxia, miRNAs and soluble mediators such as COX-2, GM-CSF and IL-6. For example, hypoxia inducible factor 1α (HIF1α) and HIF2α affect immune cell polarization in the TME regulating inducible nitric oxide synthase (iNOS) and arginase 1 (ARG1) expression. In the presence of low IFN-γ, HIF-2α promotes a T helper 2 (T_H2) phenotype through the induction of Arg1 and the downregulation of NO production (Keith B, 2012).

The organization of the extracellular matrix (ECM), whose mechanical properties affect malignant cell differentiation and invasiveness, is another relevant characteristic of the TME. Increased stromal stiffness in breast tissue is correlated with breast cancer malignancy (Levental KR, 2009) (Butcher D.T, 2009). Mechanistically, tissue stiffness promotes activation of Rho/ROCK signalling pathway, which in turn induces collagen deposition through mechanisms linked to activation of Wnt/β- catenin signaling and expression of inflammatory cytokines, including CCL2 and GM-CSF, that promote the recruitment of BM-derived cells into the TME (Chaudhuri O, 2014).

These evidences have suggested that the ECM cannot be considered as only an inert scaffold, indeed it can regulate all the key properties enabling tumour cells transformation and metastatic progression (Pickup M.W, 2014). The relevance of the ECM in BC is supported by data showing the existence of ECM-related prognostic signatures able to discriminate patients with worse prognosis. Among them the ECM3 signature was able to discriminate grade 3 patients with the worse survival probability related to the acquisition of features such as stemness and epithelial-mesenchymal transition (EMT) (Bergamaschi A, 2008). Furthermore, data from the hosting laboratory have contributed in showing that the ECM3 actively contributes in defining the suppressive microenvironment of BC. Indeed collagens are able to regulate COX-2 production and in turn GM-CSF and IL-6, two key factors involved in the differentiation of tumour promoting myeloid cells (Sangaletti S, 2016).

Other ECM proteins can contribute to local immunoregulation. Indeed the matricellular secreted protein acidic rich in cysteine (SPARC) promotes T_H2-type polarization by regulating the activation of TGF-β1 and in turn modulating macrophage production of TNF-α. In the absence of SPARC, macrophages did not down-modulate TNF-α in response to TGF-β1, fostering inflammation (Sangaletti S, 2011). Finally by regulating the nuclear translocation of p50/p65, SPARC has been shown to be involved in the acquisition of suppressive properties in myeloid cells (Sangaletti S, 2019).

A key responsible of ECM remodelling in the TME are cancer-associated fibroblasts (CAFs) that can favour ECM remodelling, inflammation and reduce anti-tumour immunity (Costa, 2018). Vascular cells, not only favour angiogenesis in the TME but also contribute to tumour growth providing nutrients and oxygen (Schaaf MB, 2018), and facilitate cancer cell dissemination and metastasis seeding (Bergers G, 2003).

1.4.1) Innate immune cells in the TME: tumour-associated myeloid cells

Two types of myeloid cell subsets actively participate and modify the TME: tumor-associated macrophages (TAMs) and the so-called myeloid derived suppressor cells (MDSCs) (Fig 16). Both cells play different roles during many stages of disease: starting with hyperplasia and dysplasia phases, in situ cancer, ultimately leading to tumour growth and metastatic dissemination.

The presence of myeloid cells in the TME is associated with the clinical stage, poor prognosis and worse overall survival (Zhang Q, 2012) (Diaz-Montero C.M, 2009) (Bergenfelz C, 2015).

Furthermore, tumour-associated myeloid cells contribute to therapeutic resistance by immune and/or non-immune mechanisms; thus different preclinical studies are ongoing to inhibit their recruitment and/or to reprogram their activity (Ahn GO, 2010) (Zhang W, 2018).

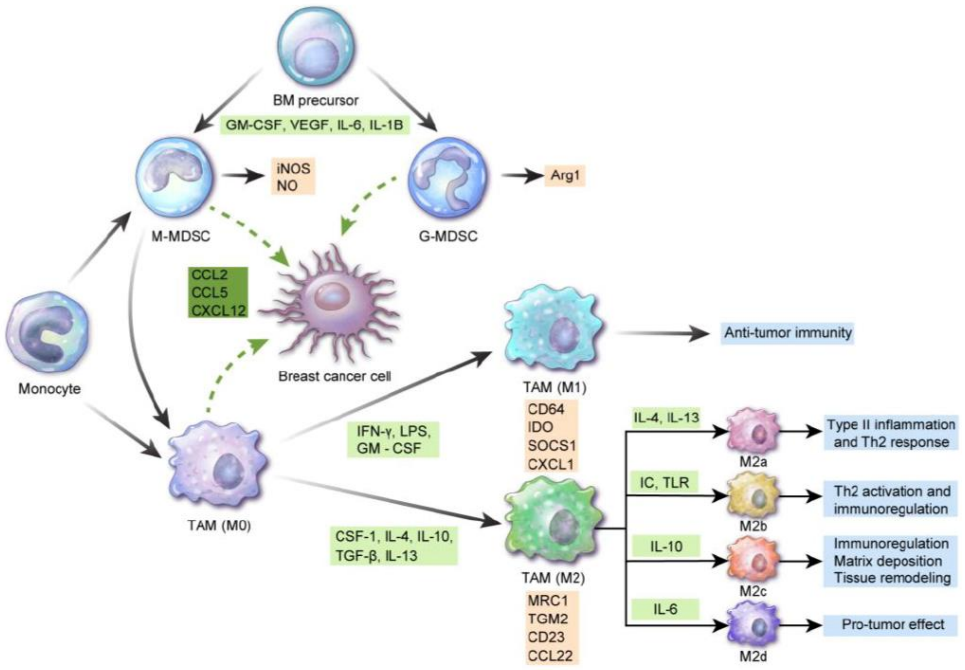

Figure 16. Origin and activity of tumour-associated myeloid cells. Adapted from Cha YJ, 2020.

1.4.2) Origin and function of tumour-associated macrophages

Based on their origin, macrophages infiltrating the TME can be subdivided into tissue-resident macrophages or BM- derived macrophages (Lahmar Q, 2016).

Tissue resident macrophages derive from the primitive yolk sac whereas those from the BM are differentiated from circulating monocytes (human $CD14^{+}CD16^{-}$, mouse $CD11b^{+}Ly6C^{+}$). In mice, the $Ly6C^{hi}CX_3CR1^{low}$ pool represents the main tumor-infiltrating monocyte subset that replenishes non proliferating TAMs (Movahedi K, 2010).

Macrophages are plastic cells that according to the microenvironmental stimuli could be directed towards different states of activation, a functional heterogeneity that can be intercepted through omic approaches such single-cell RNA sequencing (scRNAseq). As an example Zilionis et al. in the context of lung cancer have shown that macrophages can exist in almost 9 subtypes that cannot be ascribed to one of the "classic M1" or "alternative M2" classification, rather they represent a continuum different state of activation (Zilionis R, 2019). Nevertheless we can assume that TAMs have basically an M2-like MHC-II^{low} phenotype, which is induced by tumour hypoxia (Sica A, 2006) (Lewis C, 2005) (Laoui D, 2014).

The M1-macrophages are the classically inflammatory macrophages that are activated by IFN-γ and TNF released by type 1 T helper cells (T_h1). M1 macrophages, expressing

high levels of CD86 costimulatory molecules, major histocompatibility complex class II (MHCII) and CD40 on the membrane surface, have cytotoxic function and exhibit antitumor activity (Pan PY, 2010).

In contrast, M2-like macrophages are induced by IL-4, IL-13 and IL-10, released by the type 2 T helper cells (T_h2) and express CD206 and CD163 markers on their membrane surface. The alternatively activated M2 macrophages also express high levels of resistin-like molecule α (FIZZ1) and chitinase-like protein (Ym1) (Raes G, 2002).

The scavenger receptors, that mediate the phagocytic activity of macrophages, also contribute to the characterization of polarized macrophages (CD36 in M1 and SR-A1 and CD163 in M2 macrophages) (Canton J, 2013).

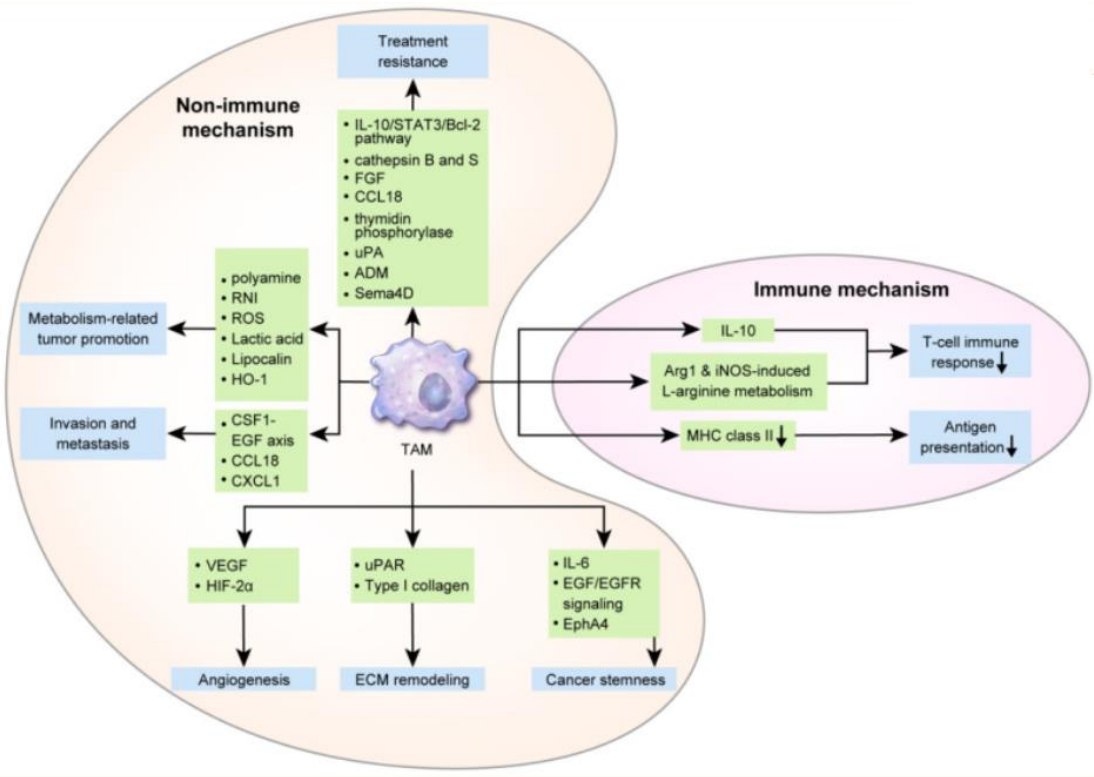

Figure 17. Activity of TAMs in the TME (Cha YJ, 2020).

Activated M1 macrophages release pro-inflammatory molecules, such as Nos2, TNF-α, IL-6, IL-12 (Biswas SK, 2010) (Martinez FO, 2014). In response to signals from breast cancer cell lines, M1-macrophages are educated toward the M2-activation states and could promote CD8+ T cell dysfunction, degradation of extracellular matrix composition and angiogenesis (Sousa S, 2015).

M2-like macrophages, through the production of IL-10, TGF-β, ARG1 and prostaglandins actively contribute to generate an immune suppressive TME (Quatromoni JG, 2012). Secretion of IL-10 suppresses CD8+ T cell activation (Ruffell

B, 2014), production of ARG1 inhibits effector T-cells (Rodriguez PC, 2004).
Furthermore, the release of chemokines from M2 macrophages, such as CCL22, favours T reg recruitment (Curiel TJ, 2004) and the production of matrix metalloproteinases (MMPs), vascular endothelial growth factor (VEGF), CCL18, epidermal growth factors (EGF) and IL-10 induces ECM disruption and local invasion (Martinez FO, 2006) (Mantovani A, 2002) (Fig 17).
Tumour hypoxia up-regulates the production of VEGF and HIF-2α in TAMs, those in turn provide multiple nutrients to cancer cells (Laoui D, 2014), induce the angiogenic switch in the TME, through the production of pro-angiogenic factors (ADM, VEGF, PDGF, MMP and TGF-β), and promote the release of reactive nitrogen intermediates and ROS (Lewis JS, 2000) (Leek RD, 2002).
TAMs are also able to induce EMT in pre-malignant lesions, which is characterized by loss of cell-cell contact and transition of epithelial cells from epithelial to mesenchymal phenotype, thereby leading to early cancer dissemination and pre-metastatic niche at distant sites (Linde N, 2018).

1.4.3) Activity of myeloid-derived suppressor cells

MDSCs are immature myeloid cells originating from BM myeloid precursors. They can be subdivided in two subsets: monocytic- (M-MDSC) and granulocytic-MDSCs (G/PMN-MDSC).
In mice, PMN and M-MDSCs are defined within the CD11b gate as $Ly6G^{+}Ly6C^{low}$ and $Ly6G^{-}Ly6C^{high}$ cells, respectively (Youn JI, 2008) (Movahedi K, 2008).
In human besides PMN- ($CD14^{-}$, $CD11b^{+}$, $CD15^{+}$) and M-MDSC ($CD11b^{+}$, $CD14^{+}$, $HLA\text{-}DR^{low/-}$, $CD15^{-}$) subsets a further population called early-stage MDSC (e-MDSC) was identified. This population of Lin^{-} $HLA\text{-}DR^{-}CD33^{+}$ cells contain a mixed group of MDSCs comprising more immature progenitor (Bronte V, 2015).
It is important to highlight that beside evaluating phenotypic markers, functional assay testing MDSC suppressive activity is mandatory to clearly define a polulation as MDSCs, being their biochemical and molecular characteristic very similar to those of neutrophils and monocytes (Bruger A.M, 2018).

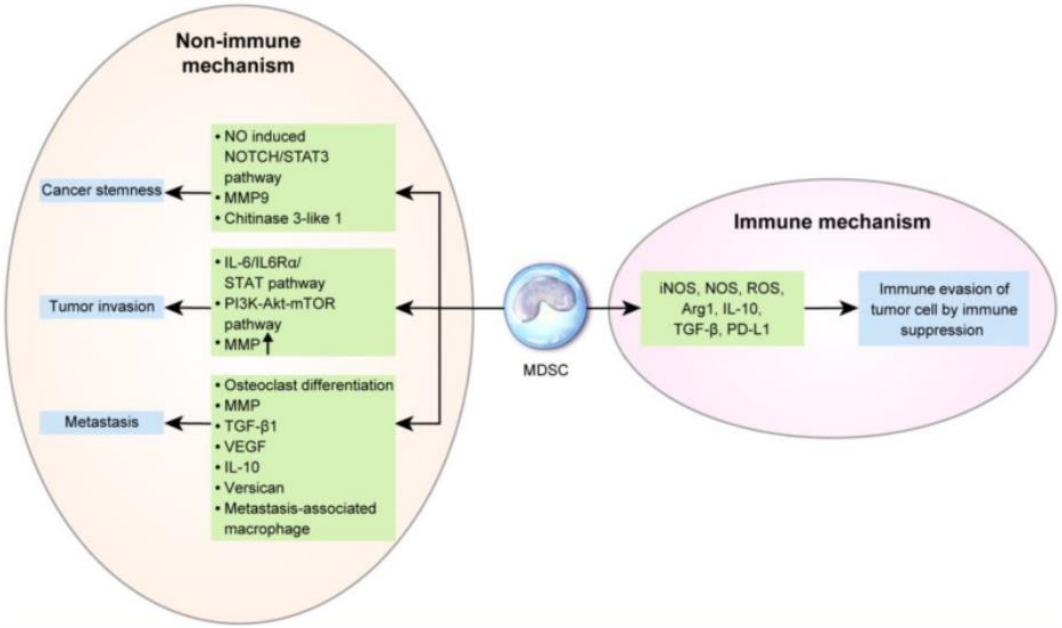

Figure 18. Activity of MDSCs in the TME (Cha YJ, 2020).

Mechanistically, M-MDSCs suppress T-cell through the release of NO, whereas PMN-MDSCs exert its suppressive activity through the production of reactive oxygen species (ROS) and ARG1 (Fig 18). Moreover the secretion of IL-10 and TGF-β by MDSCs influences the activity of regulatory T-cells and reduces the cytotoxicity of NK cells (Koike Y, 2012) (Li H, 2009) (Mao Y, 2014).

Different ratio of M-MDSC and PMN-MDSC is strictly related to the characteristic of the TME and to the inflammatory cytokines (G-CSF, M-CSF, GM-CSF, IL-1β) and chemokines (CXCL-5, CXCL-12, CCL1, CCL2 and CCL5) released in the tumour sites. Most cancers display more M-MDSCs (Haverkamp J.M, 2011). Breast cancer shows a higher proportion of PMN than M-MDSC subpopulation (Messmer MN, 2015).

1.4.4) Recruitment of myeloid cells into tumours

Emergency BM- and extramedullary myelopoiesis contribute to accumulation of circulating myeloid cells. Peripheral blood myeloid cells are then recruited into tumour tissue through specific factors (CXCL12, CCL2, CSF1, CXCL8) that attract different type of immune cells, according to their different expression of chemokine receptors. Finally, tumour-derived signals and microenvironmental conditions, such as immunosuppressive molecules (IL-10, TGF-β) and hypoxia determine their functional reprogramming (Bolli E, 2017) (Kiss M, 2018) (DeNardo DG, 2019) (Fig 19).

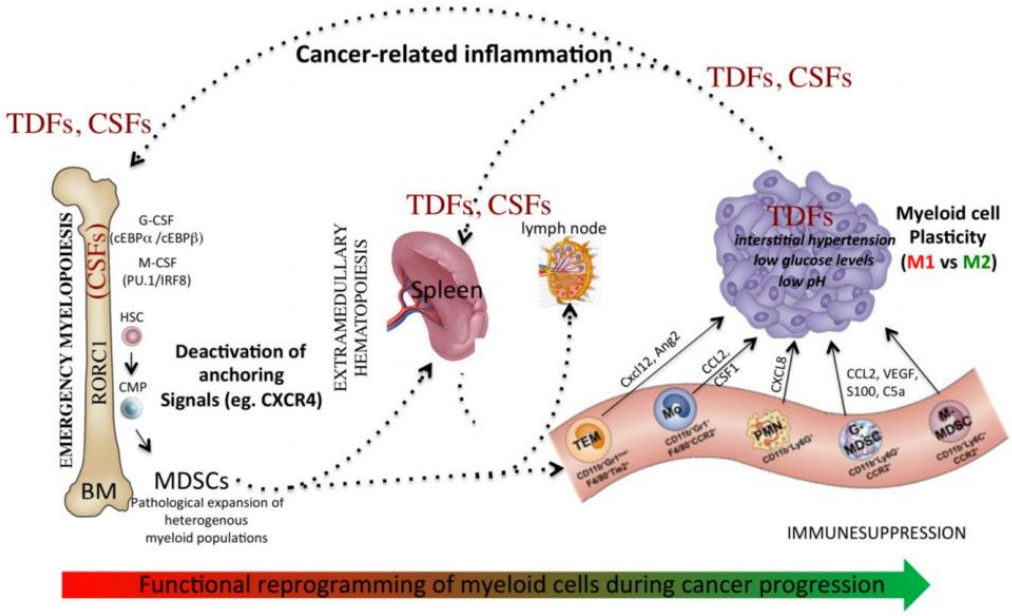

Figure 19. Myeloid cell reprogramming starts in the BM and ultimately leads to a release of circulating myeloid cells in the peripheral blood. RORC1 is a key TF that drives emergency myelopiesis. TFD- tumour-derived factors, CSF – colony-stimulating factor, TEM- TIE2-expressing monocytes (Sica A. 2019).

In detail monocytes are attracted in the TME by colony stimulating factor 1 (CSF1), C-C motif chemokine ligand 2 (CCL2), IL-6, VEGF-A and platelet-derived growth factor (PDGF). Hypoxic tumour-environment and Angiopoietin-2 (Ang-2) are also able to induce the recruitment of monocytes expressing high levels of tyrosine-protein kinase receptor Tie-2 (Murdoch et al, 2007).

In mice $Ly6C^{high}$ inflammatory monocytes express high levels of the CC-chemokine receptor 2 (CCR2) and are rapidly attracted into the inflamed tissues and tumours (Kurihara T, 1997) (Kuziel WA, 1997). Differently, the $Ly6C^{low}$ counterpart expresses high levels of CX_3C-chemokine receptor 1 (CX_3CR1) (Palframan RT, 2001). This subset patrols blood vessels and joins to non-inflamed tissue (Geissmann F, 2003).

G-MDSCs are attracted in the tumour sites primarily by CCL3, CCL4 and CCL5 chemokines (Hawila E, 2017). M-MDSC are recruited though CCL2/CCR2 signaling axis (Qian BZ, 2011) (Serbina NV, 2006).

The number of myeloid cells in the blood, reflecting the abundance of tumour-infiltrating macrophages, could be a predictive factor of disease progression and correlates with worse prognosis (Hayashi T, 2017).

Recently, transcriptional alterations of circulating myeloid cells have been detected in the peripheral blood of cancer patients, suggesting that gene expression changes could be used as diagnostic biomarker, also in patients with localized early stages of disease

(Cassetta L, 2019) (Ramos RN, 2020) (Hamm A, 2016) (Kiss M, 2020) (Chittezhath M, 2014).

1.4.5) Adaptive immune cells in the TME

Characterization of tumour-infiltrating lymphocytes (TILs) during different stages of cancer progression has been shown to have prognostic value in patients with solid tumours.

In breast cancer TILs are mainly rapresented by CD8+ T cells and by a low number of CD4+T cells.

CD8+ T cells, activated in response to immune surveillance mechanisms, kill cancer cells expressing the major histocompatibility complex (MHC) class I molecules (Bui JD, 2007). Expression of co-stimulatory receptors (ICOS, OX40 CD40L, CD28) on CD8+ T cells is a clear characteristic of T cell activation state. This process is articulated in two phases: priming and effector (Fig 20).

During the first step dendritic (DCs), natural killer (NK) and $CD4^+$ T cells provide stimuli for $CD8^+$ T cell priming (Spranger S, 2018) (Borst J, 2018).

In the second stages, activated $CD8^+$ T cells, namely cytotoxic T cells (CTLs), release IFN-γ and TNF-α or induce granule exocytosis and/or FasL/TRAIL ligand-mediated apoptosis pathways to destroy their tumour target cells (Thomas DA, 2005). In general, infiltrating T cells show a type I interferon transcriptional signature indicative of their activation state.

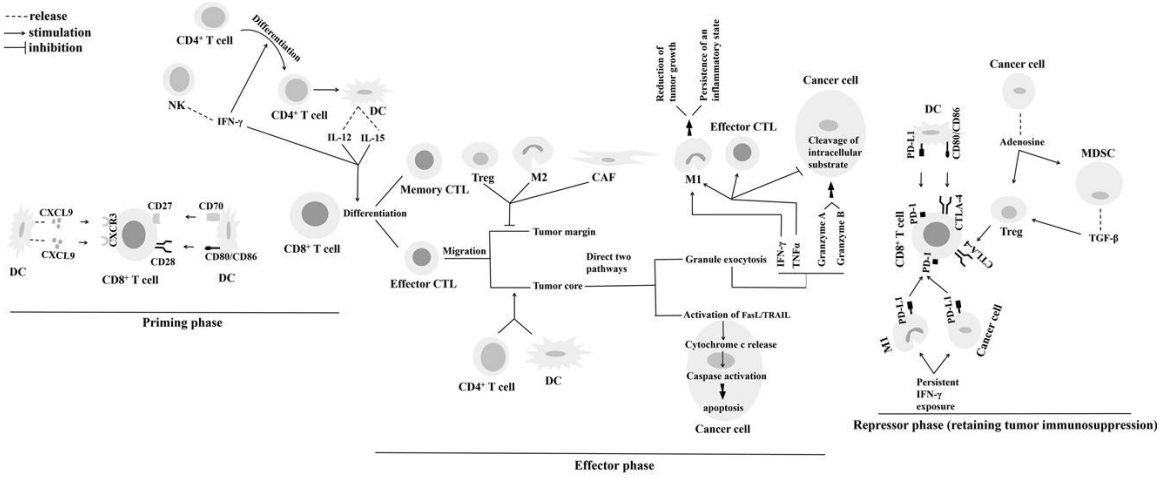

Figure 20. Sequence of events generated during CD8+ T cells activation-deactivation in the TME (Farhood B, 2019).

Chronic activation of T cells in the TME led to T cell exhaustion and expression of co-inhibitory receptors on membrane surfaces (CTLA-4, PD-1, TIGIT, LAG3, TIM3).

Furthermore, functions of effector T cells could be inhibited during the repressor phase by the immunosuppressive microenvironment generated by tumour cells, CAFs, regulatory T cells (T_{regs}) and MDSCs.
Generally, T cell infiltrate in the TME of solid tumour positively correlates with good prognosis (Mahmoud SM, 2011) Rusakiewicz S, 2013).

1.5) Mouse models of breast cancer: a useful tool to study breast cancer progression

Although animal models reflect only in part the complex landscape of human diseases, they certainly represent a useful tool to dissect the different phases of tumour progression and the crosstalk generated with local tissue and systemic organs. Furthermore, they are invaluable tools to test novel therapeutic approaches in a pre-clinical setting. In this context the use of patient-derived xenograft (PDX) models, in which human tumour tissues are implanted heterotopically (subcutaneously) or orthotopically (into mammary fat pad), further accelerate the translatability of oncology research, although in this case, the lack of a functional adaptive immune system precludes their use in immunological studies.
Different types of mouse models are available to study distinct tumour types (Byrne A.T, 2017) (Zitvogel L, 2016) (Le Magnen C, 2016) (Kersten K, 2017) (Day C.P, 2015).
Syngeneic mice models are the most common tools used in basic and pre-clinical cancer research (Gengenbacher N, 2017). Syngeneic models allow to studying the role of the immune system during tumour progression. In these mice tumour cells can be injected by different routes, such as orthotopically or systemically. Orthotopically injection is employed to better mimic tumour growth in its organ of origin. For example, PyMT41c tumour cell line, which originally derives from the MMTV-PyMT (mouse mammary tumour virus-polyoma middle tumour-antigen) mouse model of breast cancer, grows rapidly when injected into the mammary fat pad of a syngeneic mouse (Majorini M.T, 2020).
Systemically injection (intravenously or intraperitoneally) of tumour cell lines is often adopted to study the metastatic spread.

1.5.1) MMTV-HER2/NeuT mice, a genetically engineered mouse model

Genetically engineered mouse (GEM) model, the second most common type of mouse used in oncology research, represent an invaluable source for studying tumour establishment and progression. These models have genetic alteration in one or several genes involved in malignant transformation.

Tissue-specific expression of an oncogen drives tumour initiation and progression within a fairly defined time window, allowing sampling and analysis of different stages of disease. Several promoters have been used to induce the expression of the transgenes in the mammary fat pad, such as polyoma middle T antigen (PyMT) and simian virus 40 (SV40) T antigen.

MMTV-NeuT and MMTV-PyMT are both examples of transgenic mice in which the MMTV promoter drives the expression of the rat HER2 oncogene in the mammary epithelium with 100% of penetrance.

In the MMTV-HER2/NeuT transgenic model of luminal B breast carcinoma, the overexpression of the activated rat HER2/neu oncogene transduces proliferative signals in the mammary epithelium. HER2, also known as ErbB2 or Neu in rat, is a member of the transmembrane epidermal growth factor receptor (EGFR) family, composed by an extracellular ligand-binding domain and a cytoplasmic domain with tyrosine kinase activity (Yarden Y, 2001). The binding of the extracellular region of the EGFR receptor or the interaction with other Erb2 receptors induces the activation of HER signaling pathways (Garrett T.P, 2003). Activation of the RAS-RAF-MEK-MAPK pathways and PI3K/Akt signaling induces cell proliferation and survival, respectively (Wieduwilt M.J, 2008)

HER2, a well-known oncogene, is amplified in about 20-30% of primary breast cancer patients (Slamon D.J, 1987) (Paik S, 1990) (Pauletti G, 1996), but its overexpression is associated also with ovarian, lung and colon cancers (Niehans G.A, 1993) (Neve R.M, 2001).

The MMTV-HER2/NeuT mouse model allows studying all the key phases of tumour development as its progression recapitulates the hyperplasia/dysplasia, carcinoma in situ, invasive carcinoma and metastasis stages found in human breast cancer (Muller W, 1988) (Lucchini F, 1992).

Immunohistochemical characterization of the mammary glands in the NeuT mice model indicates that epithelial cells start to proliferate at 3-5 weeks of age generating a hyperplastic condition. At around 15 weeks of age the transition from hyperplasia to

carcinoma in situ occurs and at 20 weeks mammary glands display palpable tumours and multifocal lesions (Quaglino E, 2008). At 24 weeks of age neoplastic cells infiltrate the myoepithelium and the surrounding adipose tissue. Metastatic spread in the lung could occur in this model (Muller W, 1988), although rarely (Fig 21).

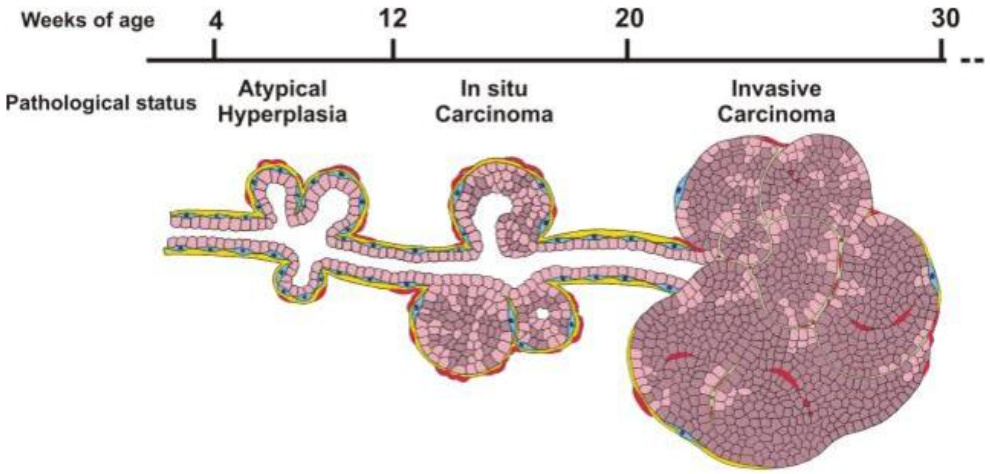

Figure 21. Representative time course of mammary tumour development in MMTV-HER2/NeuT female mice. (Iezzi M, Bentham Sci. Publ. Transl. Anim. Models Drug Discov. Dev, 2012).

MMTV-NeuT mouse model was used in the hosting laboratory to study emergency haematopoiesis along tumour development (Chiodoni C, 2020) (Melani C, 2003) (Melani C, 2007), as well as the role of different molecules such as CD40 and SPARC during transformations (Chiodoni C, 2006) (Sangaletti S, 2003).

1.5.2) Cre-lox tissue specific knockout mice

Oncogene-bearing transgenic mice or tumour-suppressor knockout mice provide useful informations regarding the role of key genes and their mutation during cancer progression.

Nevertheless, some gene mutations in the germ line led to early embryonic lethality in the specific GEM models (Papaionnou VE, 2012).

To fill this gap, other strategies were employed in the second generation of GEM models, based on inducible gene targeting (Sauer B, 1998), control of the oncogene expression (Berns A, 1999) and specific gene delivery (Fisher G.H, 1999).

Site-specific recombinase systems, such as Cre-loxP are used to generate conditional knockout mice. This tool allows to studying the role of a gene of interest in a specific tissue/cell type and/or during an established temporal frame.

Cre recombinase is a tyrosine site-specific enzyme, derived from the P1 bacteriophage, which recognizes a specific sequence of DNA, called *lox*P site (Sternberg N, 1978) (Sternberg N, 1981) (Nagy A, 2020). The *loxP* site is a 34 bp sequence: the core sequence contains 8 bp and at both extremities an inverted and palindromic sequences of 13 bp is present. The binding of Cre enzyme on the recognized regions mediates the specific excision and deletion of DNA between two *lox*P sites (Sauer B, 1998) (Fig 22A).

This system is used in particular to inactivate a pre-selected gene, but it is also able to generate the inversion or the translocation of a region of interest between two *lox*P sites (Meinke G, 2016) (Branda CS, 2004).

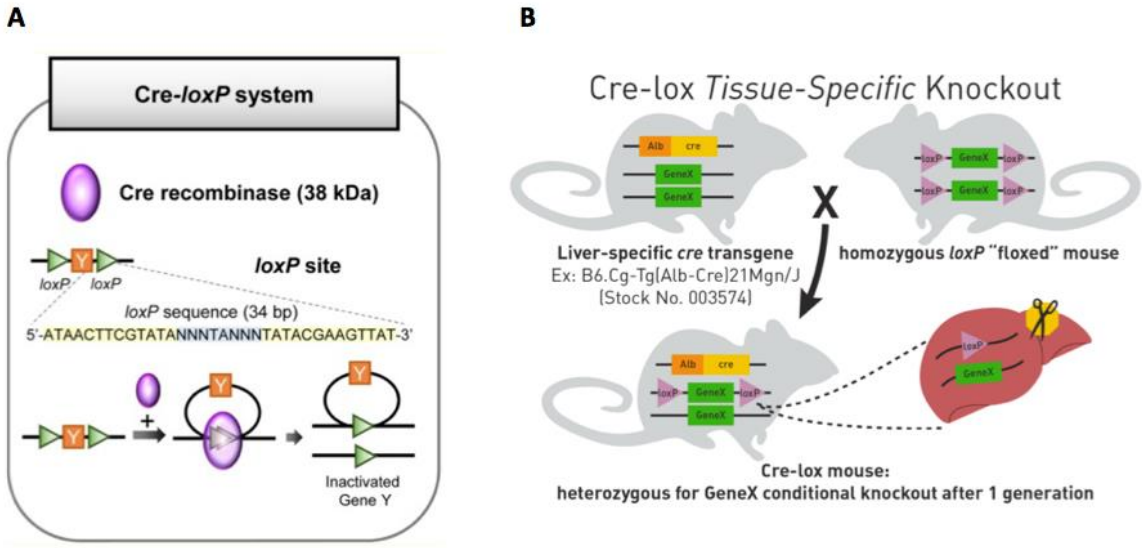

Figure 22. Inducible gene targeting in mice using the Cre/lox system. A) Mechanism of Cre-loxP system: Cre recombinase recognizes two loxP sites and creates a circular, excised and inactivate sequence of the target gene. Adapted from Kim H, 2018. B) General breeding strategy adopted to generate Cre-lox Tissue specific knockout mice. The Jackson Laboratory.

A specific promoter/enhancer drives the Cre-*lox*P system in a tissue/cell of interest. Various tissue-specific promoters have been developed to study the role of selected genes in different organs and cells: as examples, Alb for the liver (Yakar S, 1999), Aqp2 for the kidney (Ge Y, 2005), Lyz2 for macrophages (Clausen B.E, 1999), CD11c for dendritic cells (Caton M.L, 2007) and Col1a1 for osteoblasts (Kim J.E, 2004).

To generate conditional knockout mice, initially one mouse is genetically modified in order to obtain two floxed sequences in the gene of interest. Then, is necessary the generation of another mouse, carrying the Cre recombinase enzyme under a tissue specific promoter and/or enhancer. The breeding between the Cre-driver strain and the floxed mouse strain generates the tissue-specific conditional knockout mice (Fig 22B).

2) MATERIALS AND METHODS

2.1) Animal studies

We take advantage of three different mouse strains. The first is the MMTV-NeuT (NeuT, BALB/c background) mouse model of mammary carcinoma, in which we originally identified *Atf3* among the top genes modulated in the bone marrow (BM). BALB-NeuT female mice, carrying the oncogene c-erbB2 (Her-2/neu) under the mouse mammary tumor virus (MMTV) promoter, naturally develop mammary carcinoma with a clear-cut tumour progression well defined during a specific time frame (Lucchini, 1992) (Boggio, 1998). The 6, 12 and 24 weeks of age in these mice are representative respectively of pre-malignant, pre-invasive and invasive stages of mammary transformation (Chiodoni, 2020).

NeuT positive female mice were identified for the presence of NeuT transgene by polymerase chain reaction (PCR). Aged-matched controls BALB/c mice (non-transgenic littermates) were used as wild type (WT) counterparts.

Experiments performed in BALB-NeuT mice were further validated in C57BL/6 mice. Tumour cell lines generated in the hosting laboratory from MMTV-PyMT mice (PyMT41c) was used as transplantable model to be injected *in vivo* into syngeneic C57BL/6 mice ($1*10^6$ cells).

The third mouse model used for animal studies is the $Atf3^{fl/fl}LysMCre^{+/-}$ mice (C57BL/6 background), carrying a specific deletion of the ATF3 in the myeloid compartment. To generate tissue-specific ATF3-knockout mice, homozygous Atf3 floxed mice ($Atf3^{fl/fl}$ mice) were crossed with a LySMCre mouse strain. The progeny, mice heterozygous for the Atf3 allele and heterozygous for the Cre transgene ($Atf3^{fl/-}LySMCre^{+/-}$) were cross again with mice homozygous for the Atf3 floxed allele ($Atf3^{fl/fl}$ mice). The offspring, homozygous for the Atf3 floxed allele and heterozygous for the LySMCre transgene ($Atf3^{fl/fl}LySMCre^{+/-}$) were used as experimental mice. The progeny homozygous for the Atf3 floxed allele but without Cre transgene ($Atf3^{fl/fl}LySMCre^{-/-}$) were used as controls.

Being $Atf3^{fl/fl}LysMCre^{+/-}$ mice on a C57BL/6 background, PyMT41c tumour cell line was injected in the mammary fat pad of these mice ($1*10^6$ cells).

Primary tumour growth was monitored twice a week with a caliper and the volume was calculated with the following formula: $(Widght^2 \times Length)/2$.

Experiments with chronic LPS administration were performed in female BALB/c mice, purchased from Charles River Laboratories. Mice were injected intraperitoneally (i.p.) with 10ug of lipopolysaccharide (LPS) (O111:B4, Sigma Aldrich) or phosphate-buffered saline (PBS), three times per week for four weeks (chronically administration) and sacrificed the day after the last treatment.

All mice were stored under germ-free and pathogen-free conditions and maintained in a filter top cage system at the animal facility of Fondazione IRCCS Istituto Nazionale dei Tumori, Milan, Italy. All animal studies and technical procedures, executed in accordance with National Law (D.Lgs 26/2014), were approved by the Institutional Committee for Animal Welfare and by the Italian Ministry of Health.

2.2) Sample collections

Hind legs of laboratory mice were collected to analyze the BM: femurs were used to perform immunohistochemistry (IHC) and immunofluorescence (IF) analyses; tibias were used to obtain BM fresh cells for Flow Cytometry (FC) and Fluorescence-Activated Cell Sorting (FACS) analyses. Briefly, skin and muscle tissues were removed from the legs, nippers were used to cut both bone extremities and cells were obtained by flushing the marrow cavity with PBS-1X, using a 22-gauge needle attached to a 1-mL syringe.

Whole mounts of mice were collected for mammary gland histology (H&E). For FC analysis on mammary tumors, primary lesions were collected, minced and filtered through a 40um-pores cell strainer to obtain a single-cell suspension.

Organs used for IHC staining were fixed after surgical removal with 10% neutral buffered formalin overnight, washed twice in water and then paraffin embedded. For IHC staining bones were decalcified.

Blood was collected from mice by intracardiac puncture with 20µl of EDTA (0.5mol/L pH 8) and used for FC analysis. For serum separation, blood was collected from the retro-orbital sinus, maintained at 37°C for 30 min and at 4°C for 1 hour before centrifugation (13.000 rpm per 1 min at 4° C).

2.3) Evaluation of disease in tumour-bearing mice

Disease score at early time points was calculated on H&E-stained sections using a DMD-108 digital microscope (Leica, Germany).

The disease was obtained considering the following variable: extension (focal, 1; multifocal, 2; diffuse, 3) and severity (mild, 1; moderate, 2; severe, 3) of hyperplasia, dysplasia, in situ carcinoma and stromal reaction (peri-ductal inflammatory infiltrate and adipose tissue inflammation).

To obtain the disease score, each variable analysed to evaluate mammary lesions in individual mice were weighted, as percentage of 100 and scored as follows:

- Hyperplasia (2,5% extension and 2,5% severity), total 5%;
- Dysplasia (10% extension and 15% severity), total 25%;
- Carcinoma (10% extension and 25% severity), total 35%;
- Stromal remodelling (10% extension and 5% severity), total 15%;
- Periductal inflammatory 10%;
- Adipose tissue inflammation 10%.

The sum of each variable identifies the weighted score, shown in the table below.

Weighted values		2.50%	2.50%	10%	15%	10%	25%	10%	5%	10%	10%	
ID	Sample	Hyperplasia (severity)	Hyperplasia (extension)	Periductal inflammatory infiltrate	Dysplasia (severity)	Dysplasia (extension)	Carcinoma (severity)	Carcinoma (extension)	Stromal reaction (severity)	Stromal reaction (extension)	Phlogosis of adipose tissue	score
AM27	NeuT 12 weeks	0.05	0.075	0.3	0.45	0.3	0.75	0.2	0.1	0.2	0	**2.425**
AM28	NeuT 12 weeks	0.05	0.075	0.1	0.45	0.3	0.75	0.1	0.1	0.2	0.1	**2.225**
AM29	NeuT 12 weeks	0.05	0.075	0.1	0.45	0.3	0.25	0.2	0.1	0.2	0	**1.725**
AO31	NeuT 12 weeks	0.05	0.075	0.1	0.45	0.2	0.5	0.2	0.05	0.2	0	**1.825**
AO32	NeuT 12 weeks	0.05	0.075	0.1	0.45	0.2	0.5	0.2	0.1	0.2	0	**1.875**
AO33	NeuT 12 weeks	0.05	0.075	0.1	0.45	0.3	0.75	0.2	0.1	0.2	0	**2.225**
AO34	NeuT 12 weeks	0.05	0.05	0.2	0.45	0.2	0	0	0.1	0.2	0	**1.25**
AM65	NeuT 12 weeks	0.075	0.05	0.2	0.45	0.2	0.25	0.2	0.05	0.2	0	**1.675**
AM66	NeuT 12 weeks	0.075	0.05	0.2	0.45	0.2	0.25	0.1	0.05	0.1	0.1	**1.575**
AM67	NeuT 12 weeks	0.075	0.05	0.3	0.45	0.2	0.25	0.2	0.1	0.2	0	**1.825**

2.4) Flow cytometry and cell sorting

Single-cell suspensions were treated with ammonium chloride potassium (ACK) lysis buffer (150 mM NH4Cl, 10mM KHCO3, 0.1 mM EDTA in sterile H_2O) to remove red blood cells. Fc-blocked solution (eBioscience) was used to avoid unspecific ligation of conjugated antibodies. After that, cells were incubated with specific antibodies at (5ug/mL) and acquired using a BD LSRFortessa™ Flow Cytometer (BD Biosciences). Analyses were performed with FlowJo software (version 10.4.2).

Progenitors and myeloid cells were sorted by FACS from the BM using a FACSAria BD instrument. At least 3 mice per group were sacrificed in each experiment.

The following monoclonal antibodies, purchased from eBiosciences, BD Biosciences and BioLegend were used:

Fluorescence	Antigen	Clone
PE	CD45	30F11
PE	CD11b	M170
PE	CD3	I45-2C11
PE	CD11c	M418
PE	B220	RA3-6B2
PE	Gr1	RB6-8C5
PE	F4/80	BM8.1
PE	Ter119	TER119
APC	c-Kit	ACK2
Pe-Cy7	CD16/32	93
FITC	CD34	RAM34
BB700	CD11b	M1/70
FITC	B220	RA36/32
PE	Ly6G	1A8
APC	Ly6C	HK1.4
FITC	CD45	30-F-11
FITC	Ter119	TER119
FITC	CD31	390
PerCp-Cy5.5	CD44	IM7
PE-Cy7	CD29	eBioHMb1-1
APC	Sca1	D7
PE	c-Kit	2B8
PE	Ly6G	1A8
BV421	Ly6C	AL21
APC	Gr1	RB6.8C5

2.5) Cell cultures

Mouse breast cancer cell lines (PyMT41c and 4T1) and 293T Human embryonic kidney cell line were maintained in DMEM (Gibco®), supplemented with 10% fetal bovine serum (FBS), 2mM L-glutamine, Hepes, sodium pyruvate (NaPyr) and non-essential amino acids (NAAA). The PyMT41c was generated and characterized in the hosting laboratory from spontaneous tumours collected from MMTV-PyMT mice (C57BL/6 background) (Majorini M.T, 2020). 4T1 and 293T cell lines were purchased from the American Type Culture Collection (ATCC).

All cell lines were cultured in humidified incubators at 37°C with 5% of CO_2.

2.6) Isolation of hematopoietic stem cells from the bone marrow

Hematopoietic stem cells (HSCs) were isolated from the BM of mice by immunomagnetic beads (Lineage cell depletion kit, Miltenyi Biotec). After separation,

purity of cells was checked by FC analysis. Cell suspension was expanded in StemSpan SFEM medium (STEM CELL Technologies) supplemented with SCF (50ng/mL), TPO (15ng/ml), IL-3 (30ng/mL), Flt3 ligand (50ng/mL) and IL-6 (20ng/mL).

For HSCs stimulation and co-culture experiment, cells were seeded at a density of $1*10^5$cells/cm^2.

2.7) Lentivirus production and infection of hematopoietic stem cells

Progenitor cells were infected with two ATF3-encoding lentiviral vectors. The first was the pLVX-EF1α-ATF3-IRES-ZsGreen in which ATF3 expression is under the constitutively active human elongation factor 1 α (EF1α) promoter and carrying the ZsGreen fluorescent protein as reporter. The second is a myeloid specific lentiviral vector, pRRL.CD68.ATF3.WPRE.PGK.hNGFR, in which the CD68 specific myeloid promoter drives ATF3 sequence and the hNGFR reporter is under the PGK promoter.

pLVX-EF1α-IRES-ZsGreen and pRRL.CD68GFP.WPRE.PGK.hNGFR were used as controls.

Lentiviral vectors were obtained by cloning the ATF3 sequence (from pUC57-Atf3 plasmid, from DBA Italia) into the two-lentiviral backbones (pLVX-EF1α-IRES-ZsGreen and pRRL.CD68GFP.WPRE.PGK.hNGFR).

Viral stocks were produced in 293T cells by Ca_3PO_4 transfection of four plasmids: two packaging plasmids (pMDLg/pRRE and pRRSV-REV), an envelope plasmid (pMD2-VSV-G) and the DNA of the lentiviral vectors of interest.

The supernatants of 293T containing viral particles were collected 16-18 hours post transfection. Supernatants were purified with Corning®bottle-top vacuum filters with a pore size of 0.45μm (Sigma-Aldrich) and ultra-centrifuged at 13.000 rpm at 4°C for 2 hours (De Palma M, 2002). Purified viral particles were stored at -80°C.

Viral titre was checked by FACS analysis on 293T cells, using different dilution of the virus.

For infection of HSCs, expanded lineage negative (Lin-) cells were washed, re-suspended in their medium and lentiviral particles were added at multiplicity of infection (MOI) 100. Efficiency of transduction was evaluated after 24 hours by FACS (percentage of ZsGreen or hNGFR positive cells).

2.8) Colony forming unit assay

Colony forming unit (CFU) assay was performed with BM-derived HSCs infected or not with ATF3-expressing vector. Progenitor cells were plated in triplicate in 35-mm dishes (at the density of $2*10^4$ cells per dish) and cultured in MethoCult™ M3434 medium (StemCell Technologies) for 13 days, at 37°C and 5% CO_2-humidified incubator.

Two independent researchers evaluated the morphology of the colonies with an EVOS™ XL Core Imaging System. Hematopoietic progenitors were scored for their ability to generate granulocyte-macrophage (GM-), granulocyte (G-) and macrophage (M) progenitor cells.

2.9) Monocyte/macrophage differentiation

HSCs were isolated from the BM and differentiated toward monocytes in the presence of macrophage-colony stimulating factor (M-CSF). Briefly, HSCs cells were expanded in their medium for 3 day in order to increase the percentage of CD34+ cells. Cells were then resuspended in IMDM (10% FBS) containing only M-CSF (40ng/mL) and differentiated for next 9 days. Monocyte/macrophage differentiation was evaluated by FACS, measuring the percentage of CD11b, Ly6C and or F4/80 positive cells.

2.10) Isolation of mesenchymal cells from the bone marrow

Mouse BM mesenchymal cells (MSCs) were purified from the femurs and tibias of mice. The internal BM cellular fraction was removed, the bone and the trabecular fraction were incubated with collagenase I (Sigma-Aldrich) (1 mg/mL) for 1h at 37°C. Then, cell suspension was filtered through a 70µM cell strainer, in order to remove debris. After treatment of single-cell suspension with ACK lysis buffer, cells were incubated with the following PE-conjugated antibody: CD45, B220, CD3, CD11b, CD11c, Gr1, F4/80, Ter119 (all markers of hematopoietic cells). Anti-PE microbeads (Miltenyi Biotec) were used to collect the unlabeled cells that are eluted as PE-negative with a MACS® column separator. After separation, MSCs were phenotypically characterized by FC analysis with the following markers: CD45, Ter119, CD31, Sca-1, CD29, CD44.

Pericyte-vascular cells were isolated from the BM medullary cavity using anti-NG2/AN2 microbeads (Miltenyi Biotec).

For *in vitro* experiments, BM-derived mesenchymal cells were expanded and differentiated with MesenCult™ MSC Basal Medium supplemented with Mesenpure cocktail (StemCell Technologies) for 10 days. Cells were cultured under hypoxic conditions: 5% of O_2 and 5% of CO_2 at 37°C in humidified incubators.
In vitro experiments were performed using MSCs between the 2^{nd} and the 3^{rd} passages. For MSCs stimulation and co-culture experiment, cells were seeded at a density of $1*10^5$cells/cm^2.

2.11) Co-culture experiment

For the co-culture experiment we used primary stabilized MSCs and fresh-sorted HSCs. In detail, when MSCs reached 80-90% of confluence, cells were detached and seeded on 24 well plates. Fresh naïve HSCs, isolated from WT mice and expanded overnight with StemSpan™ Hematopoietic cell media, were added to MSCs seeded the day before, using Transwell®-24-well permeable support (0.4μm pore polycarbonate membrane). After 24 hours, cells were washed with PBS and collected for molecular analysis.

2.12) *In vitro* and *In vivo* neutralization of IL-1β

Recombinant IL-1β and anti-IL-1β monoclonal antibodies were initially tested in a dose-dependent manner to detect the best concentration.
In all experiments shown, HSCs were stimulated for 24 hours with 25ng/mL of recombinant IL-1β (211-11B, PeproTech).
Anti-IL-1β neutralizing antibody (B122, BioXCell) and relative Isotype control (Hamster IgG, BioXCell) were added to the medium prior to co-culture experiments at the dose of 5 μg/ml.
Both antibodies were used also for *in vivo* studies. The B122 monoclonal antibody was injected in NeuT mice starting from 12 weeks of age. C57BL/6 mice started anti-IL-1β treatment three days after the injection of the PyMT41c tumour-cell line.
Both mice were treated with anti-IL-1β and relative isotype control, two times a week for four weeks. Antibodies were injected intraperitoneally (i.p) at the rate of 50 μg per mouse in 200 ul of physiologic saline water.

2.13) Immunostaining and histopathology on paraffin-embedded (FFPE) sections

Four-micrometers-thick tissue sections of bone and mammary glands were deparaffinized, rehydrated and unmasked using Novocastra Epitope Retrieval Solutions pH6 or pH9 in a thermostatic bath at 98°C for 30 minutes. Subsequently, the sections were brought to room temperature and washed in PBS. After neutralization of the endogenous peroxidase with H2O2 (3%) and Fc-blocking by a specific protein solution, the samples were incubated with primary antibodies overnight at 4 C°. Staining was revealed using IgG (H&L) specific secondary antibodies (Life Technologies) and AEC (3-Amino-9-Ethylcarbazole) or DAB (3-3' diaminobenzidine) chromogenic substrate. The slides were counterstained with Harris hematoxylin (Novocastra).

Primary antibodies used for IHC are the following: mouse Monoclonal CXCL12/SDF-1 (79018; R&D Systems); Rabbit Monoclonal CXCR4 (UMB2; Epitomics); Mouse Monoclonal Nestin (rat-401; Millipore); Rabbit Polyclonal ATF3 (HPA001562; Sigma-Aldrich); Mouse Monoclonal CD8 (4SM15; Invitrogen); Mouse Monoclonal CD206 (C068C2; BioLegend).

2.14) Confocal microscopy analysis

Immunofluorescence analyses were performed on frozen OCT-embedded BM samples.

For ATF3 intracellular staining, four-micrometre-thick sections were fixed for 10 min with 4% paraformaldehyde (PFA) and permeabilized for 10 min at room temperature with 0.2% Triton X-100. For cell membrane staining, sections were fixed for 15 min with cold acetone.

Sections were blocked in PBS1X with 5% BSA and incubated with primary antibody for 2 hours and secondary antibody for 30 min. Anti-rat and anti-rabbit (Alexa Fluor 633- and 555-conjugate) secondary antibodies were used for fluorescence detection (Life Technologies).

Conjugated antibodies (c-kit PE/FITC; Lineage markers: CD45, CD3, CD11b, CD11C, B220, Gr1, Ly6C/ FITC; CD29 APC, CXCR4 PE) were further added as third step. Nuclei were counterstained with the 4',6-diamidino-2-phenylindole (DAPI) stain.

Negative controls were mouse and rabbit immune sera instead of the primary antibodies. All sections were analysed under a Zeiss AXIO Scope.A1 optical microscope and microphotographs were collected using a Zeiss Axiocam 503 Color digital camera using the Zen 2.0 imaging software.

Primary antibodies used for IF are the following: ATF3 (44C3a, SantaCruz), FcγR (93, eBioscience), SPARC (AF492, R&DSystems), CXCL12 (79018; R&D Systems).

2.15) RNA extraction and qPCR analysis

RNA was extracted from cells using Direct-zol RNA Microprep kit (ZymoResearch), following the manufacturer's instruction and quantified with NanoDrop™2000/2000c Spectrophotometer (ThermoFisher). QIAamp ® RNA blood Mini Kit (Qiagen) was used to isolate RNA from mouse peripheral blood.

For gene expression analysis, RNA (at least 300ng) was reverse transcribed with SuperScript™ IV VILO™ Master Mix with exDNase™ Enzyme or with High-Capacity cDNA Reverse Transcription kit. Quantitative PCR (qPCR) was executed with ABU Prism 7900 HT (AB) using the TaqMan Fast Advanced PCR MasterMix (Applied Biosystem). Gene expression levels were normalized with β-Actin expression. The following primes were used: Atf3 Mm00476033_m1; Actb Mm02619580_g1; Irf8 Mm00492567_m1; F480 Mm00802529_m1; IL-1β Mm00434228_m1.

2.16) Graph and Statistical analysis

Data analyses were performed using GraphPad Prism Software (Version 9.0). Statistical analyses, assuming that both populations have the same SD, were evaluated using a parametric test for continuous variables (two tailed paired and unpaired Student's t-test or one-way ANOVA followed by multiple comparison) with confidence intervals of 95%. Dot plots report mean ± standard deviation.

In vivo experiments were performed at least two times and for *in vitro* experiments two or more biological replicates were used. Data were accepted statistically significant at $P < 0.05$ (*, $P < 0.05$; ** $P < 0.01$; ***, $P < 0.001$).

The number of animals used for *in vivo* experiments were defined on the basis of statistical principles to assure the significance of the results with the smallest number of animals.

Public dataset analysis was performed using R software:

- Normalized RNA-Seq data derived from mouse normal hematopoietic cells were obtained from GSE60101. ATF3 expression was checked across all datasets, composed of 16 different cell types.

- Pre-processed gene expression data derived from 38 populations of human hematopoietic cells were downloaded from GSE24759 with *GEOquery* package. Data were imported into R software and collapsed with maxRowVariance method from *WGCNA package*. ANOVA test was performed between all 38 populations of hematopoietic cells. P value was corrected through the Benjamini & Hockeberg method. *Atf3* variation across all different cell populations was charted through a boxplot.

- BALB/c and NeuT mice gene expression profile pre-processed data were downloaded from GSE117071 with *GEOquery package* and multiple probes that matched the same genes were collapsed selecting the most detected probe all over the dataset. Batch effect was corrected through *Harman package*.

- GSE61055 were downloaded with GEOquery package and probes that matched the same gene were collapsed with the WGCNA package with method maxRowVariance. Class comparison between $Atf3^{-/-}$ mouse macrophages and wild type mouse macrophages, both untreated, were calculated through Limma package and genes were considered significant with a FDR < 0.05 (p.value was corrected through Benjamini & Hochberg method).

- Peripheral blood mononuclear cell raw data were downloaded from GSE27562 with the *GEOquery package* and then normalized with RMA function from *affy package*. Data were collapsed with the maxRowVariance method imported from *WGCNA package*. Class comparison between normal initial mammograms and malignant breast cancer patients were performed through *limma package* and p value obtained from comparison was corrected with Benjamini & Hochberg method. Genes with a FDR < 0.05 were considered significant. ATF3 variation between normal and malignant samples was charted through a boxplot for a graphical purpose.

3) AIM OF THE STUDY

Cancer development is not entirely a neoplastic cell-autonomous process, but it also relies on the ability of accessory cells, mostly immune cells of bone marrow (BM) origin, to establish a pro-tumorigenic state. Indeed, starting from pre-malignant stage, the release of growth factors, cytokines, chemokines and miRNAs in the blood activates a stress response in the BM niche and shifts the normal haematopoiesis towards myeloid cell expansion.

Studying the BM hematopoietic and stromal perturbation occurring during breast cancer development, we identified BM stromal changes occurring at the initial step of mammary transformation and anticipating the expansion of myeloid cell populations at the expense of erythroid and B cells. These changes were associated with a transcriptional reprogramming of the BM haematopoietic niche, guided by the activation of the immune transcription factors *Atf3*.

We picket *Atf3* as the front gene candidate to promote BM niche alterations. Indeed, *Atf3* was among the top up-modulated genes in the BM of MMTV-NeuT (NeuT thereafter) model, at both pre-invasive and late stage of disease.

Despite this evidence, the molecular mechanisms promoting *Atf3* activation in the BM niche and inducing a systemic tumour-emergency myelo-granulopoiesis were unknown. This gap led us to investigate the role of ATF3 during the BM hematopoietic reprogramming associated with tumour progression. Furthermore, being the balance between hematopoietic stem cell (HSC) quiescence, proliferation and differentiation tightly dictated by the cross-talk between HSCs and mesenchymal stem cells (MSCs) in the BM microenvironment, we investigated which BM stromal-derived signals activate ATF3 during HSC differentiation.

The project was articulated to reach four specific aims:

1. Evaluate ATF3 expression in BM populations during different stages of breast carcinogenesis.
2. Test *in vitro* the effects of ATF3 on BM progenitor cells.
3. Identify the upstream regulators of ATF3.
4. Assess *in vivo* the role of ATF3 during breast cancer progression.

This project might define a new player involved in the early phase of cancer-adapted myelopoiesis and provide the rationale for novel strategies to prevent cancer progression.

4) RESULTS

4.1) *Atf3* expression in the bone marrow correlates with different stages of breast carcinogenesis

To assess ATF3 expression along disease progression, transgenic NeuT and control sibling BALB/c mice were sacrificed at 12 and 24 weeks of age, two time points representing early and late stages of breast cancer progression, respectively (Chiodoni C, 2020).

Particularly, at 12 weeks of age the mammary glands of NeuT mice are characterized by the absence of palpable tumour masses. This stage of mammary gland transformation was scored by an expert pathologist, which evaluated the histological grade on H&E-stained sections subdividing mammary glands samples into hyperplasia, dysplasia or in situ carcinoma status.

At 24 weeks of age, all mammary glands of NeuT mice have developed palpable tumours with extensive stromal remodelling and inflammatory immune cell infiltrate, which are representative of more invasive stages of neoplastic progression (Fig 23A).

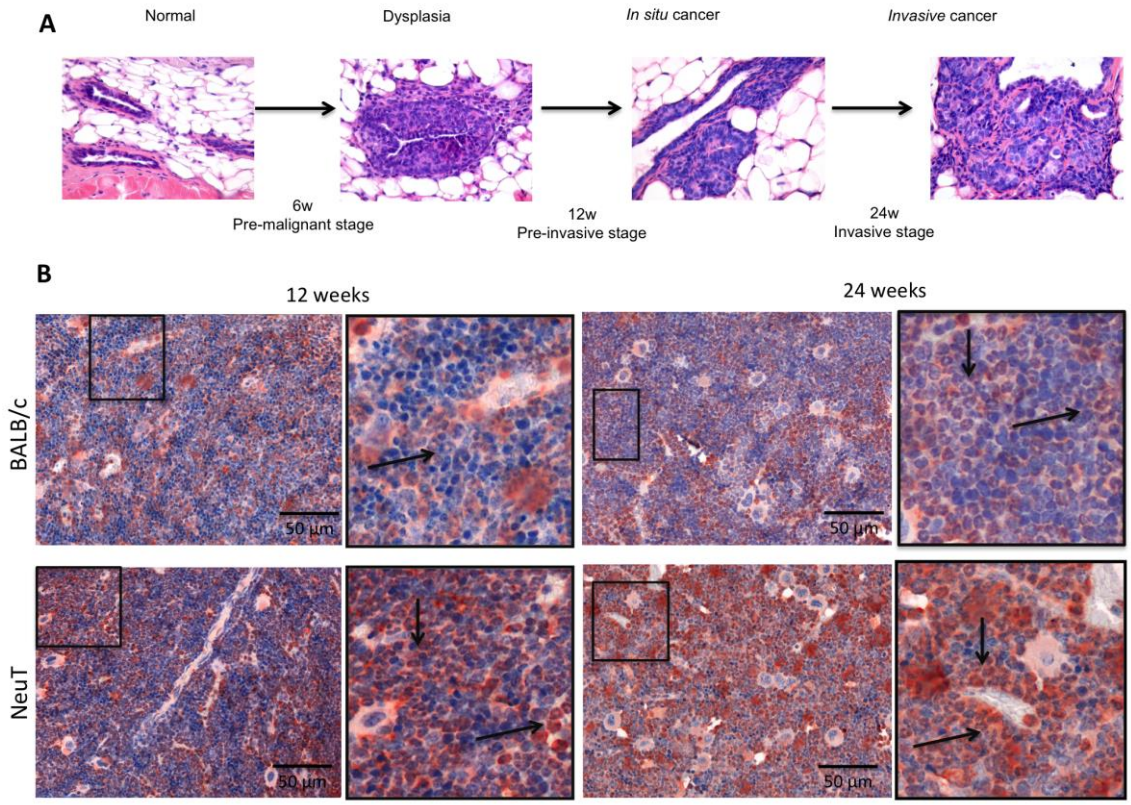

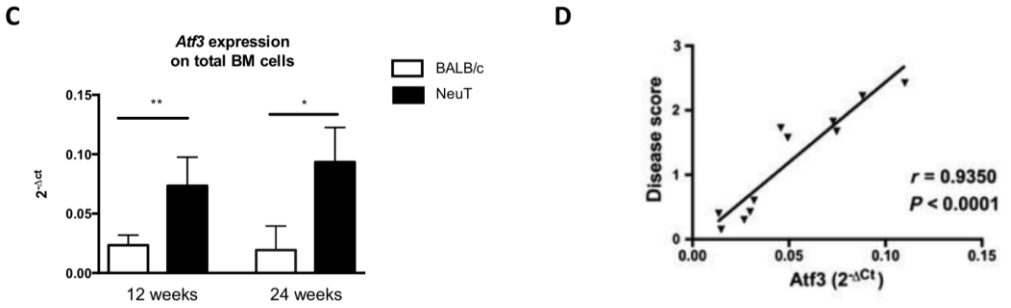

Figure 23. A) Expected tumour progression in NeuT mouse model along disease progression. B) Representative IHC staining for ATF3 in the BM of 12-24 week-old BALB/c and NeuT mice. Scale bars, 50 μm. Figure enlargement indicates that ATF3 *expression is confined in the myeloid cells only in the NeuT mice at both time points. C) Evaluation of Atf3 expression on total BM samples by qPCR. BALB/c white colomns (n=5) vs NeuT black columns (n=5) at 12 and 24 weeks of age. D) Correlation between Atf3 expression by qPCR in NeuT BM samples and disease score of each animal (n=11).*

For both time points, ATF3 expression was evaluated by IHC and qPCR analyses on FFPE sections or total BM cells, respectively.

Results in Fig. 23B show ATF3 up-modulation in the BM of both 12 and 24 weeks of age in NeuT mice in comparison to age-matched BALB/c controls. Figure enlargement highlights that ATF3 staining is confined to myeloid cell elements in NeuT mice. Furthermore, ATF3 expression increased along disease progression (comparison of the BM of NeuT at 12 and 24 weeks).

In line with IHC data, qPCR analysis confirmed the *Atf3* up-modulation at transcriptional levels (Fig 23C).

Subsequently, we evaluated whether the disease score assigned to the mammary glands of NeuT mice at 12 weeks of age was correlated with changes in *Atf3* expression, quantified by qPCR on total BM cells.

To obtain the disease score, all variables analyzed to evaluate the mammary lesions in individual mice were weighted by an expert pathologist (see Material and Methods section).

Results showed that *Atf3* expression in the BM correlated with the pathologic disease score assigned to the mammary glands (r = 0,9350; p value < 0,0001) (Fig 23D).

4.2) ATF3 is activated in different cells of the myeloid lineage during tumour-progression

To investigate in which specific BM cell populations *Atf3* is more expressed, we interrogated public available gene expression datasets. Firstly, we checked *Atf3* expression in a dataset of the mouse normal hematopoietic system (GSE60101).

Hierarchic differentiation tree generated with BloodSpot shows that during the different stages of hematopietic stem cell (HSC) maturation the expression of *Atf3* was mostly restricted to monocytes (Fig 24A).

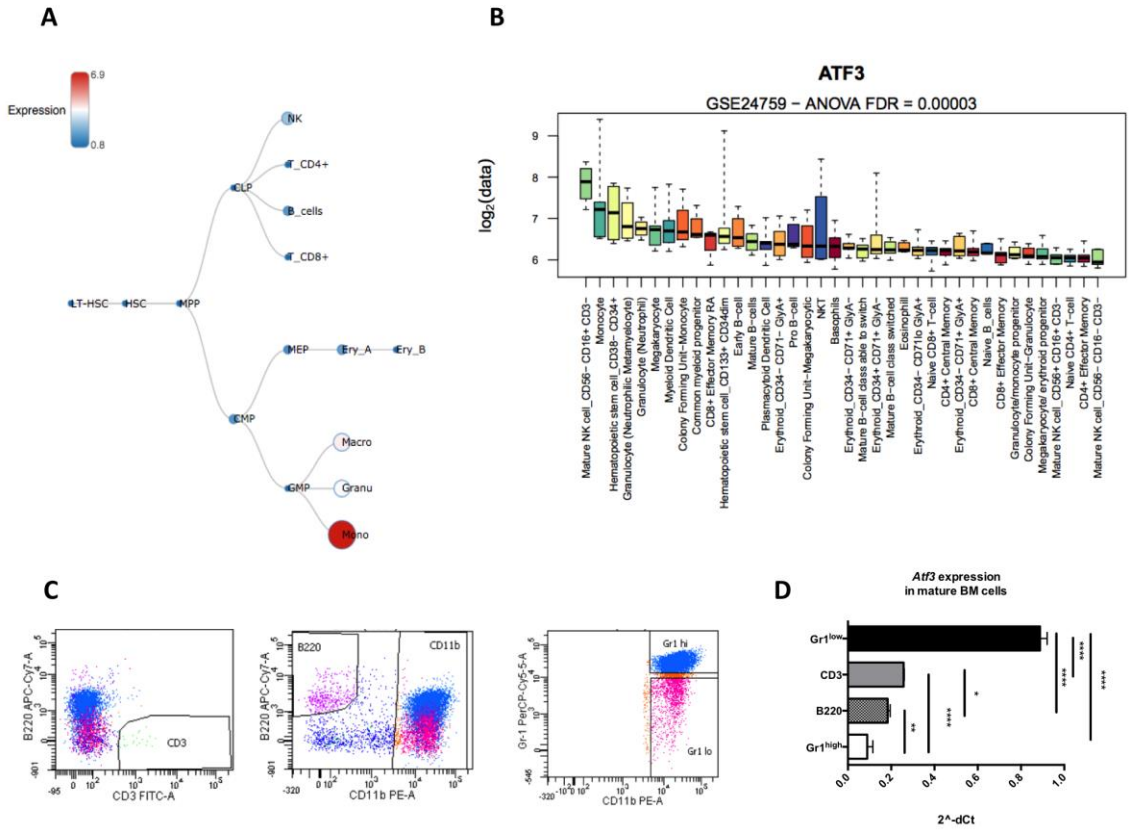

Figure 24. A) Output generated with BloodSpot that displays Atf3 expression during mouse normal haematopoiesis. B) ATF3 expression during human hematopoietic stem cell differentiation. C) Gating strategy adopted to sort the different mature BM cell populations from naïve BALB/c mice. CD11b, B220, CD3, Gr1 markers were used to discriminate the different subsets. D) Atf3 expression evaluated by qPCR on sorted BM cell populations (n=4). Ordinary one-way ANOVA with Tukey's multiple comparisons test was used as statistical analysis.

Human gene expression profile (GSEA24759) shows that *Atf3* expression was detectable very early, being expressed by CD38-CD34+ HSCs (Fig 24B), and confirmed data in the mouse dataset, showing the highest *Atf3* expression in the monocytes.

The data obtained with bioinformatics tools were then validated *in vivo* quantifying *Atf3* expression on T- ($CD3^+$) and B- ($B220^+$) lymphocytes, granulocytes ($Gr1^{high}$) and monocytes ($Gr1^{low}$) FC-sorted from the BM of naïve mice (Fig 24C). As expected, *Atf3* expression was enriched in the monocyte fraction (Fig 24D).

As monocyte differentiation occurs from myeloid progenitors, we assessed *Atf3* expression along different stages of myeloid differentiation. To this end, progenitor and mature myeloid BM populations were FC-sorted using the gating strategies displayed in Figure 25.

Lineage negative (Lin-) cells, which represent a fraction of BM cells enriched in stem cells and progenitors, were initially enriched using the mouse lineage cell depletion kit (Miltenyi Biotec). This kit works through a negative selection, staining total BM cells with a cocktail of biotinylated antibodies against a panel of differentiation markers (CD5, CD11b, B220, Gr1 (Ly6G/C), 7-4, Ter119), leading to the enrichment of the more immature and progenitor fractions. The different progenitor populations were distinguished according to the expression of CD34 and CD16/32. Based on these markers we isolated megakaryocyte/erythroid progenitors [MEPs ($CD34^{-}CD16/32^{-}$)], common myeloid progenitors [CMPs ($CD34^{+}CD16/32^{low}$)] and granulocyte-monocyte progenitors [GMPs ($CD34^{+}CD16/32^{high}$)] (Fig 25A).

The mature populations [(monocytes ($Ly6C^{high}$) and granulocytes ($Ly6G^{high}$)] were sorted from total BM cells, in the $CD11b^{+}B220^{-}$ gate. Using the same gate we also sorted myeloid cells expressing low levels of Ly6C and Ly6G markers, which likely represent a more immature fraction (Fig 25B).

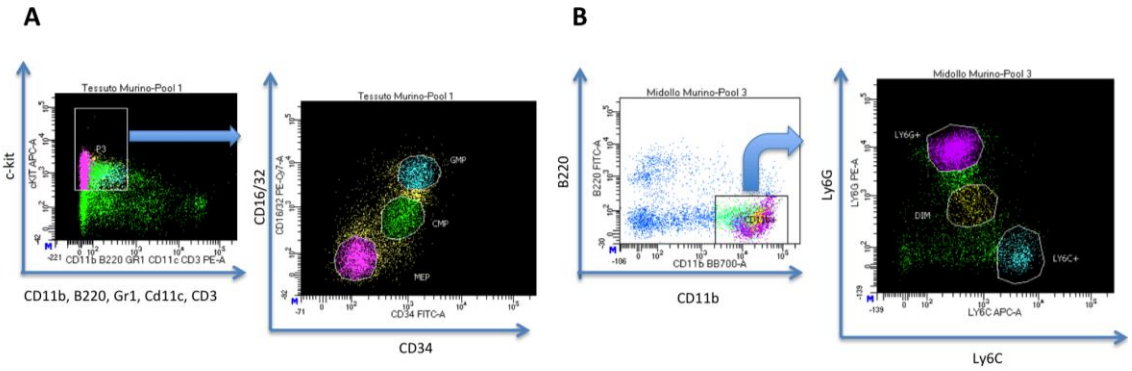

Figure 25. Gating strategies used to FC-sort progenitor cells (CMPs, GMPs, MEPs) within the $Lin^{-}c\text{-}Kit^{+}$ gate. GMPs in cyan were identified as $CD34^{+}CD16/32^{high}$, CMPs in green as $CD34^{+}CD16/32^{low}$, MEPs in pink as $CD34^{-}CD16/32^{-}$. B) Myeloid cells (neutrophils, monocytes and more immature myeloid cells) were sorted within the $CD11b^{+}B220^{-}$ gate. Neutrophils in pink ($Ly6G^{high}$), monocytes in cyan ($Ly6C^{high}$) and more immature myeloid cells in yellow (expressing Ly6G and Ly6C markers at low levels).

All these progenitor and mature BM populations were obtained from 12 and 24 week-old NeuT and control BALB/c mice.

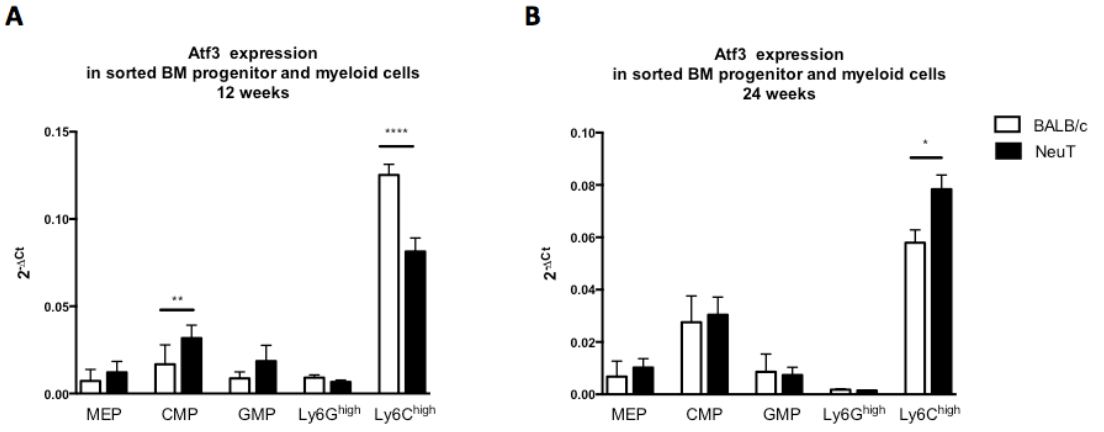

Figure 26. Evaluation of Atf3 expression by qPCR in sorted cells isolated from the BM of BALB/c and NeuT mice at both time points: A) 12 and B) 24 weeks of disease. In vivo experiments were performed two times (n=5 for each group). Ordinary one-way ANOVA with Sidak's multiple comparisons test was used as statistical analysis.

At pre-invasive stage, qPCR analysis identified in NeuT mice higher *Atf3* expression in CMP and GMP cells, which reached statistical significance in the CMP population, and its down-regulation in monocytes (Ly6C^{high}), compared to BALB/c control (Fig 26A). This pattern was different at the invasive stage of disease, where the difference in *Atf3* expression between BALB/c and NeuT mice was appreciated only in the monocytic (Ly6C^{high}) fraction (Fig 26B).

To assess whether the above results were limited and specific for the NeuT tumour model, data were confirmed in a different transplantable luminal breast cancer model. To this end, the PyMT41c (41c thereafter) breast cancer cell line, established in our laboratory from a spontaneous tumor originated in MMTV-PyMT mice (C57BL/6 background), has been injected into the mammary fat pad of naïve mice.

To mimic an early time point, mice were sacrificed 9 days after 41c cell injection, when tumours were not yet palpable and disease were similar to the pre-invasive stages of mammary transformation in NeuT mice.

The late time point was established at 30 days after cell injection, when the tumours reached approximately 100 mm^3 of volume.

At the end of the experiment, mice were euthanized and *Atf3* modulation was evaluated by qPCR on FC-sorted BM progenitor and mature myeloid cells.

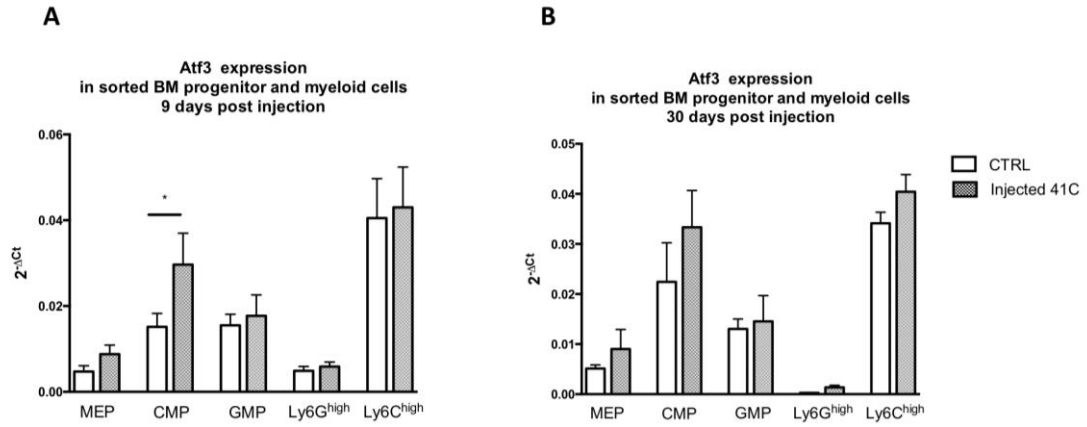

Figure 27. Evaluation of Atf3 expression in sorted BM cell populations of B6 mice injected or not with 41c tumour cell line. A) Mice were sacrificed at day 9 post injection when tumour was not palpable. B) Mice were sacrificed when tumour was well established, 30 days after injection. In vivo experiments were performed two times (n=5 for each group). Ordinary one-way ANOVA with Sidak's multiple comparisons test was used as statistical analysis.

In line with the NeuT model, *Atf3* expression was induced in the CMPs (Fig 27 A-B), particularly at the early time point and increased in the Ly6C^{high} cell fraction at late time point (Fig 27B). However, in this transplantable model we did not observe *Atf3* down-modulation in the fraction of Ly6C^{high} cells at the early time point (Fig 27 A), as previously showed in the NeuT mice model.

As transcription factor, ATF3 exerts its function when translocate into the nucleus, therefore the only expression of *Atf3 mRNA* is not sufficient to claim its activity. To evaluate ATF3 nuclear translocation, confocal microscopy analysis was performed on BM samples collected from NeuT and control BALB/c mice. Frozen OCT-embedded BM samples were stained with antibodies to ATF3, CD16/32 (FcγR) and lineage (Lin) markers (CD11b, Gr1, F4/80, B220, CD11c).

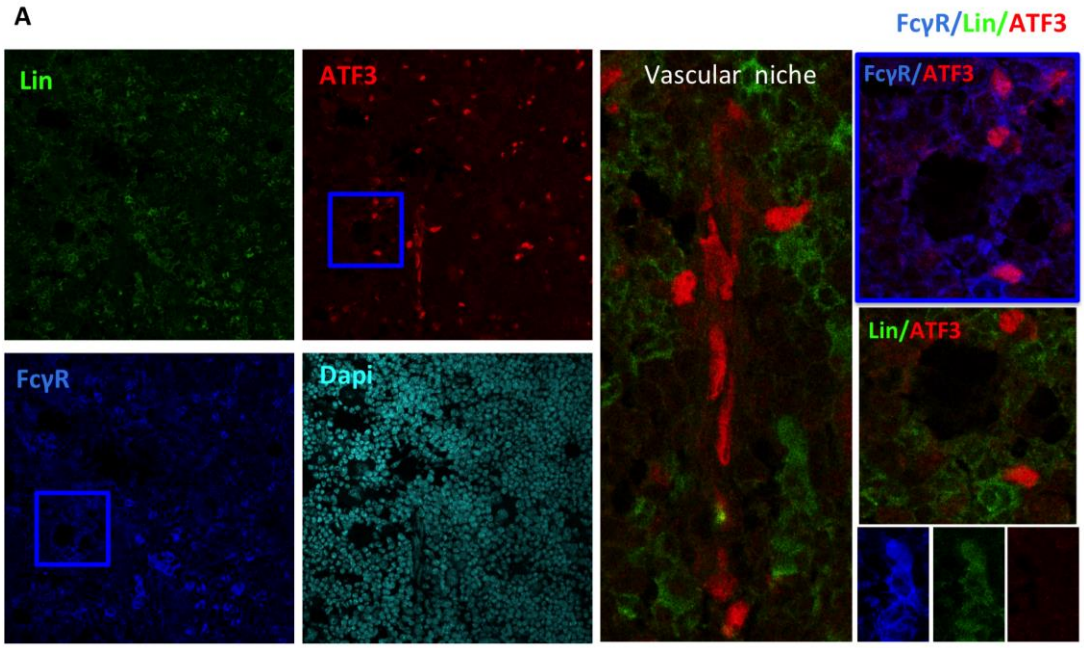

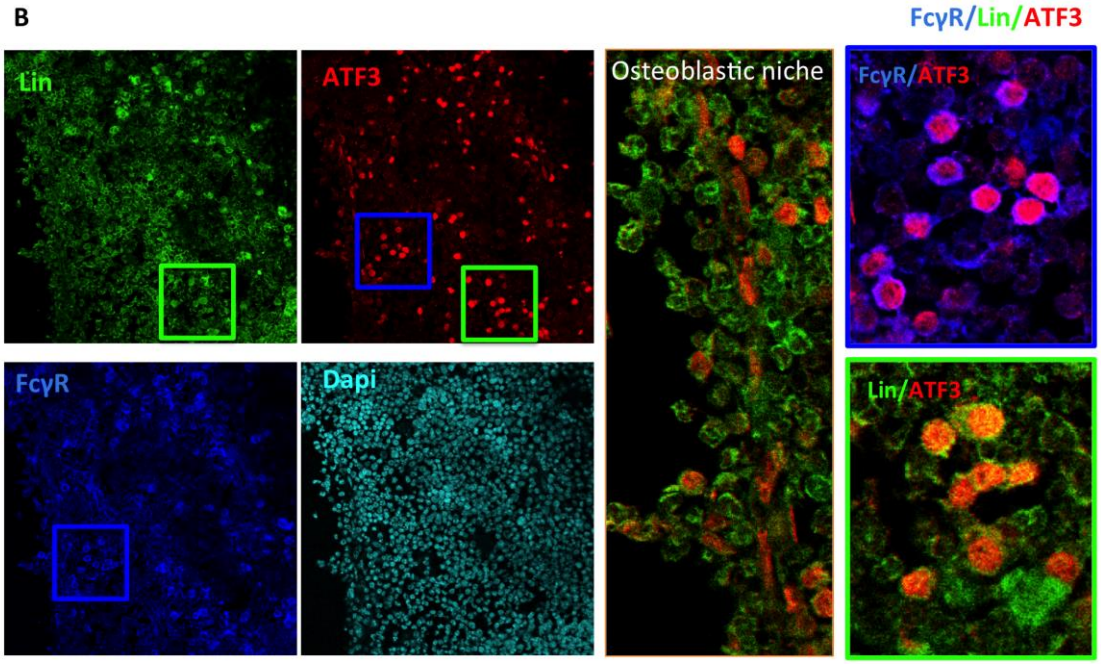
B
FcγR/Lin/ATF3
Lin
ATF3
Osteoblastic niche
FcγR/ATF3
FcγR
Dapi
Lin/ATF3

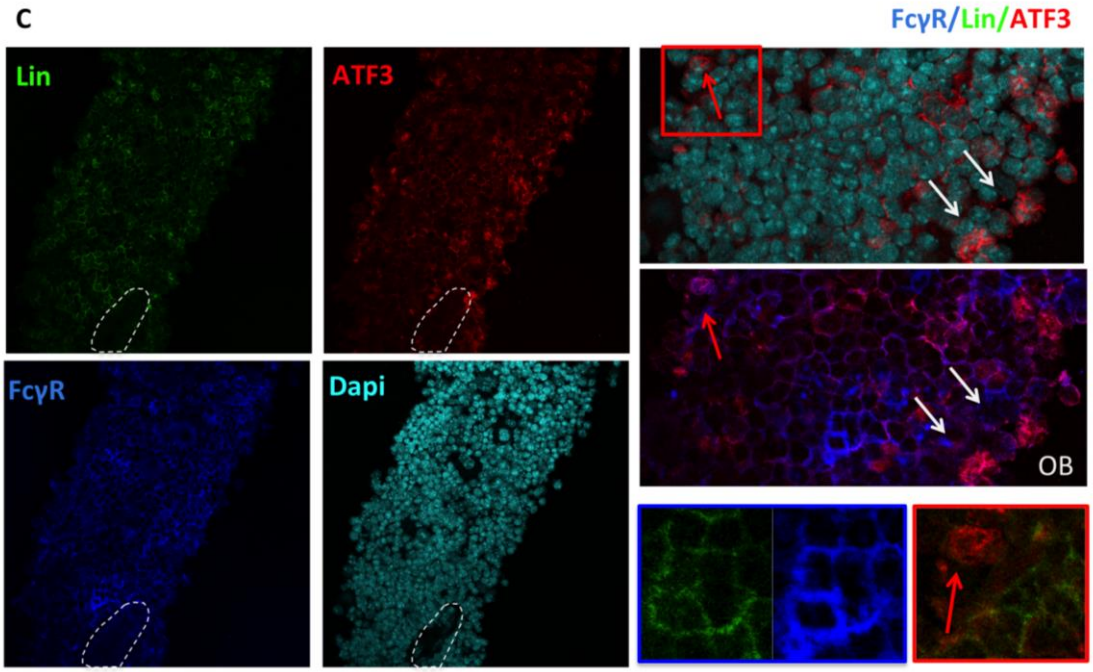
C
FcγR/Lin/ATF3
Lin
ATF3
FcγR
Dapi
OB

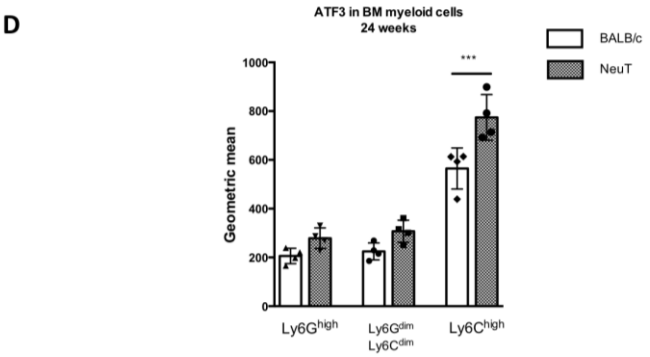
D
ATF3 in BM myeloid cells
24 weeks
BALB/c
NeuT
***
Geometric mean
1000
800
600
400
200
0
Ly6G^high
Ly6G^dim Ly6C^dim
Ly6C^high

Figure 28. Confocal microscopy analysis showing ATF3 *expression in the BM of NeuT mice at both A) early and B) late time points. Figure C) shows* ATF3 *expression in the BM of naïve BALB/c mice.* ATF3 *(red), FcyR (blue), Lineage CD11b, Gr1, F4/80 markers (green), DAPY (cyan) D) Evaluation of* ATF3 *expression by FACS in the BM of BALB/c (n=4) and NeuT mice (n=4) at 24 weeks of age. Fluorescence intensity of* ATF3 *was evaluated as MFI. Ordinary one-way ANOVA with Sidak's multiple comparisons test was used as statistical analysis.*

Confocal microscopy analysis showed high ATF3 expression and nuclear localization in myeloid progenitors (Lin-/FcγR+), localized in proximity of the vascular niche at pre-invasive stage of disease (12 weeks) (Fig 28A). This feature was maintained at the invasive stage of mammary transformation (24 weeks), when ATF3 became also more expressed in Lin+/FcγR+, likely mature monocyte/macrophage cells (Fig 28B).

Notably, the nuclear localization of ATF3, indicative of its activation, was a clear characteristic of tumour-bearing mice, whereas in the BM of BALB/c mice ATF3 staining was mainly confined to the cytoplasm of cellular elements surrounding the osteoblastic niche (Fig 28C).

FACS analysis performed on mature BM myeloid cell subsets confirmed a higher ATF3 expression, evaluated as mean fluorescence intensity (MFI), in monocytes (Ly6C+) compared to the other myeloid populations: granulocytes (Ly6G+) and more immature cells (Ly6GLy6C^{dim} cells).

4.3) ATF3 activation in myeloid progenitor clusters is a feature of emergency haematopoiesis

The activation of ATF3 in BM precursors at early stage suggested to evaluate whether this condition was paralleled by changes in BM cell composition, as expected during cancer-induced haematopoiesis. To this end, a deep characterization of BM cells was performed analysing myeloid precursors and mature cells, in both spontaneous NeuT and transplantable 41c model.

To quantify progenitors we used FACS (in the 41c model) and an IF approach allowing the *in situ* detection of the so-called "CMP/GMP clustering" (in the NeuT model). As described by Hérault et al. GMP clustering is a feature of emergency haematopoiesis and could be detected using antibodies to Lin/ckit/FcγR markers (Hérault A, 2017).

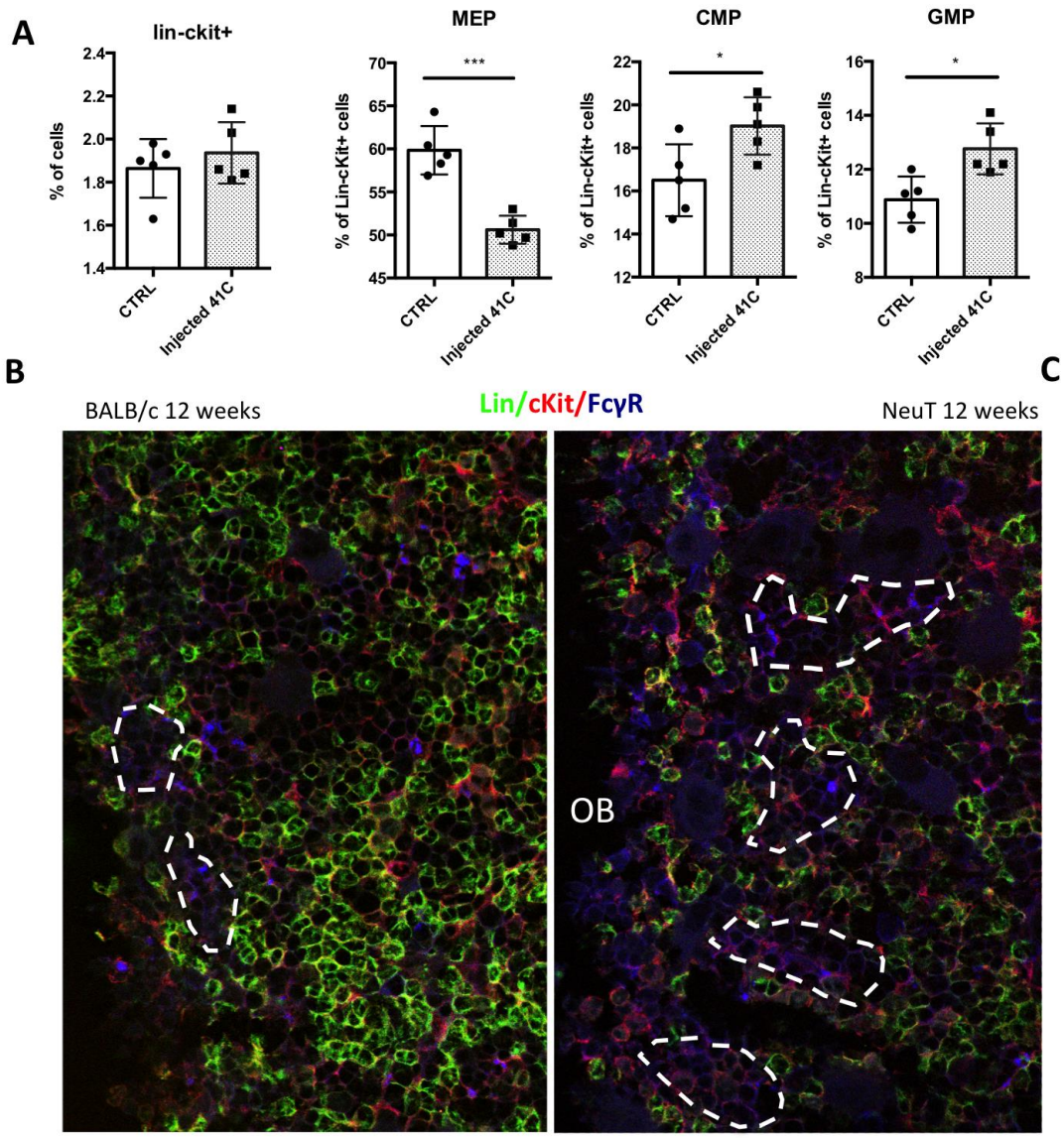

Figure 29. A) Quantification by FC analysis of the different progenitor cell subsets (MEPs, CMPs, GMPs within the Lin⁻ c-Kit⁺ cells) in the BM of mice injected with 41c tumour cell line and euthanized after 9 days (n=5 for each group). The same markers used to FC-sort the different BM populations were employed also for FACS staining. Unpaired t-test with equal SD was used as statistical analysis. Imaging of GMP clustering in the BM of B) naive and C) tumour-bearing NeuT mice at early stages of disease.

At the early stage of tumour take in the 41c transplantable model we observed a significant increase in CMP and GMP progenitors, at the expense of MEPs, a picture suggestive of a myeloid-skewed haematopoiesis (Fig 29A). The same increase in CMPs/GMPs was confirmed through confocal microscopy analysis performed in NeuT model at 12 weeks of age. IF of BM sections collected from BALB/c mice revealed that GMPs/CMPs (Lin-/c-Kit+/FcγR+) were organized in clusters composed by few cells, mainly close to the osteoblastic (OB) niche (Fig 29B). Differently, in the BM of tumour-bearing NeuT mice, clusters of GMPs/CMPs were not restricted to the sole OB

niche, being localized in all the BM parenchyma, particularly close to the vascular niche, and were composed by a higher number of cells (Fig 29C).

At late time point we observed an expansion of mature CD11b+ myeloid cells, evaluated by FACS analysis, in both models (Fig 30). One difference between the two models was in the subpopulation of expanded CD11b+ cells, which were monocytes in NeuT-tumour bearing mice (Fig 30A) and granulocytes in 41c-transplantable model (Fig 30B).

CMP/GMP clustering, as an early marker of emergency haematopoiesis, was not different in the BM of NeuT mice compared to the normal counterpart at 24 weeks (Fig 30C). This is in line with the interpretation that emergency haematopoiesis occurs in response to early transformation, while established tumours might preferentially promote myeloid cell differentiation of expanded precursors.

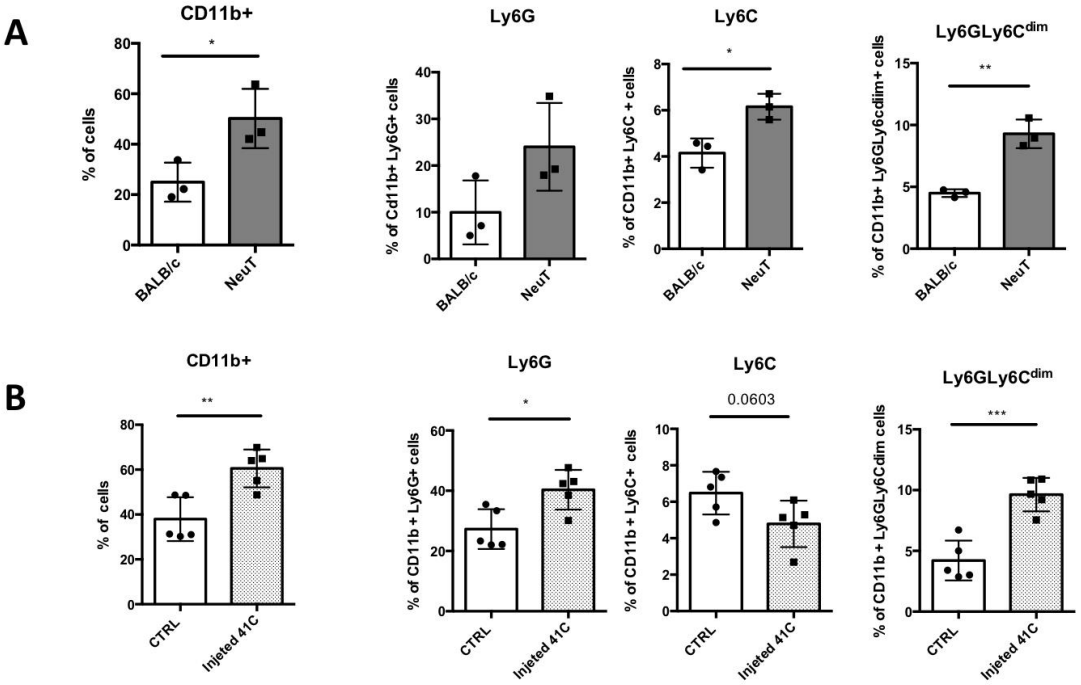

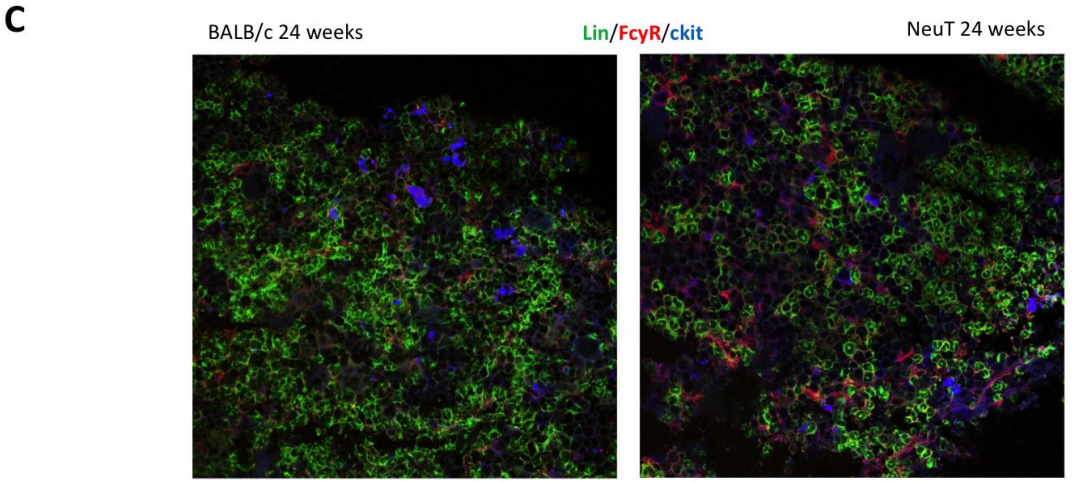

Figure 30. Quantification by FACS of mature myeloid cells in the BM of A) NeuT tumour bearing (n=3 for each group) and B) mice injected with 41c tumour cell line (n=5 for each group). The same markers used to FC-sort the mature myeloid BM populations were also employed for FACS staining. Unpaired t-test with equal SD was used as statistical analysis. C) IF analysis of CMP/GMP clustering performed on frozen BM OCT samples from BALB/c and NeuT at 24 weeks of age.

Overall these data suggest that the nuclear activation of ATF3 in progenitor cells of tumour-bearing mice could drive the formation of granulocyte/macrophage progenitor clusters. Furthermore, the biphasic ATF3 expression in BM progenitors and mature myeloid cells could be relevant to drive a myeloid cell expansion and differentiation, respectively.

4.4) The nuclear activation of ATF3 is a hallmark of tumour-promoting myelopoiesis

Cancer represents a chronic state of smoldering inflammation. To study whether ATF3 activation in myeloid progenitor cells occurs in response to a general stress conditions or represents a specific characteristic of BM response to malignant transformation, ATF3 modulation was assessed in a model of chronic inflammatory condition, obtained through chronic LPS administration.

BALB/c mice were intraperitoneal (i.p) injected with 10 ug of LPS, three times per week, for four consecutive weeks, and sacrificed the day after the last treatment. Control mice were treated with PBS alone.

At the end of the experiment, ATF3 expression was evaluated by IF analysis on frozen OCT-embedded BM samples, and by qPCR on flow-sorted BM cell populations.

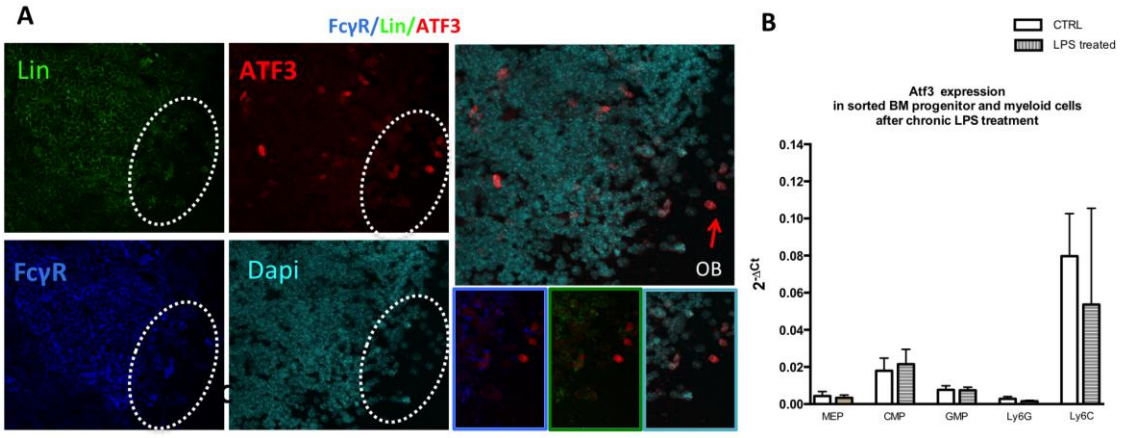

Figure 31. A) Confocal microscopy analysis showing ATF3 *expression in the BM of BALB/c mice treated chronically with LPS.* ATF3 *(red), FcγR (blue), Lineage CD11b, Gr1, F4/80 markers (green), DAPY (cyan). B) qPCR for Atf3 expression performed on progenitor and mature myeloid cells FC-sorted from total BM of BALB/c treated or not with LPS. In vivo experiments were performed two times (n=3 for each group). Ordinary one-way ANOVA with Sidak's multiple comparisons test was used as statistical analysis.*

Administration of LPS in mice induced ATF3 nuclear translocation in the BM stromal cells of the OB niche, but had no effect in the fraction of myeloid progenitor cells (Fig 31A), which instead characterized the BM of tumor-bearing mice. In addition, qPCR analysis of FC-sorted progenitors and mature myeloid cells showed similar *Atf3* expression in mice stimulated with chronic LPS administration and in PBS-treated controls (Fig 31B), whereas ATF3 up-regulation characterized NeuT mice.

Notably, the lacks of ATF3 induction in myeloid progenitors of LPS-treated mice was in line with no substantial changes in the fraction of precursor and mature myeloid subsets, evaluated in term of frequency on total BM cells by FACS (Fig 32 A-B).

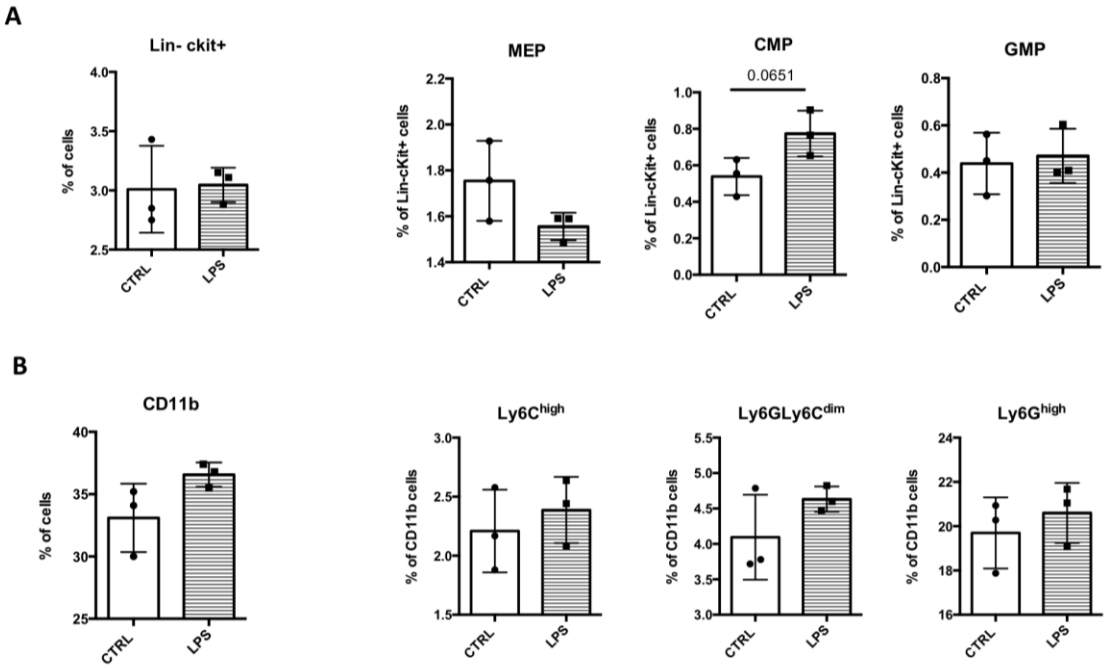

Figure 32. FACS analysis on total BM of BALB/c mice treated or not with chronically LPS (n=3 for each group). A) Evaluation of different progenitor cell subsets (MEPs-CMPs-GMPs) within the Lin-ckit+ cells. B) Quantification of granulocytes (Ly6G^{high}), monocytes (Ly6C^{high}) and more undifferentiated (Ly6GLy6C^{dim}) cells within the gate of CD11b+ B220- cells after chronic LPS treatment. Unpaired t-test with equal SD was used as statistical analysis.

To validate our data in a different setting, we checked *Atf3* expression on a publicly available gene expression profile (GSE108892) of mouse BM stromal cells under homeostatic conditions (Fig 33A) and in response to 5-FU treatment (Fig 33B) (Tikhonova A.N., 2019).

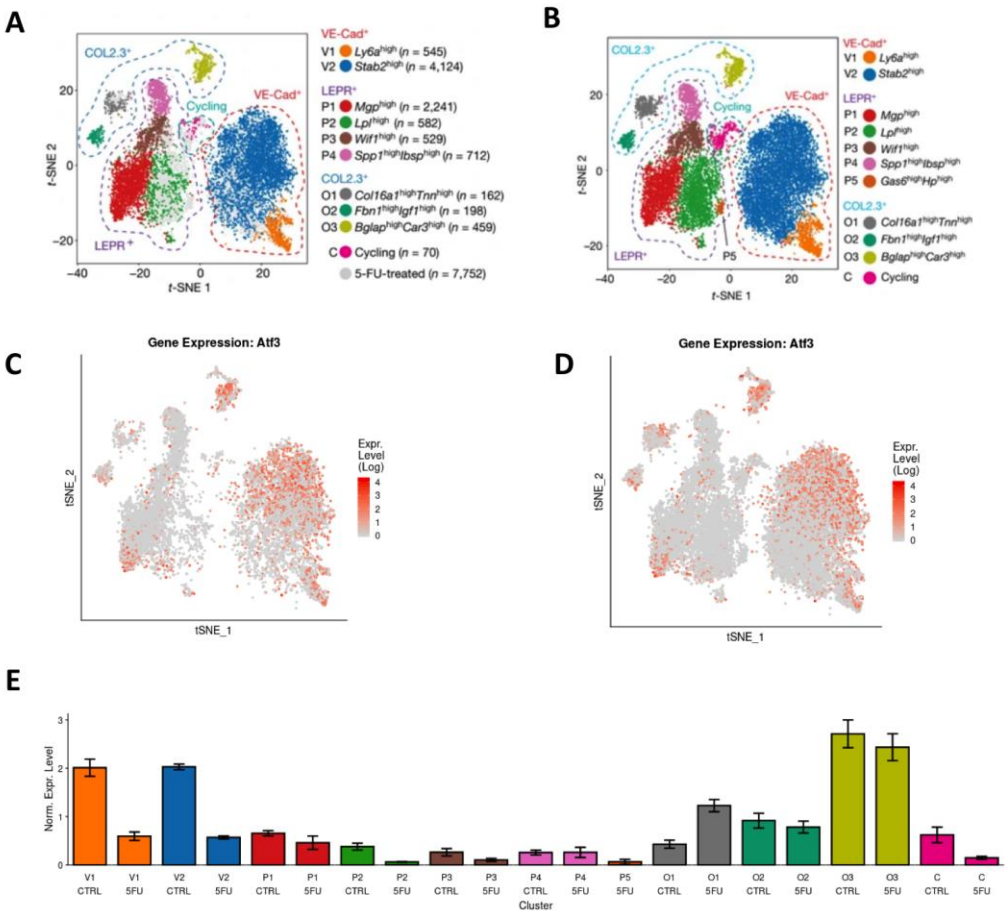

Figure 33. Visualization obtained with the interactive tool (http://aifantislab.com/niche) based on GSE108892 dataset. t-SNE plot indicating the different clustering of bone marrow stromal niche: osteoblast (COL2.3), perivascular (LEPR+) and vascular (VE-Cad+) cells under A) steady state and B) in response to stress-induced haematopoiesis. Atf3 distribution in the different clusters of BM stromal cells generated with the tSNE plot during C) normal and D) after 5-FU treatments. E) Bar plot indicating Atf3 expression levels in the different compartment of the bone marrow niche split by treatment.

Single cell-data analysis revealed that in normal condition *Atf3* was more expressed in the fraction of vascular (VE-Cad+) and osteoblastic (COL2.3+) cells. Lower *Atf3* expression was identified in perivascular (LEPR+) cells (Fig 33 C-E).

In line with our IF staining, stress-induced haematopoiesis (5-FU treatment) induced *Atf3* expression in the OB cells expressing high levels of Osteocrin, Angiopoietin like 2 and Del-1. On the contrary, *Atf3* was down-regulated in the vascular cells (VE-Cad+) of the BM niche (Fig 33 D-E).

Collectively, these findings indicate that ATF3 activation and modulation in immature myeloid cells is a specific feature of tumour-induced emergency myelopoiesis. As expected, being ATF3 an adaptive response gene, its activation could be induced in different cell types. Further investigation is required to explore its role in BM stromal cells under normal conditions and malignancies.

4.5) ATF3 drives the expansion and the differentiation of monocyte/macrophage cells

The lower ATF3 expression in mature neutrophils compared to monocytes (shown in fig. 28D) prompted the idea of testing whether ATF3 is a functional checkpoint for monocyte differentiation from BM precursors.

Therefore, Lin- cells from naïve mice were cultured in IMDM medium in presence of macrophage colony-stimulating factor (M-CSF) for 9 days (Fig 34A). Cells were collected every 3 days to analyze *Atf3* expression by qPCR and differentiation markers (CD11b, Ly6G, Ly6C and F4/80) by FACS.

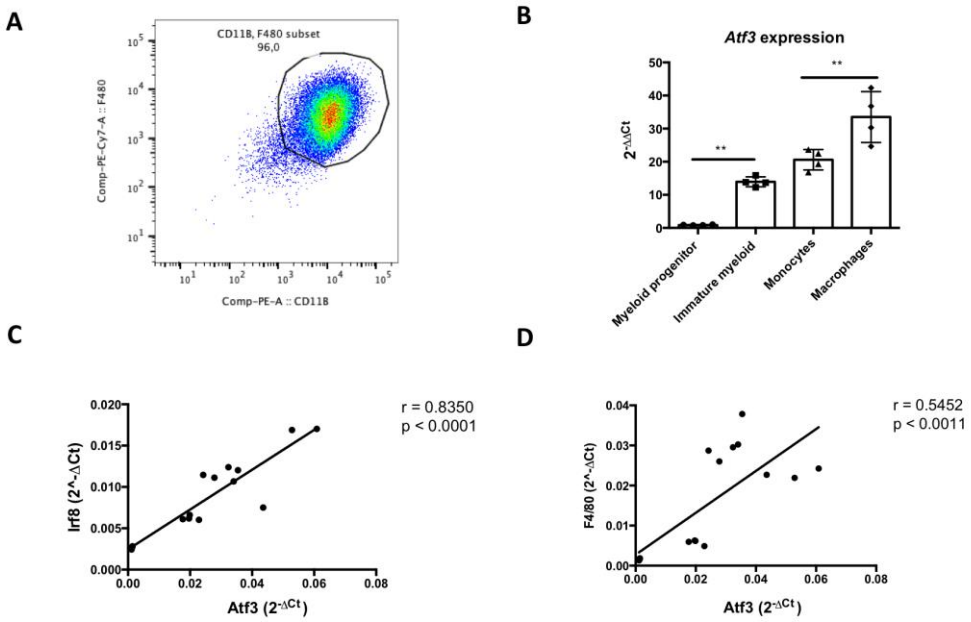

Figure 34. A) Representative evaluation by FACS analysis of macrophage maturation induced by M-CSF after 9 days. B) Atf3 expression evaluated by qPCR during different stages of monocyte/macrophage cell differentiation. For in vitro experiments four biological replicates were used. Ordinary one-way ANOVA with Tukey's multiple comparisons test was used as statistical analysis. Pearson correlation analysis between the levels of Atf3 and the expression of C) Irf8 and D) F4/80, markers of macrophage maturation. R^2 and P values are shown in the graphs.

Confirming the hypothesis, *Atf3* mRNA increased during differentiation of Lin- cells toward monocytes/macrophages (Fig 34B). Notably, this phenotype was correlated with the expression of *Irf8* ($p<0.001$, $r=0.83$) (Fig 34C), a transcription factor involved in monocyte differentiation (Friedman AD, 2007), and with the surface macrophage-specific F4/80 marker ($p<0.001$, $r=0.54$) (Fig 34D).

To confirm through a different approach that ATF3 in Lin- cells could skew progenitor differentiation toward the monocytic lineages, Lin- cells were infected with 2 different lentiviral vectors designed to force ATF3 expression. The first one uses the constitutive EF1α promoter to express ATF3 in total BM cells, the second one uses the myeloid-specific CD68 promoter, which is expressed in progenitors starting from the CMP/GMP

stage and in differentiated myeloid cells (DC, monocytes and, at low levels in granulocytes) (Strobl H, 1995) (Lotti F, 2002) (Gough PJ, 2001).

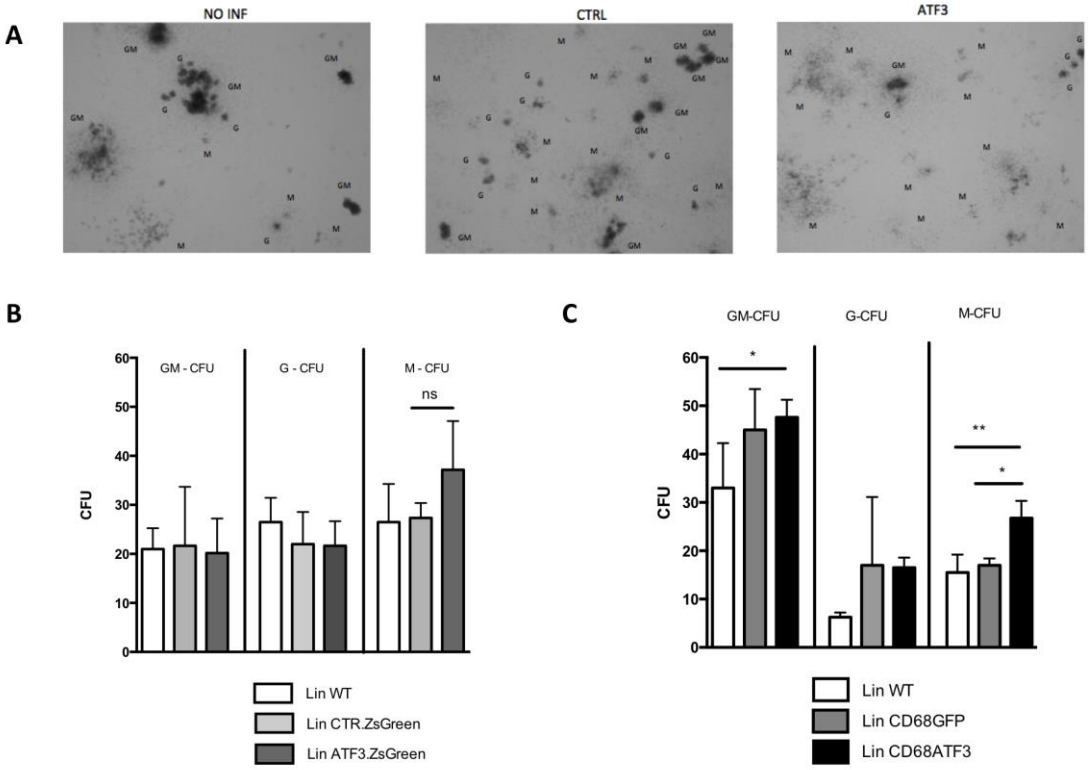

Figure 35. A) Photographs of different granulocytes/macrophages GM-, granulocytes G- and macrophages M-colony forming unit (CFU) obtained in MethoCult™ Media overexpressing ATF3 in BM progenitor cells. Cell count of CFU obtained overexpressing ATF3 under a B) constitutively (EF1α) or C) myeloid specific (CD68) promoter. For in vitro experiments three biological replicates were used. Ordinary one-way ANOVA with Tukey's multiple comparisons test was used as statistical analysis.

Cell lineage differentiation was evaluated through a colony forming unit (CFU) assay. The cytokines included in the semi-solid culture medium support the formation of granulocyte (G-CFU), macrophage (M-CFU) and granulocyte/macrophage (GM-CFU) colonies, which can be identified on the basis of their morphology (Tripodo C, 2012) (Fig 35A).

The number and the morphology of colonies were evaluated 13 days post infection. The infection with both ATF3 lentiviral vectors increased the differentiation of M-CFU (Fig 35 B-C) if compared to the relative controls (pLVX-EF1α-IRES-ATF3.ZsGreen and pRRL.CD68.GFP.WPRE.hPGK.NGFR).

These results suggest that ATF3 over-expression promotes the expansion and differentiation of monocyte/macrophage cells.

4.6) Hematopoietic switch fronted by ATF3 activation in the BM myelopoiesis is linked with detectable changes in the BM stromal niche organization

We next investigated whether the hematopoietic switch observed in the BM of tumour-bearing mice and guided by ATF3 activation in progenitors was associated with alteration in the BM stromal architecture. Indeed, the hosting laboratory has previously shown that the chronic nature of signals coming from the periphery (ie autoimmunity) is responsible for long lasting changes in the BM stromal architecture (Tripodo C, 2017). Such changes are eventually responsible for specific hematopoietic switches along differentiation. Therefore, considering that tumour represents a chronic condition, we evaluated whether NeuT tumourigenesis was associated to BM stromal changes and whether these alterations anticipated ATF3 activation in the progenitor compartment.

A particular attention has been given at the early time points. To this end, BM specimens from NeuT mice were collected at 6 and 12 week of age. As marker of stromal remodeling we used secreted protein acidic and rich in cysteine (SPARC) in combination with CD29 and c-Kit. SPARC was used according to data obtained in pre-leukemic NPMc+ mice showing that the down-modulation of SPARC expression in CD29+ stromal cells licenses immature myeloblast and c-Kit+ progenitor expansion under an autoimmune spur (Tripodo C, 2017).

IF analysis of SPARC expression in $CD29^{+}$ BM stromal cells, associated to the staining of c-Kit (SPARC/CD29/c-Kit), allows visualizing the distribution and frequency of the HSC population in the BM.

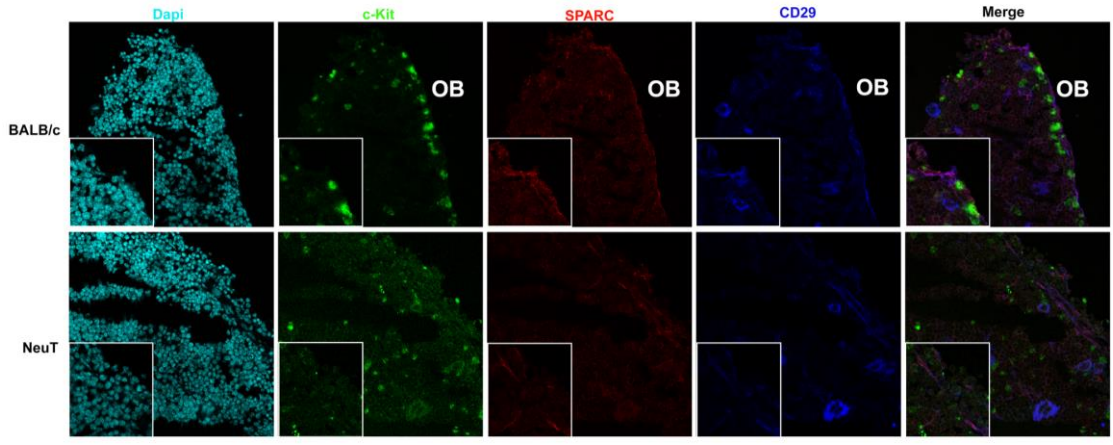

Figure 36. IF staining for SPARC (red), CD29 (blue), c-Kit (green) and DAPI (cyan) highlights the cell lining the osteoblastic (OB) niche in the BM of BALB/c (upper panels) and NeuT (lower panels) mice at 12 weeks of age.

Confocal microscopy analysis showed a down-modulation of SPARC expression in the osteoblastic cells of 12-week old NeuT mice along with the relocalization of c-Kit+

HSCs from the osteoblastic niche (OB) to interstitial areas. HSCs were also more numerous in NeuT samples in comparison to normal BALB/c counterparts (Fig 36).

Since CXCL12/CXCR4 axis is known to play a pivotal role in regulating the localization of HSCs within specialized niches, IHC analysis was used to test the expression of the prototypical stromal-derived chemotactic factor CXCL12 and its receptor CXCR4. Mesenchymal cells were highlighted with the Nestin marker.

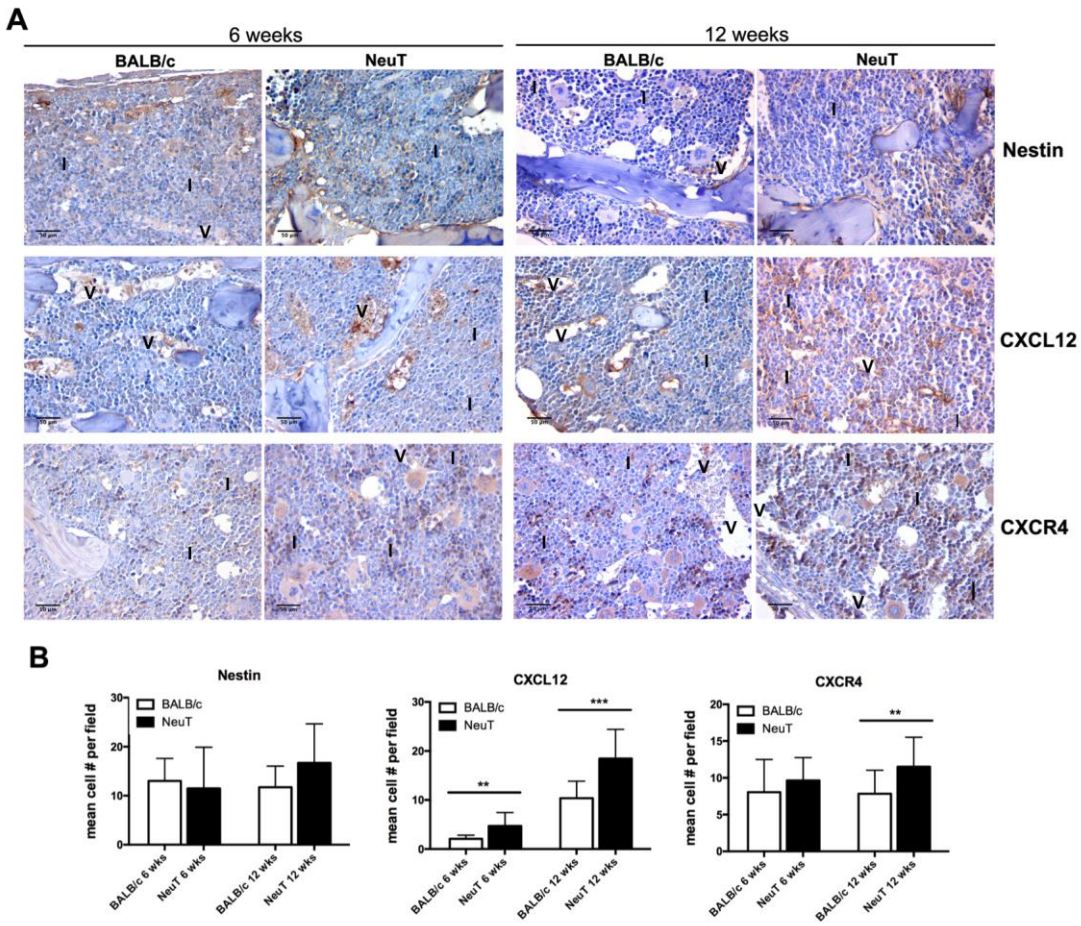

Figure 37. A) Immunohistochemical stainings of Nestin+ mesenchymal stromal cells, CXCL12 chemotactic stromal factor and CXCR4 receptor in BM sections of 6 week and 12 week BALB/c and NeuT mice. Scale bars, 50 µm. Vascular (V) and interstitial (I) areas are indicated in the figure. B) Quantitative immunolocalization analysis of the same marker relative to panel A. The quantitative evaluation is expressed as the average percentage of marked areas. Two-tailed t test was performed for statistical analysis.

In control BALB/c mice, Nestin+ and CXCL12+ cells were mostly confined to the vascular area. Differentially, an increase in the density and relocalization of Nestin+ mesenchymal stromal cells, associated with CXCL12-expressing elements, was observed in the vascular and interstitial areas of NeuT tumour-bearing mice (Fig 37A). Quantification of stromal markers, performed with a software analysis associated with a digital microscope high-power-field (HPF), confirmed the increase of CXCL12 in the hematopoietic niche of transgenic NeuT than control mice, at both pre-malignant (6

weeks) and pre-invasive (12 weeks) stages of disease (Fig 37B). Consistently with CXCL12 modulation, in the same BM samples, we observed an enrichment in CXCR4-expressing elements, likely HSCs, in the interstitial area of 6 and 12 week-old NeuT mice (Fig 37A) that was confirmed by quantification analysis at 12 weeks of disease (Fig 37B).

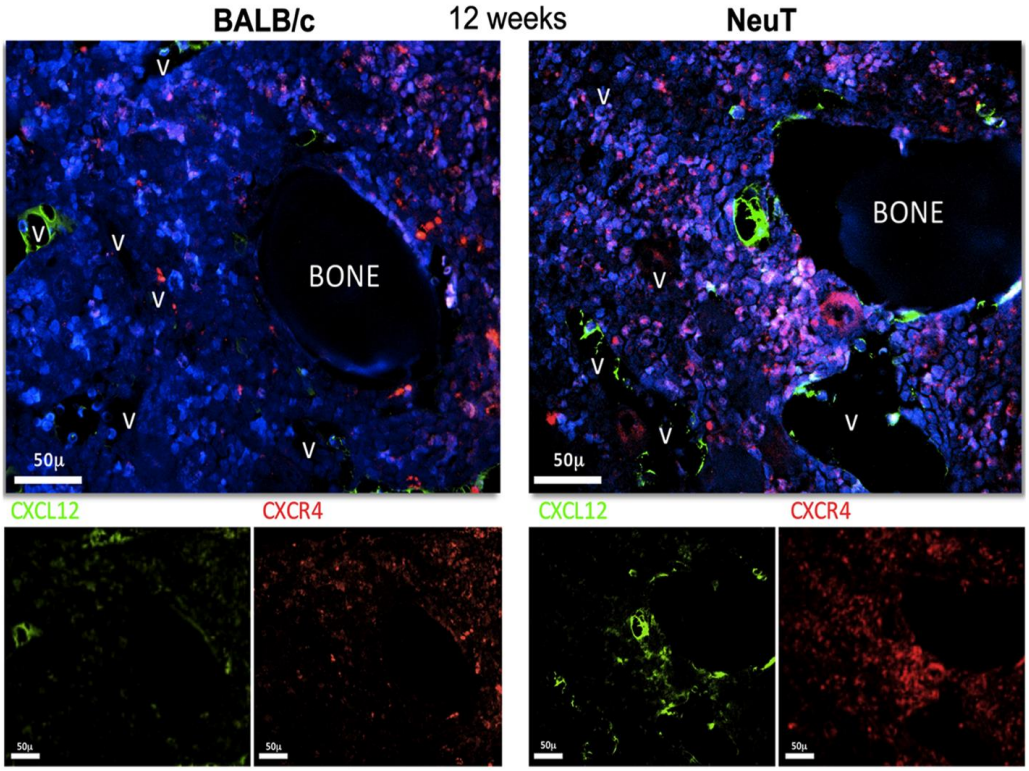

Figure 38. A) Immunolocalization of CXCL12 and CXCR4 expression on BM sections of BALB/c and NeuT mice. Vascular (V) area is indicated in the figure. CXCR4 (red), CXCL12 (green), DAPI (Blue).

Double immunofluorescence analysis for CXCL12 and CXCR4 markers confirmed the remodeling of this axis in the BM hematopoietic interstitium of NeuT mice (Fig 38), which could explain the observed redistribution of c-Kit+ cells (showed in Fig 36).

Overall, these data support the association between BM stromal changes and the modification in the distribution of hematopoietic populations.

Furthermore, the above results suggest that changes in the BM stromal niche organization might anticipate the emergency haematopoiesis characterizing NeuT mice and starting at 12 weeks of age with ATF3 induction in CMP and GMP progenitors.

4.7) IL-1β signaling drives ATF3 activation in HSCs and initiates a specific lineage commitment

Stromal-derived BM niche signals have been largely involved in driving emergency haematopoiesis. Therefore we analyzed if signals coming from the remodeled stroma of

NeuT mice could activate *Atf3* expression in haematopoietic stem cells to sustain myeloid cell expansion.

In order to identify the up-stream regulator of *Atf3*, we started analyzing by Ingenuity Pathway Analysis (IPA) software the GEP (GSE117071) performed in the BM of tumour-bearing NeuT mice, in which we initially identified *Atf3* among the top up-modulated genes starting from pre-invasive stage of disease (12 weeks) (Chiodoni C, 2020).

Reults identified IL-1β, a pro-inflammatory cytokine able to stimulate HSCs proliferation, GMP clustering and myeloid differentiation (Pietras EM, 2016), among the up-stream regulator of *Atf3*, probably through an indirect interaction (Fig 39A). In addition, bioinformatic analysis showed that *Atf3* expression in the BM correlated with the IL-1 receptor 2 (IL1R2) expression (Pearson=0.785, p value=0.00012) in the longitudinal analysis between 6 and 12 week-old NeuT mice but not in control mice (Fig 39B).

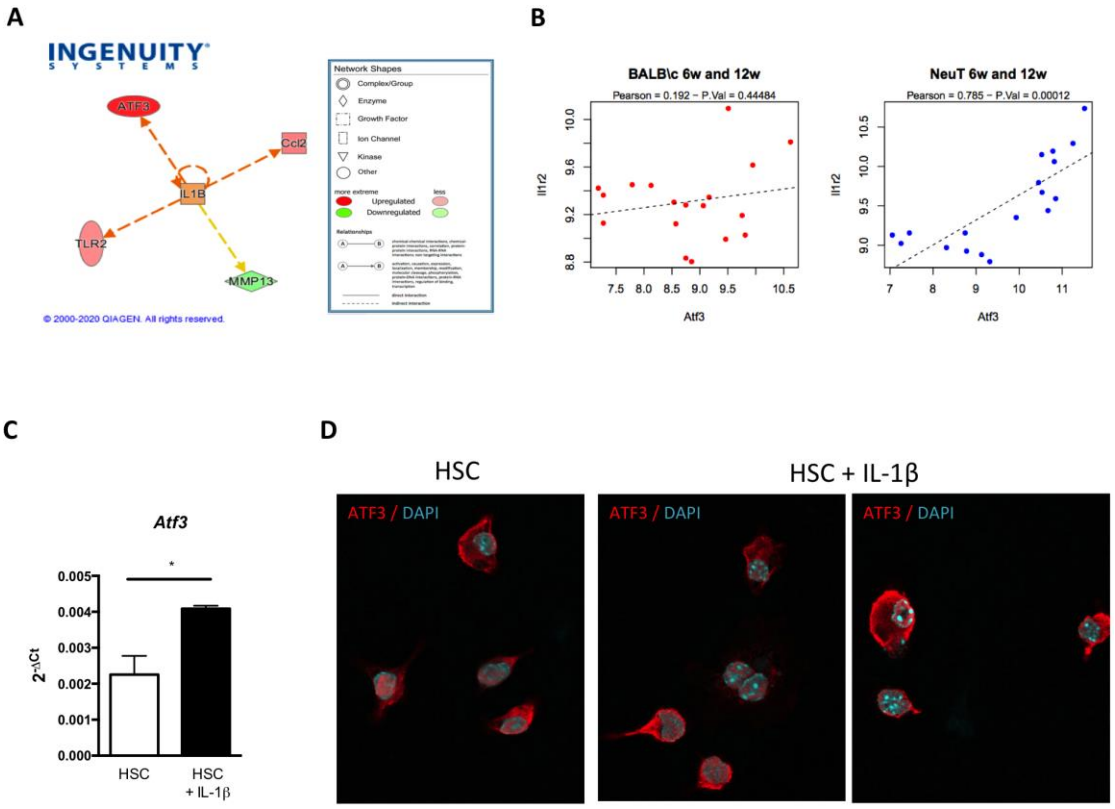

Figure 39 A) Output of IPA software analysis showing the probably relation between IL-1β and Atf3 B) Correlation between Atf3 and IL1R2 expression in the BM samples of BALB/c and NeuT mice in the GSE117071 dataset. C) qPCR and D) IF analysis of Atf3 expression on IL-1β-treated HSCs. Two-tailed t test was performed for statistical analysis.

To assess IL-1β effect on ATF3 activation, HSCs cells were isolated from the BM of BALB/c mice and stimulated with IL-1β (25ng/ul) for 24h. *Atf3* modulation was

evaluated through qPCR and IF. Both analyses showed a significant induction of *Atf3* expression (Fig 39C) and its nuclear translocation (Fig 39D) in IL-1β-treated HSCs.

The next step was the analysis of IL-1β expression in mesenchymal stromal cells (MSCs) ($CD45^-$, $Ter119^-$, $CD11b^-$, $CD11c^-$, $CD3^-$, $Gr1^-$, $B220^-$) (Fig 40A) and pericyte-vascular cells ($AN2^+$) (Fig 40B) isolated by immunomagnetic beads from the BM of 12 week-old NeuT mice. qPCR analysis showed that BM-MSCs and pericyte-vascular cells from NeuT mice expressed higher levels of *IL-1β* in comparison to BALB/c control animals.

These results suggested the hypothesis that BM-MSCs could be the first sensors of peripheral tumours, which through the release of IL-1β could stimulate ATF3 expression and activation in BM precursors.

To test this hypothesis, primary MSCs isolated from the bone of BALB/c and C57BL/6 mice were expanded and differentiated in hypoxic conditions with MesenCult™ MSC Basal Medium supplemented with Mesenpure cocktail for 10 days.

MSCs, between the 2^{nd} and the 3^{rd} passages, were stimulated with the serum collected from tumour-bearing and control BALB/c mice. Both BALB/c and C57BL/6 naïve MSCs up-regulate IL-1β expression when cultured in the presence of serum collected respectively from NeuT (Fig 40C) or C57BL/6 mice injected with 41c tumour-cell lines (Fig 40D).

Induction of IL-1β was detected also after stimulation of MSCs with supernatants collected from BALB/c-derived 4T1 (Fig 40E) or PyMT-derived 41C tumor cell lines (Fig 40F).

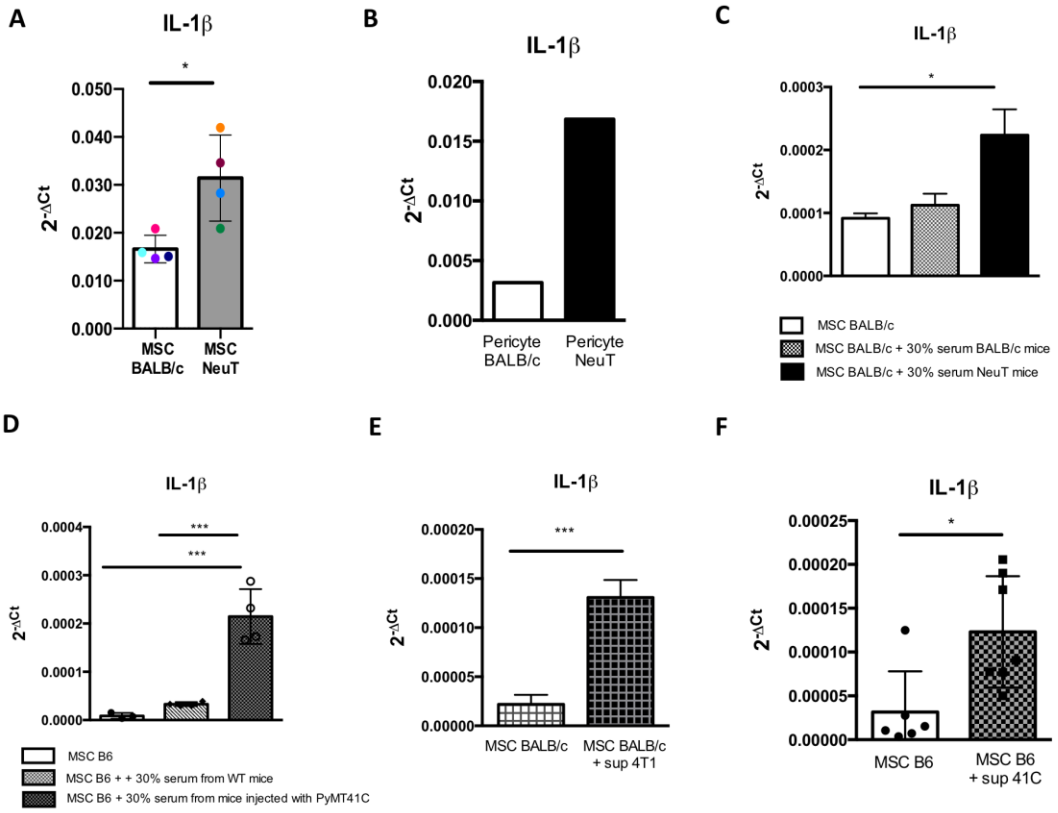

Figure 40. Expression of IL-1β on A) MSCs and B) pericytes isolated from the BM of BALB/c and NeuT mice at early stage of disease (12 weeks). Up-regulation of IL-1β after stimulation (30%) of C) BALB/c-derived and D) B6-derived BM-MSCs with serum collected respectively from NeuT mice and B6-mice transplanted with PyMT41c tumor cell-line or with tumor supernatant collected from E) 4T1 or F) 41c carcinoma cell lines. t test was applied for statistical analysis. The dots indicate the biological replicates for each condition. Two-tailed t test or Ordinary one-way ANOVA with Tukey's multiple comparisons test were used as statistical analysis.

To evaluate whether the release of IL-1β from MSCs was able to activate *Atf3* in HSCs, naïve HSCs (Lin- cells) were co-cultured using transwell with MSCs isolated and then differentiated *in vitro* from the compact bone of BALB/c and NeuT-tumour bearing mice (Fig 41B). FC analyses were performed to evaluate the purity of cells before the co-culture and showed a good enrichment of HSCs cells, sorted by magnetic beads (Fig 41A), and a homogenous population of MSCs (CD45-; CD29+; CD44+, Sca1+), with a low $CD45^{+}$ contamination in MSC cultures (Fig 41D).

Co-culture experiments showed that IL-1β, which is produced only by NeuT-derived MSCs (Fig 41E), is able to induce *Atf3* expression on naïve HSCs (Fig 41C).

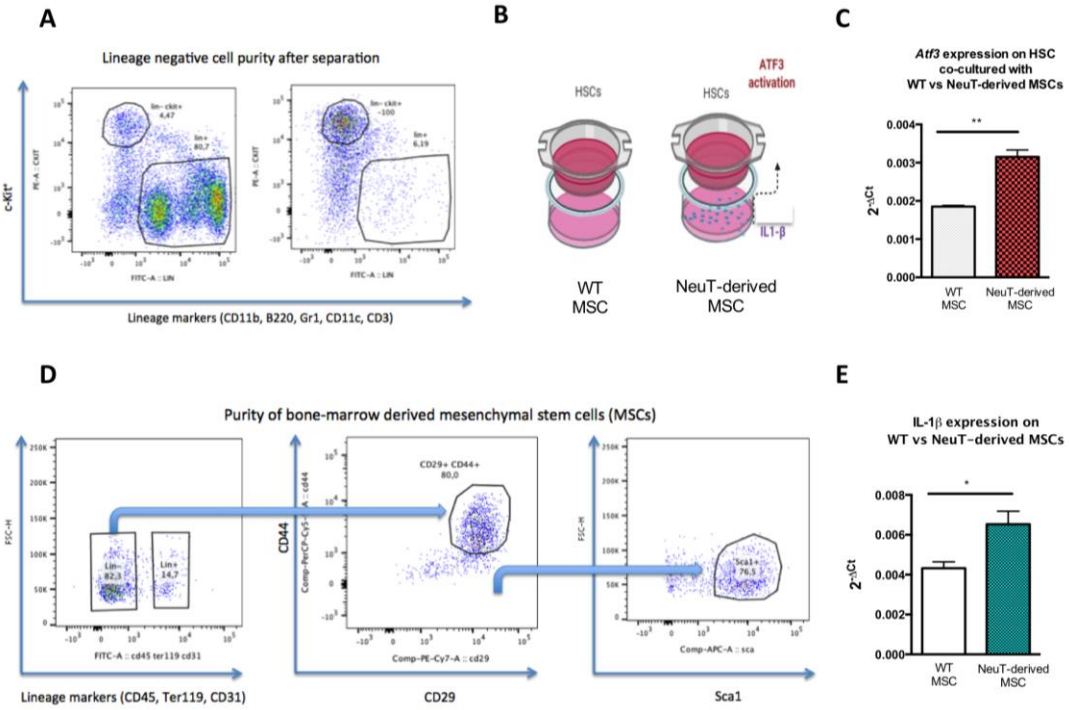

Figure 41. A) Evaluation of Lin⁻c-Kit⁺ cell purity after separation by FC analysis. c-Kit and lineage markers were employed. B) BALB/c and NeuT-derived BM-MSCs were co-cultured for 24h with naïve HSCs C) Atf3 expression on HSCs co-cultured respectively with WT (blank) vs NeuT-derived BM-MSCs (red). D) Characterization of MSCs isolated from BALB/c and NeuT mice and differentiated with MesenCult ™ MSC Basal Medium for 15 days. E) qPCR for IL-1β on BALB/c (blank) and NeuT derived (green) MSCs. For co-culture experiments three biological replicates were used. Two-tailed t test was used as statistical analysis.

To confirm that the activation of *Atf3* is specifically mediated by the release of IL-1β from MSCs, co-culture experiment was performed in presence of an anti-IL-1β antibody.

Firstly, anti-mouse IL-1β and relative isotype control were tested *in vitro* on HSCs stimulated with recombinant IL-1β. ATF3 nuclear activation on stimulated HSCs was blocked after incubation with anti-IL-1β neutralizing antibody (Fig 42A).

Then, BM-derived MSCs generated from BALB/c and NeuT mice were co-cultured with naïve HSC ± anti IL-1β antibody. After 24 hours, cells were washed and qPCR was used to evaluate *Atf3* expression on HSCs. As expected, blocking IL-1β in NeuT-derived BM-MSCs was able to inhibit *Atf3* expression on HSCs (Fig 42B). No effects were identified on HSCs co-cultured with BALB/c derived MSCs (Fig 42C).

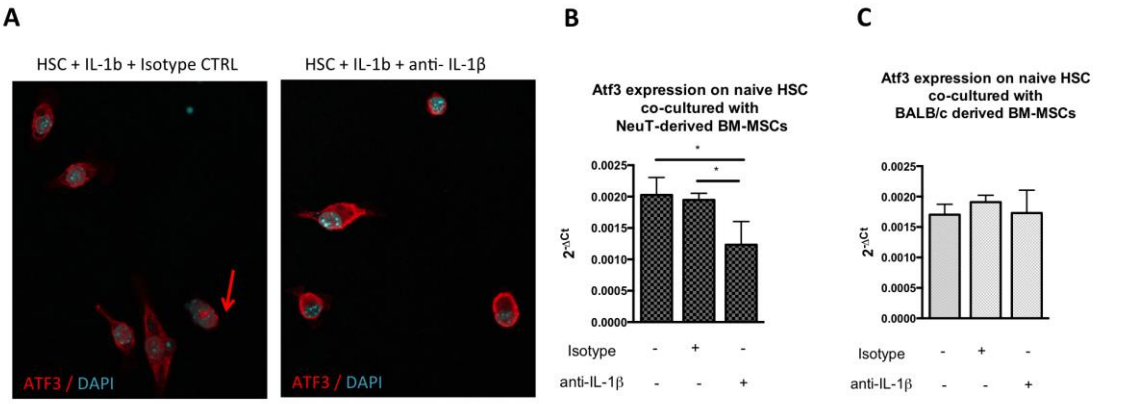

Figure 42. Neutralization studies performed with anti-IL-1β (5 ug/ml) specific for the precursor and mature secreted form of IL-1β. A) IF staining for ATF3 expression performed on naïve HSCs stimulated in vitro with recombinant IL-1β ± anti-IL-1β or isotype CTRL. Evaluation of Atf3 expression on naïve HSC co-cultured with B) NeuT-derived or C) BALB/c-derived MSCs ± anti-IL-1β or isotype CTRL. For co-culture experiments three biological replicates were used. Ordinary one-way ANOVA with Sidak's multiple comparisons test was used as statistical analysis.

These results suggest that MSCs, normally involved in the maintenance and regulation of haematopoiesis, through the release of IL-1β could activate *Atf3* expression in haematopoietic progenitor cells.

4.8) Blocking IL-1β inhibits *Atf3* activation and the emergency-myelopoiesis observed in the BM of tumour-bearing mice

In order to investigate the effects of IL-1β blockade *in vivo*, NeuT mice were treated with anti-IL-1β and relative isotype control antibodies, two times a week for four consecutive weeks starting at 12 weeks of age.

The day after the last treatment, mice were euthanized and BMs were collected in order to evaluate *Atf3* modulation on sorted immature and mature myeloid cell populations. Quantification of progenitor and mature BM cells were performed by FC analysis.

IF staining was employed to evaluate ATF3 activation and CMP/GMP clustering in treated mice.

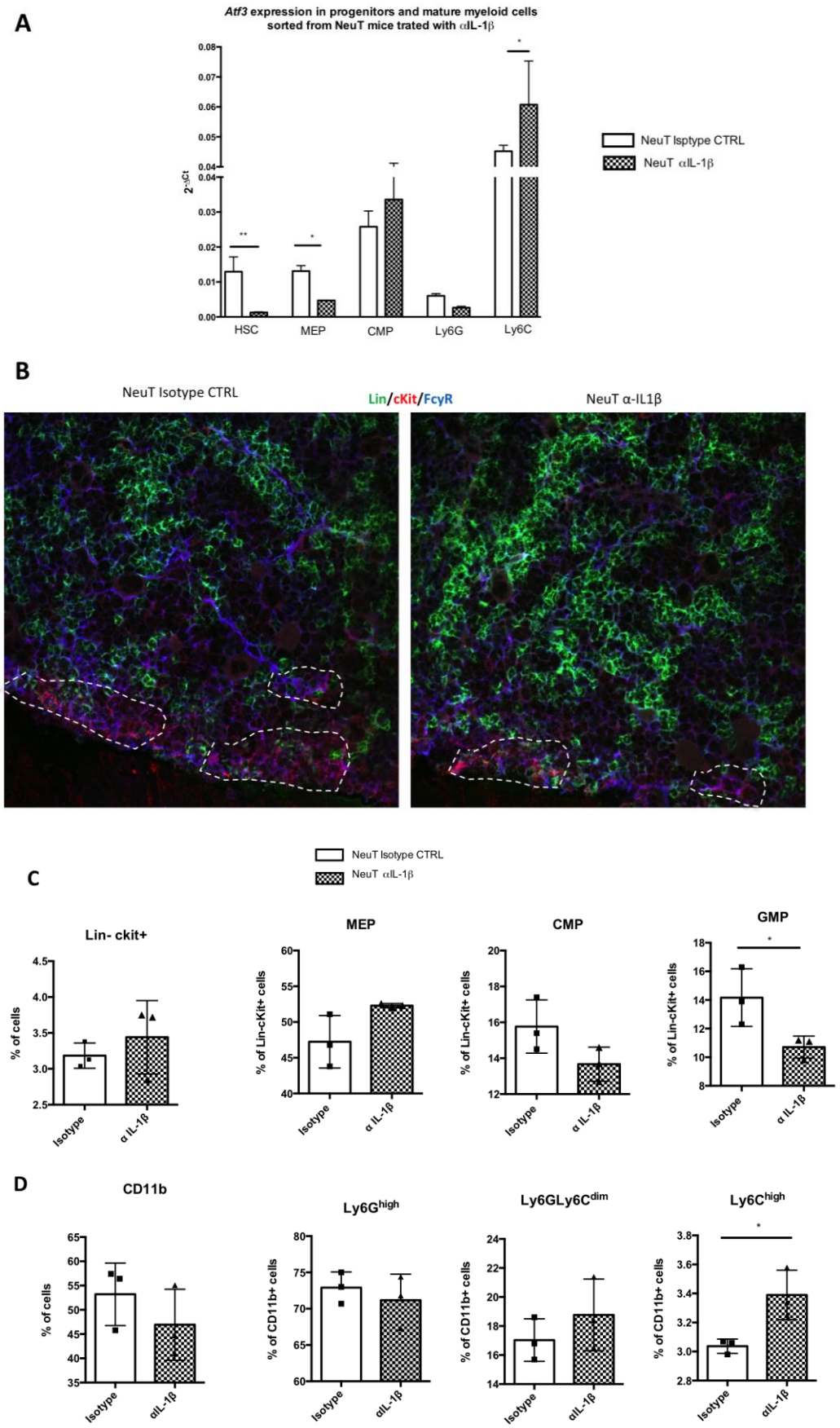

Figure 43. A) Atf3 expression on progenitor and mature myeloid cells sorted from the BM of NeuT mice, at pre-malignant stage of disease, treated or not with αIL-1β antibody for 4 weeks. In vivo experiments were performed two times (n=3 for each group). Ordinary one-way ANOVA with Sidak's multiple comparisons test was used as

statistical analysis. B) Evaluation of CMP/GMP clustering on OCT-embedded BM sections: Lin (green) c-kit (red) FcyR (blue) DAPI (cyan). FACS analysis performed on BM collected from the same animals in order to evaluate the percentage of C) progenitors and D) mature myeloid cells (n=3 for each group). Two-tailed t test was used as statistical analysis.

Blocking IL-1β in NeuT mice induces *Atf3* down-modulation in HSCs cells (Fig 43A). This modulation was associated with a substantial decrease, in the HSC fraction, of both CMP and GMP cells in NeuT-treated compared to control mice, as evaluated by both IF and FACS-analyses (Fig 43 B-C). This might suggest that *Atf3* induction in HSCs could be a necessary step toward CMP and GMP differentiation. Notably, the reduction of GMP cells after IL-1β treatment did not allow us to evaluate *Atf3* expression through qPCR, owing to the low number of FC-sorted cells.

No significant alterations were detected by FACS analysis in the number of mature CD11b+ cells (Fig 43D).

In order to evaluate whether blocking IL-1β is able also to affect tumour progression, we moved to the transplantable 41c model.

To this end, the 41c cell line was injected into the mammary fat pad of C57BL/6 mice that were treated with αIL-1β Ab starting 3 days after cell injection. Tumour onset was monitored for 33 days. At the endpoint mice were sacrificed and their BM analyzed.

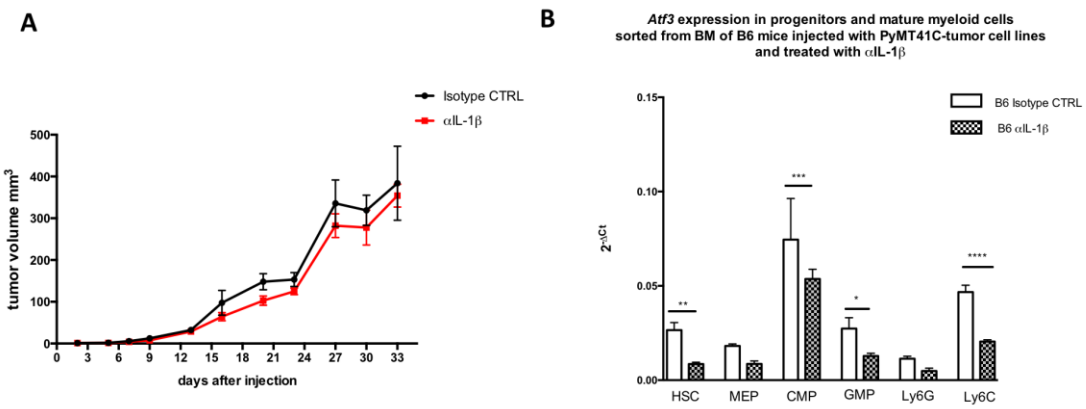

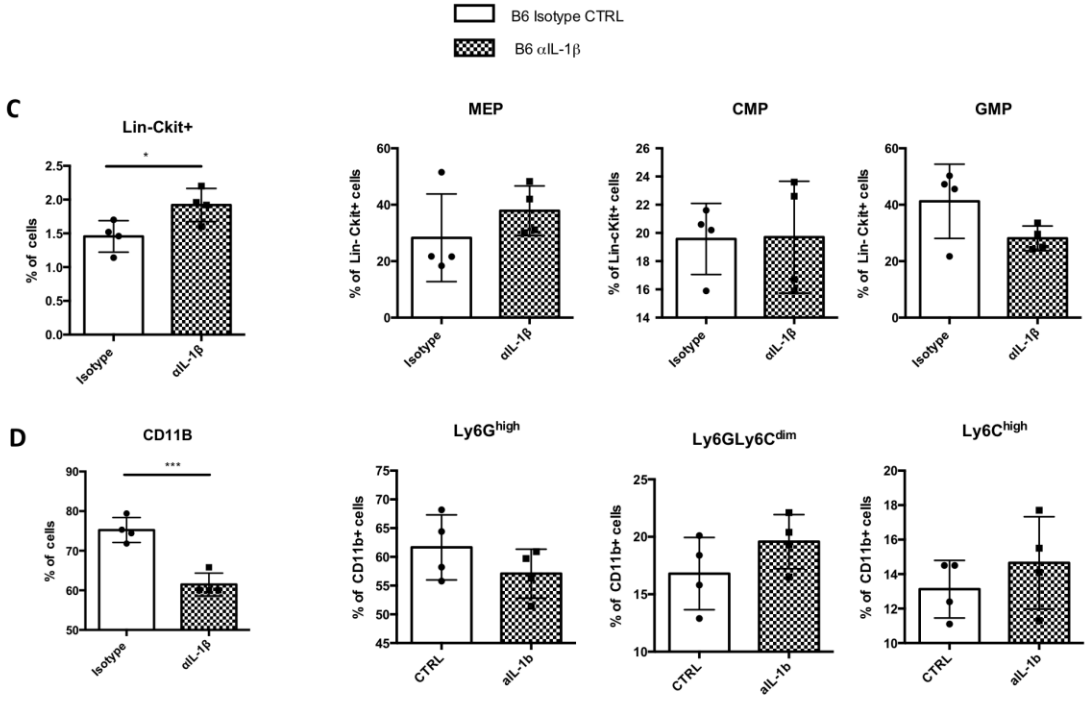

Figure 44. A) Evaluation of tumour growth measured with the following formula: (Widght² x Length)/2 on B6 mice injected with 41c tumour cell line and treated or not with αIL-1β Ab (n=4 for each group). Mutiple t test was used to compare differences along tumor progression. B) Evaluation of Atf3 expression by qPCR on sorted progenitor and mature myeloid cells. Ordinary one-way ANOVA with Sidak's multiple comparisons test was used as statistical analysis. FACS analysis performed on C) progenitors and D) mature BM cells isolated from the same animals (n=4 for each group). Two-tailed t test was used as statistical analysis.

Despite the tumour growth was very similar between the two groups (Fig 44A), we observed the down-modulation of *Atf3* expression in both immature (CMPs-GMPs) and mature (Ly6C) myeloid cells sorted from the BM of αIL-1β treated mice (Fig 44B).

Furthermore, we observed that treatment with anti-IL-1β reduces GMPs (Fig 44C) and induces a significant decrease of mature myeloid population (CD11b+) in the BM of the same mice (Fig 44D).

Collectively, results show that anti-IL-1β treatment is able to decrease *Atf3* up-regulation in both immature and mature myeloid cell populations during cancer progression and to reduce the myeloid switch occurring during tumour-induced BM emergency myelopoiesis.

At early time points in NeuT mice the treatment affected CMP/GMP clustering, a necessary step towards the establishment of emergency hematopoiesis. At late stages of tumour progression, blocking IL-1β reduced CD11b+ myeloid cell expansion.

4.9) Changes in the BM immune composition are reflected also in the primary tumour site

To assess whether the changes in immune populations observed in the BM of tumour-bearing mice at early time point were present also at the primary tumor site, the mammary glands of NeuT and control sibling mice were analyzed by flow cytometry at 12 weeks of age.

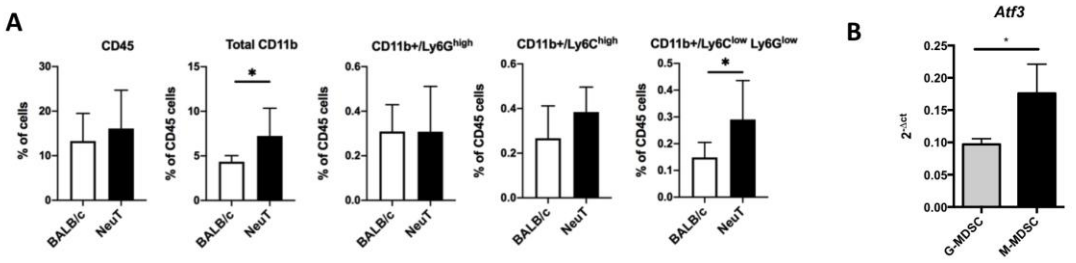

Figure 45. A) FC analysis showing changes in myeloid cells in the mammary glands of NeuT mice at 12 weeks of age (n=5 for each group). B) qPCR analysis for Atf3 expression in the two MDSC subsets (G-granulocytes and M-monocytes) isolated by immunomagnetic beads (Myeloid-derived suppressor cells isolation kit Miltenyi Biotec) from the tumours of NeuT mice (n=3).

Results showed an enrichment of myeloid cells, mainly with an immature phenotype ($CD11b^{+}/Ly6C^{low}/Ly6G^{low}$) (Fig 45A).

In addition, starting from the observation that in the BM of NeuT mice ATF3 was mainly expressed by an immature myeloid subset and that under pathologic conditions, such as cancer, immature myeloid cells are expanded and converted into myeloid-derived suppressor cells (MDSC), we analyzed *Atf3* expression in the G-MDSCs and M-MDSCs isolated by immunomagnetic beads from mammary tumors of NeuT mice.

Results showed an increase in *Atf3* expression in the M-MDSC fraction (Fig 45B).

4.10) ATF3 deletion in the myeloid compartment affects myeloid cell recruitment

To study the role of ATF3 in differentiated myeloid cells, we took advantage from the availability of $ATF3^{fl/fl}LysMCre^{+/-}$ mice (C57BL/6 background). These mice carry a deletion of the ATF3 in the myeloid compartment. Specifically, the homozygous ATF3 floxed alleles are deleted by the Cre recombinase, which expressed under the lysozyme M promoter allows generating myeloid cells (monocytes/macrophages and neutrophils) deficient for ATF3 (Fig 46A). The efficiency and specificity of LysMCre in $ATF3^{fl/fl}LysMCre^{+/-}$ mice was evaluated on sorted BM myeloid cell population and on peritoneal macrophages, isolated *ex vivo*, checking *Atf3* expression through qPCR.

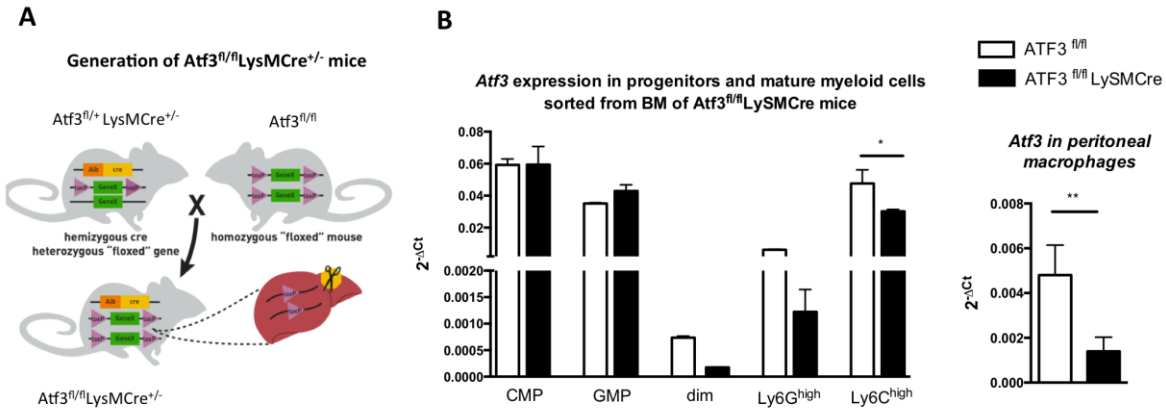

Figure 46. A) Schematic representation indicating the generation of Atf3$^{fl/fl}$LySMCre mice. Atf3$^{fl/+}$LySMCre$^{+/-}$ mice were obtained crossing Atf3$^{fl/fl}$ mice with LySMCre transgenic mouse strain. Adapted from Kim H, 2018. B) Evaluation by qPCR of the deletion efficiency of the Atf3 floxed exon in sorted BM progenitor and mature myeloid cells and in peritoneal macrophages isolated from ATF3$^{fl/fl}$ (white) and ATF3$^{fl/fl}$LySMCre (black) mice (n=5 for each group). A) Ordinary one-way ANOVA with Sidak's multiple comparisons test and two-tailed t test was used as statistical analysis.

As expected, *Atf3* expression was not abrogated in the CMP/GMP cells, however efficient recombination of the ATF3 floxed alleles was obtained in the more immature myeloid cells (Ly6GLy6C^{dim}), neutrophils (Ly6G^{high}), monocytes (Ly6C^{high}) and peritoneal macrophages (Fig 46B).

To define whether the deletion of ATF3 in the myeloid compartment was able to affect tumour progression, the 41c cell line was injected into the mammary fat pad of Atf3$^{fl/fl}$LysMCre$^{+/-}$ and Atf3$^{fl/fl}$LysMCre$^{-/-}$ (Atf3$^{fl/fl}$ thereafter) control mice.

At 30 days after cell injection mice were sacrificed, tumours and peripheral blood (PB) were analysed to assess any differences in immune cell composition.

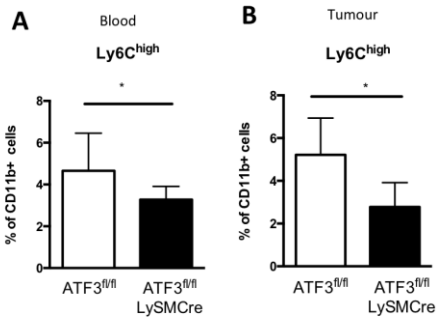

C

ID	Entrez_ Gene_ID	Symbol	logFC	P.Value	adj.P.Val	FC
ILMN_2735184	12822	Col18a1	-2.980013301	5.80E-09	0.000174987	-7.889934375
ILMN_2998658	170942	Erdr1	-3.884649228	3.56E-08	0.000304372	-14.77052528
ILMN_1240615	56177	Olfm1	-1.014484945	6.37E-08	0.000384753	-2.020181541
ILMN_2785648	246278	Cd207	-1.71098507	2.26E-06	0.004447398	-3.273842845
ILMN_2737710	21844	Tiam1	-0.843223021	5.21E-06	0.007102887	-1.794053635
ILMN_2641678	69772	Bdh2	-1.232383514	5.65E-06	0.007102887	-2.349548444
ILMN_2589768	15559	Htr2b	-1.103884738	9.76E-06	0.010390468	-2.149326621
ILMN_1250421	17381	Mmp12	-1.19264372	1.01E-05	0.010390468	-2.285712134
ILMN_2605212	102857	Slc6a8	-0.964334366	1.32E-05	0.01210602	-1.951163082

Figure 47. Quantification of monocytes (Ly6C^{high}) in the A) tumours and in the B) peripheral blood of Atf3$^{fl/fl}$ and Atf3$^{fl/fl}$LySMCre mice after injection of PyMT41C tumour cell line (n=5 for each group). Two-tailed t test was used as statistical analysis. C) Evaluation of potential ATF3 target genes based on publicly available GEP performed on WT and ATF3$^{-/-}$ BM-derived macrophages. Genes related to cell migration were highlighted in red.

Flow cytometry analyses showed a significantly decrease in monocytes (Ly6C^{high}) in the PB and in the tumours of Atf3$^{fl/fl}$LySMCre$^{+/-}$ mice (Figure 47 A-B).

This result suggests that ATF3 might be involved in the regulation of genes controlling

the release of monocytes/macrophages from the BM into the circulation.

To identify genes potentially regulated by ATF3, we looked at a publicly available gene expression profile (GSE61055) in which WT and *Atf3-/-* BM-derived macrophages were compared (Labzin L.I, 2015). We found that genes related to cell migration (*Col18a1, Erdr1, Olfm1, Tiam1*) were strongly down regulated in *Atf3-/-* macrophages (Fig 47C).

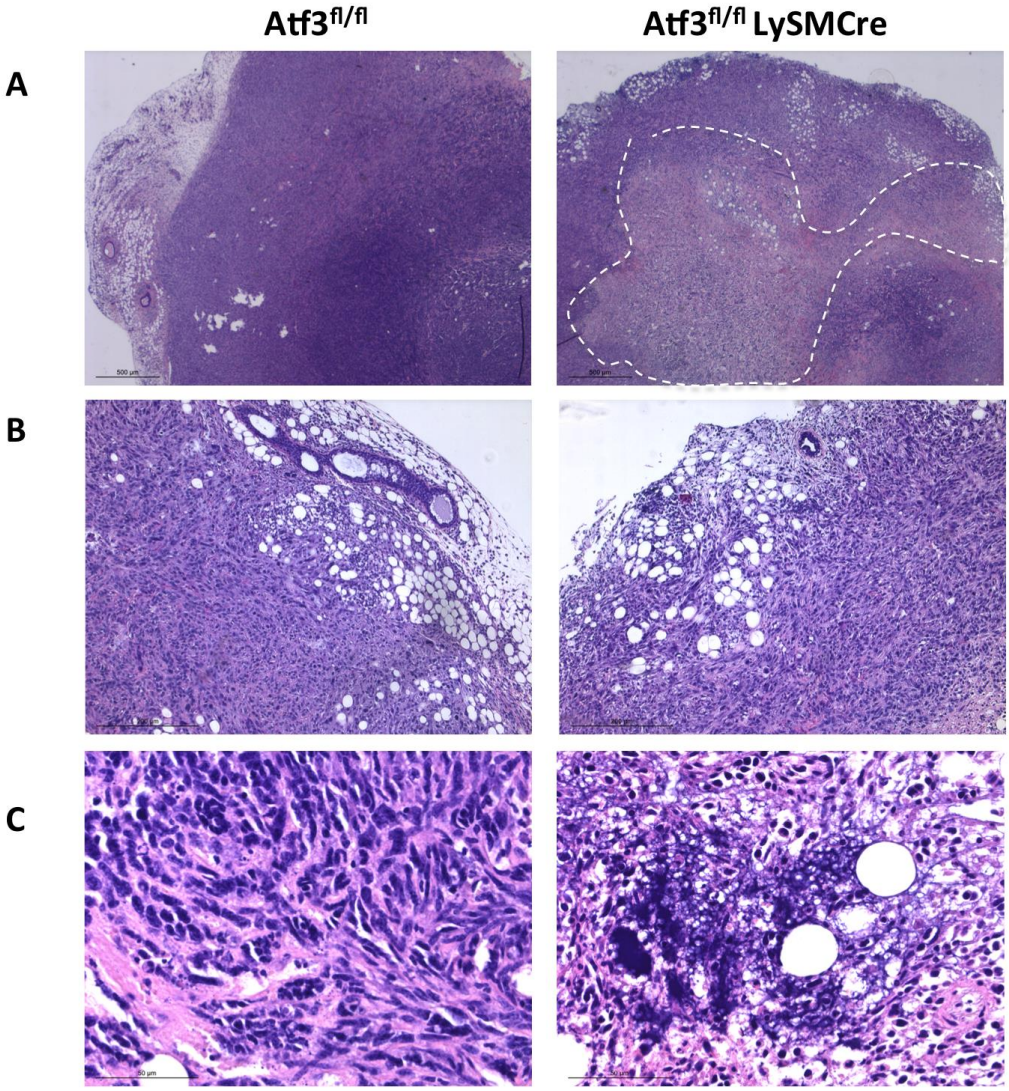

Figure 48. H&E staining performed on tumours of Atf3$^{fl/fl}$LysMCre$^{+/-}$ showing A) hypoxic and necrotic areas B) invasion margins and c) abnormal deposition of nuclear material compared to Atf3$^{fl/fl}$ control mice.

Having shown the possible role of ATF3 in promoting macrophage differentiation and migration, we next evaluated the presence of macrophages in situ in tumours obtained from Atf3$^{fl/fl}$LysMCre$^{+/-}$ and Atf3$^{fl/fl}$ control mice. IHC analysis showed a reduction in CD206+ macrophages in tumours from Atf3$^{fl/fl}$LysMCre$^{+/-}$ mice (Fig 49B). This phenotype was paralleled by morphological changes associated to the presence of larger hypoxic and necrotic areas (Fig 48A), more evident infiltrative growth with better integration with the surrounding tumour stroma and increased lymphocytes (Fig 48B) in

tumours from Atf3$^{fl/fl}$LysMCre$^{+/-}$ compared to controls. Such morphological changes on H&E sections were confirmed by IHC analysis showing higher CD8+ T cells in tumours obtained from Atf3$^{fl/fl}$LysMCre$^{+/-}$ than control mice (Fig 49 A).

Notably tumors from Atf3$^{fl/fl}$LysMCre$^{+/-}$ mice also showed areas of abnormal deposition of fibrotic nuclear material, a picture compatible with the absence of scavenger tumour-associated macrophages (TAMs) (Fig 48C).

This picture is suggestive of an overall decrease of local macrophage differentiation, which is in line with the reduced mobilization of monocytes from the BM in Atf3$^{fl/fl}$LysMCre$^{+/-}$mice.

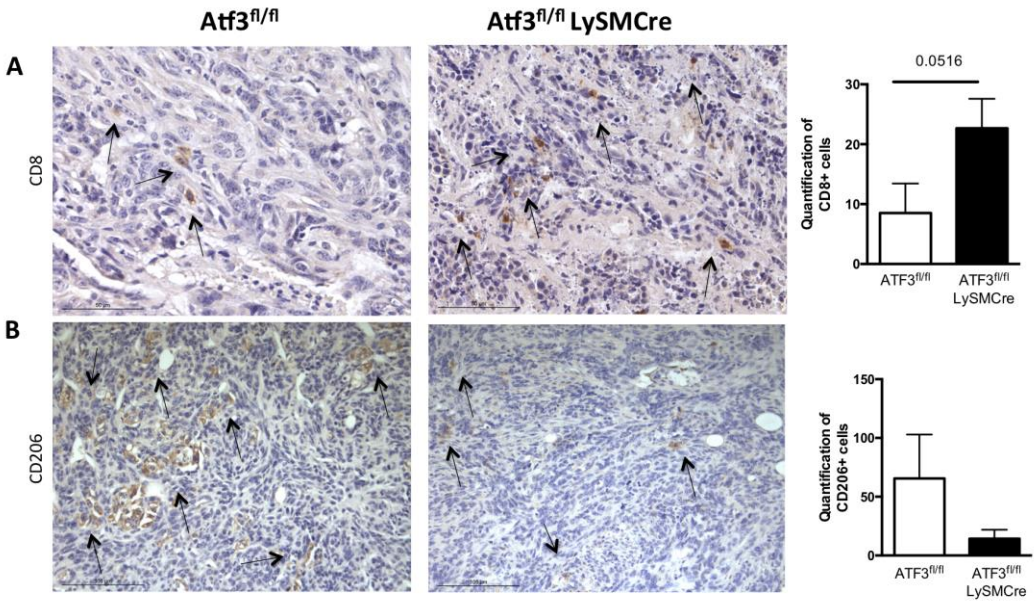

Figure 49. Immunohistochemical staining of A) CD8+ T cells and B) CD206+ macrophages in tumour sections of Atf3$^{fl/fl}$LysMCre$^{+/-}$ and relative Atf3$^{fl/fl}$ control mice injected with 41c cancer cell line (n=5 for each group). Quantification of CD8+ or CD206+ cells were performed by counting the number of positive cells out of four non-overlapping high-power (x400) microscopic field for every tumour sections. Two-tailed t test was used as statistical analysis.

As in the study from Wolford et al. in which the activity of ATF3 was characterized in TAMs, no differences in terms of tumour take and volume were observed between Atf3$^{fl/fl}$LysMCre$^{+/-}$ and control mice. In this paper they reported substantial difference in metastasis formation after injection of MVT-1 mammary carcinoma into conditional ATF3 knockout mice (Wolford CC, 2019), suggesting a role of ATF3 in metastasis formation that prompt our future analysis in a metastatic model of breast carcinoma.

4.11) *ATF3* expression in the peripheral blood is able to distinguish breast cancer patients from healthy individuals

Having shown that ATF3 is an early functional marker of tumour-induced haematopoiesis, we tested whether *Atf3* induction could be detected also in the peripheral blood. This could potentially quote *Atf3* as a circulating marker of breast transformation.

Thus, the presence of *Atf3* positive cells was evaluated on total PB cells (PBCs) collected from tumour-bearing NeuT mice at late stages of breast carcinogenesis (24 weeks), when myeloid cells (CD11b+) are significantly released into the circulation (Fig 50A).

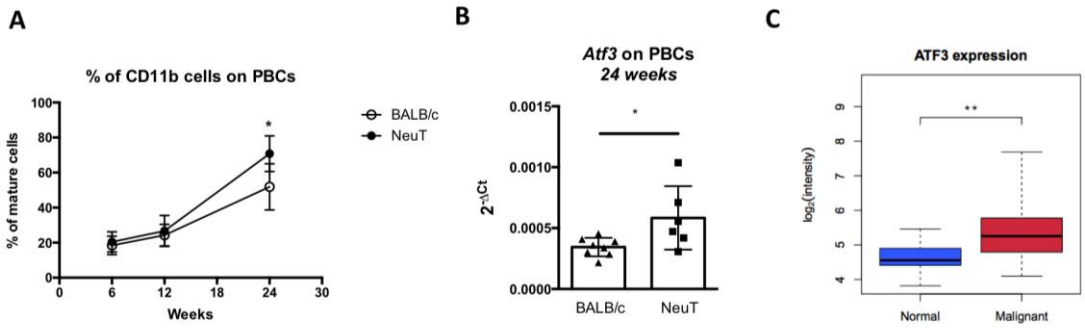

Figure 50. A) Quantification of CD11b+ cells in the blood of BALB/c (n=6) and NeuT (n=6) mice starting from 6 weeks of age. Multiple t test was used as statistical analysis. B) Atf3 expression evaluated by qPCR on total PBCs isolated from the blood of BALB/c (n=8) and NeuT mice (n=6) (24 weeks). Dots represent individual mice. Ordinary one-way ANOVA with Sidak's multiple comparisons test was used as statistical analysis. C) ATF3 expression on PBMCs collected from healthy donors (n=31) and breast cancer patients (n=57), based on GSE27562.

Results showed that *Atf3* expression evaluated by qPCR analysis was higher in the PBCs of NeuT compared to control BALB/c mice.

To investigate the translational significance of these data, *ATF3* expression was evaluated *in silico* in the PB of patients with breast cancers. To this end we analyzed a publicly available human dataset (GSE27562) (LaBreche HG, 2011) consisting of 57 patients with a diagnosis of breast cancer versus 31 healthy controls.

The analysis shows that *ATF3* is up-regulated in peripheral blood mononuclear cells (PBMCs) collected from BC patients compared to controls (fold change (FC) = -1.66563, false discovery rate (FDR) = 0.001904469) (Fig 50C).

Overall these results suggest that ATF3 induction in the BM ultimately leads to a tumour-specific release of *ATF3+* cells into the circulation, potentially making ATF3 a marker of malignant transformation that could be detected in the circulation at late time point.

To define whether *ATF3* expression could be a biomarker of breast cancer in human samples, we will analyse *ATF3* expression in PBMCs collected in our Institute from women with a benign or malignant diagnosis and from healthy donors.

5) DISCUSSION

Bone marrow (BM) is the first sensor of stress molecules that are released from peripheral tissues during infection, systemic immune activation and tumour development. These conditions alter the BM stromal activity, which is normally devoted to the maintenance of hematopoietic stem cells (HSCs) toward a reprogramming of BM haematopoiesis, and sustain the increased hematopoietic demand.

In this context, the hosting laboratory has shown that peripheral chronic immune stimulation (e.g. autoimmunity) is able to modify the BM extracellular matrix composition, mainly through the down regulation of secreted protein acidic and rich in cysteine (SPARC) and collagen-I, a condition that better supported pathological myeloproliferation in pre-leukemic mice (Tripodo C, 2017).

Growing tumours mimic low-grade chronic inflammatory conditions and are therefore potentially able to affect the BM microenvironment. Indeed, tumour-derived signals can educate the BM stromal compartment to support the expansion of immature and immune suppressive myeloid cells (Engblom C, 2017), which in turn sustain tumour growth and metastasis (Peinado H, 2012) (Casbon AJ, 2015).

Using the BALB-NeuT (NeuT thereafter) spontaneous model of mammary carcinoma we have shown the BM stromal changes characterizing initial steps of mammary transformation and that sustain the expansion of myeloid cell populations. Furthermore, we described the transcriptional reprogramming of BM hematopoietic niche during tumour development (Chiodoni C, 2020). The activating transcription factor 3 (*Atf3)* emerged among the genes significantly up modulated between NeuT and control mice, at both pre-invasive (12 weeks) and late stage (24 weeks) of disease. Further investigation indicated that *Atf3* expression in the BM correlated with the pathologic disease score, prompting the idea of ATF3 modulation supporting all the phases of tumour growth (Chiodoni C, 2020). Starting from this evidence, this project demonstrates that the induction of ATF3 in HSCs is triggered by tumour-primed BM-mesenchymal stem cells (MSCs) and represents the first signal licensing the redirection of haematopoiesis toward myeloid cell expansion, contraction of erythroid cells and reduction of B-cell lymphopoiesis. IL-1β, released at a higher levels by BM-MSCs from NeuT mice compared to controls, was responsible for ATF3 induction in HSCs. Notably, using the chronic administration of LPS, we showed that ATF3 activation in myeloid cells is a peculiarity of cancer-induced myelopoiesis, as it was not induced in

LPS-treated mice. Indeed in the BM of WT mice treated chronically with LPS, ATF3 activation was mainly confined to the osteoblastic niche. Conversely, in the BM of tumour-bearing mice, ATF3 expression was a clear characteristic of the progenitor and myeloid cell fractions.

ATF3 regulates the inflammatory response to stress signals, such as DNA damage, metabolic dysfunction, cellular injury and oxidative stress (Hai T, 1999). ATF3 is expressed at low levels under steady-state conditions; nevertheless its expression and nuclear translocation can be quickly promoted by danger signals, such as those associated with nascent tumours.

This study shows that ATF3 activation during cancer progression is a multistep process characterized by the sequential induction of ATF3 in two different subsets of BM progenitor/myeloid cells.

At early time point, corresponding to tumour onset, the nuclear translocation of ATF3 in BM progenitor (Lin-/FcγR+) cells of tumour-bearing mice promotes the formation of common myeloid/granulocyte-monocyte progenitor (CMP/GMP) clusters, which represent key features of emergency haematopoiesis (Hérault A, 2017). At late time point of tumour progression, ATF3 activation in mature monocytes drives the expansion of monocytic myeloid cells and in peripheral tissues their differentiation toward macrophages.

The involvement of ATF3 in monocyte/macrophage differentiation was supported by data showing that ATF3 expression increases during monocyte/macrophage cell differentiation and that its over-expression in BM progenitor cells enhances their ability to form monocyte/macrophage colonies in a semi-solid medium. Notably, preliminary *in vivo* data showed a low number of tumour-associated macrophages (TAMs) in PyMT41c tumour transplanted into $Atf3^{fl/fl}LysMCre^{+/-}$ mice, a result that is in line with the defective recruitment of circulating monocytes detected in the blood and in the tumours of the same mice.

This paucity in TAMs correlates with higher CD8+ T cells in tumours obtained from $Atf3^{fl/fl}LysMCre^{+/-}$ and suggests that deletion of ATF3 in the myeloid compartment could favour T cell infiltration in the tumour microenvironment and therefore antitumour immune response.

These data are also supported by chromatin-immunoprecipitation studies showing an enrichment of ATF3 binding sites on cells of monocyte lineage (Lara-Astiaso D, 2014).

Mechanistically, the effect of ATF3 on monocyte/macrophage differentiation could pass through the induction of *Irf8,* a transcription factor that drives progenitor cells to differentiate into macrophages (Friedman AD, 2007) (Strauss L, 2015).

Differently, at early time point, the induction of *Atf3* in BM progenitor cells is the result of a cross talk between MSCs and HSCs, governed by IL-1β.

Blocking IL-1β directly into NeuT mice at tumour onset impaired CMP/GMP clustering, along with ATF3 activation in HSCs. As CMP/GMP clustering is a necessary step towards myeloid cell differentiation, *in vivo* blockade of IL-1β, at late stage in transplantable PyMT41c mouse model, decreased the expansion of CD11b+ cells. This data is in line with that from Kaplanov et al. demonstrating that injection of 4T1 (BALB/c background) and PyMT (C57BL/6 background) breast cancer cell lines into *Il-1β*-deficient mice decreased the recruitment of CCR2+ myeloid cells also impairing their differentiation into immunosuppressive macrophages, a mechanism that favoured T cell-mediated immunity (Kaplanov I, 2019).

The formation of CMP/GMP clusters has been described for the first time during the development of hematologic malignancies (Hérault A, 2017). The relevance of ATF3 in leukemia is supported by recent data showing that ATF3 promotes leukemia cell cycling, survival and differentiation (Di Marcantonio D, 2021). Interestingly, the underlying mechanism could be similar to that described in the NeuT model and involving IL-1β. Accordingly, Carey et al. showed that an IL1-rich environment is able to promote cell expansion and disease progression in AML patients (Carey A, 2017). This observation fits well with the concept that myeloid cell expansion in solid tumours is the normal "non mutated" counterpart of AML blasts. Therefore, mechanisms sustaining myeloid cell expansion and differentiation could be maintained in AML cells. For example, leukemic blasts retain ad use to suppress Arginase II, a prototypical suppressive molecule produced by myeloid-derived suppressor cells (Mussai F, 2013).

Overall these data suggest that ATF3 is a key relevant and functional player of cancer associated myelopoiesis. However, at translational level, targeting ATF3, as well as other transcription factors, could be difficult to be achieved pharmacologically. Therefore the inhibition of the upstream regulators could be doable, as in the case of IL-1β, according to the Canakinumab Anti-inflammatory Thrombosis Outcomes Study (CANTOS) that showed reduced incidence of lung cancer in patients with atherosclerosis treated with anti-IL-1β monoclonal Ab (Ridker PM, 2017).

Benefits were identified also in breast cancer patients. Indeed, an IL-1 signature has been identified in Her-2 negative breast cancer with a poor prognosis and treatment with anti-IL-1R antagonist, anakinra, reduced the expression of inflammatory genes in peripheral blood leukocytes while increased the expression of several natural killer and cytotoxic T cell genes (Wu TC, 2018).

One additional emerging observation that remains to be investigated is the activation of ATF3 at early time point of NeuT tumourigenesis in perivascular stromal cells. This feature might suggest the presence of another step in cancer-induced haematopoiesis, which implies the induction of ATF3 in these peculiar mesenchymal elements. It is unclear whether such induction is due to the direct sensing of signals from the site of tumour onset or is a consequence for the mesenchymal rearrangement occurring in the BM, also due to SPARC down-modulation (Chiodoni C, 2020). Thus, the next step of this work will test the role of ATF3 in mesenchymal cells and the presence in the laboratory of Leptin receptor Cre (LepR-Cre) mice, to be crossed with $Atf3^{fl/fl}$ mice, will help answering to this question (Ding L, 2013).

In summary, the findings of this project identify ATF3 as a relevant transcription factor that, activated by tumour-primed BM-MSCs, redirects BM haematopoiesis toward myeloid cells expansion. Furthermore, the identification of the IL-1β as a key inflammatory cytokine that promotes ATF3 activation in the BM niche, provides the rationale for novel strategies able to prevent its activation.

Despite the relevance of IL-1β/ATF3 signaling pathway, strictly involved in driving a cancer-adapted myelopiesis, was demonstrated only in a pre-clinical setting, this thesis, in line with the recent literature, supports the rational to test the effective therapeutic benefits of IL-1β inhibition in breast cancer patients.

Of note, the preliminary data obtained with this work also allow us to propose ATF3 as a new marker for breast cancer transformation. Indeed the release of ATF3 positive myeloid cells from the BM during breast cancer transformation, in line with data showing *ATF3* up-modulation in the peripheral blood mononuclear cells collected from tumour-bearing NeuT mice and validated *in silico* in breast cancer patients, suggest us to test the relevance of ATF3 as predictive circulating marker in a clinical setting.

6) BIBLIOGRAPHY

1. Ahn GO, Tseng D, Liao CH, Dorie MJ, Czechowicz A, Brown JM. Inhibition of Mac-1 (CD11b/CD18) enhances tumor response to radiation by reducing myeloid cell recruitment. Proc Natl Acad Sci U S A. 2010;107(18):8363-8368. doi:10.1073/pnas.0911378107
2. Akashi K, Traver D, Miyamoto T, Weissman IL. A clonogenic common myeloid progenitor that gives rise to all myeloid lineages. Nature. 2000;404(6774):193-197. doi:10.1038/35004599
3. Baldridge MT, King KY, Boles NC, Weksberg DC, Goodell MA. Quiescent haematopoietic stem cells are activated by IFN-gamma in response to chronic infection. Nature. 2010;465(7299):793-797. doi:10.1038/nature09135
4. Balduino A, Mello-Coelho V, Wang Z, et al. Molecular signature and in vivo behavior of bone marrow endosteal and subendosteal stromal cell populations and their relevance to hematopoiesis. Exp Cell Res. 2012;318(19):2427-2437. doi:10.1016/j.yexcr.2012.07.009
5. Barnard ME, Boeke CE, Tamimi RM. Established breast cancer risk factors and risk of intrinsic tumor subtypes. Biochim Biophys Acta. 2015;1856(1):73-85. doi:10.1016/j.bbcan.2015.06.002
6. Basu S, Hodgson G, Zhang HH, Katz M, Quilici C, Dunn AR. "Emergency" granulopoiesis in G-CSF-deficient mice in response to Candida albicans infection. Blood. 2000;95(12):3725-3733.
7. Bergenfelz C, Larsson AM, von Stedingk K, et al. Systemic Monocytic-MDSCs Are Generated from Monocytes and Correlate with Disease Progression in Breast Cancer Patients. PLoS One. 2015;10(5):e0127028. Published 2015 May 20. doi:10.1371/journal.pone.0127028
8. Bergers G, Benjamin LE. Tumorigenesis and the angiogenic switch. Nat Rev Cancer. 2003;3(6):401-410. doi:10.1038/nrc1093
9. Berns, A. Turning on tumors to study cancer progression. Nat Med 5, 989–990 (1999). https://doi.org/10.1038/12421
10. Biswas SK, Mantovani A. Macrophage plasticity and interaction with lymphocyte subsets: cancer as a paradigm. Nat Immunol. 2010;11(10):889-896. doi:10.1038/ni.1937
11. Blank U, Karlsson G, Karlsson S. Signaling pathways governing stem-cell fate. Blood. 2008;111(2):492-503. doi:10.1182/blood-2007-07-075168
12. Boespflug ND, Kumar S, McAlees JW, et al. ATF3 is a novel regulator of mouse neutrophil migration. Blood. 2014;123(13):2084-2093. doi:10.1182/blood-2013-06-510909
13. Boettcher S, Gerosa RC, Radpour R, et al. Endothelial cells translate pathogen signals into G-CSF-driven emergency granulopoiesis. Blood. 2014;124(9):1393-1403. doi:10.1182/blood-2014-04-570762
14. Boggio K, Nicoletti G, Di Carlo E, et al. Interleukin 12-mediated prevention of spontaneous mammary adenocarcinomas in two lines of Her-2/neu transgenic mice. J Exp Med. 1998;188(3):589-596. doi:10.1084/jem.188.3.589
15. Bolli E, Movahedi K, Laoui D, Van Ginderachter JA. Novel insights in the regulation and function of macrophages in the tumor microenvironment. Curr Opin Oncol. 2017;29(1):55-61. doi:10.1097/CCO.0000000000000344

16. Borst J, Ahrends T, Bąbała N, Melief CJM, Kastenmüller W. CD4+ T cell help in cancer immunology and immunotherapy. Nat Rev Immunol. 2018;18(10):635-647. doi:10.1038/s41577-018-0044-0
17. Boulais PE, Frenette PS. Making sense of hematopoietic stem cell niches. Blood. 2015;125(17):2621-2629. doi:10.1182/blood-2014-09-570192
18. Branda CS, Dymecki SM. Talking about a revolution: The impact of site-specific recombinases on genetic analyses in mice. Dev Cell. 2004;6(1):7-28. doi:10.1016/s1534-5807(03)00399-x
19. Bronte V, Brandau S, Chen SH, et al. Recommendations for myeloid-derived suppressor cell nomenclature and characterization standards. Nat Commun. 2016;7:12150. Published 2016 Jul 6. doi:10.1038/ncomms12150
20. Bruger AM, Dorhoi A, Esendagli G, et al. How to measure the immunosuppressive activity of MDSC: assays, problems and potential solutions. Cancer Immunol Immunother. 2019;68(4):631-644. doi:10.1007/s00262-018-2170-8
21. Bui JD, Schreiber RD. Cancer immunosurveillance, immunoediting and inflammation: independent or interdependent processes?. Curr Opin Immunol. 2007;19(2):203-208. doi:10.1016/j.coi.2007.02.001
22. Burstein HJ, Polyak K, Wong JS, Lester SC, Kaelin CM. Ductal carcinoma in situ of the breast.N Engl J Med. 2004;350(14):1430-1441. doi:10.1056/NEJMra031301
23. Butcher DT, Alliston T, Weaver VM. A tense situation: forcing tumour progression. Nat Rev Cancer. 2009;9(2):108-122. doi:10.1038/nrc2544
24. Byrne AT, Alférez DG, Amant F, et al. Interrogating open issues in cancer precision medicine with patient-derived xenografts [published correction appears in Nat Rev Cancer. 2017 Sep 15;:]. Nat Rev Cancer. 2017;17(4):254-268. doi:10.1038/nrc.2016.140
25. Cain DW, Snowden PB, Sempowski GD, Kelsoe G. Inflammation triggers emergency granulopoiesis through a density-dependent feedback mechanism. PLoS One. 2011;6(5):e19957. doi:10.1371/journal.pone.0019957
26. Calvi LM, Adams GB, Weibrecht KW, et al. Osteoblastic cells regulate the haematopoietic stem cell niche. Nature. 2003;425(6960):841-846. doi:10.1038/nature02040
27. Canton J, Neculai D, Grinstein S. Scavenger receptors in homeostasis and immunity. Nat Rev Immunol. 2013;13(9):621-634. doi:10.1038/nri3515
28. Carey A, Edwards DK 5th, Eide CA, et al. Identification of Interleukin-1 by Functional Screening as a Key Mediator of Cellular Expansion and Disease Progression in Acute Myeloid Leukemia. Cell Rep. 2017;18(13):3204-3218. doi:10.1016/j.celrep.2017.03.018
29. Casbon AJ, Reynaud D, Park C, et al. Invasive breast cancer reprograms early myeloid differentiation in the bone marrow to generate immunosuppressive neutrophils. Proc Natl Acad Sci U S A. 2015;112(6):E566-E575. doi:10.1073/pnas.1424927112
30. Cassetta L, Fragkogianni S, Sims AH, et al. Human Tumor-Associated Macrophage and Monocyte Transcriptional Landscapes Reveal Cancer-Specific Reprogramming, Biomarkers, and Therapeutic Targets. Cancer Cell. 2019;35(4):588-602.e10. doi:10.1016/j.ccell.2019.02.009
31. Caton ML, Smith-Raska MR, Reizis B. Notch-RBP-J signaling controls the homeostasis of CD8- dendritic cells in the spleen. J Exp Med. 2007;204(7):1653-1664. doi:10.1084/jem.20062648
32. Cha YJ, Koo JS. Role of Tumor-Associated Myeloid Cells in Breast Cancer. Cells. 2020;9(8):1785. Published 2020 Jul 27. doi:10.3390/cells9081785

33. Challen, G. A., Boles, N., Lin, K. K-Y., & Goodell, M. A. (2009). Mouse hematopoietic stem cell identification and analysis. Cytometry Part A, 75(1), 14 - 24.https://doi.org/10.1002/cyto.a.20674
34. Chaudhuri O, Koshy ST, Branco da Cunha C, et al. Extracellular matrix stiffness and composition jointly regulate the induction of malignant phenotypes in mammary epithelium. Nat Mater. 2014;13(10):970-978. doi:10.1038/nmat4009
35. Chavakis T, Mitroulis I, Hajishengallis G. Hematopoietic progenitor cells as integrative hubs for adaptation to and fine-tuning of inflammation. Nat Immunol. 2019;20(7):802-811. doi:10.1038/s41590-019-0402-5
36. Cheers C, Haigh AM, Kelso A, Metcalf D, Stanley ER, Young AM. Production of colony-stimulating factors (CSFs) during infection: separate determinations of macrophage-, granulocyte-, granulocyte-macrophage-, and multi-CSFs. Infect Immun. 1988;56(1):247-251. doi:10.1128/iai.56.1.247-251.1988
37. Chen BP, Liang G, Whelan J, Hai T. ATF3 and ATF3 delta Zip. Transcriptional repression versus activation by alternatively spliced isoforms. J Biol Chem. 1994;269(22):15819-15826.
38. Chen BP, Wolfgang CD, Hai T. Analysis of ATF3, a transcription factor induced by physiological stresses and modulated by gadd153/Chop10.Mol Cell Biol. 1996;16(3):1157-1168. doi:10.1128/MCB.16.3.1157
39. Chiodoni C, Iezzi M, Guiducci C, et al. Triggering CD40 on endothelial cells contributes to tumor growth. J Exp Med. 2006;203(11):2441-2450. doi:10.1084/jem.20060844
40. Chiodoni C, Cancila V, Renzi TA, et al. Transcriptional Profiles and Stromal Changes Reveal Bone Marrow Adaptation to Early Breast Cancer in Association with Deregulated Circulating microRNAs. Cancer Res. 2020;80(3):484-498. doi:10.1158/0008-5472.CAN-19-1425
41. Chittezhath M, Dhillon MK, Lim JY, et al. Molecular profiling reveals a tumor-promoting phenotype of monocytes and macrophages in human cancer progression. Immunity. 2014;41(5):815-829. doi:10.1016/j.immuni.2014.09.014
42. Chow A, Lucas D, Hidalgo A, et al. Bone marrow CD169+ macrophages promote the retention of hematopoietic stem and progenitor cells in the mesenchymal stem cell niche. J Exp Med. 2011;208(2):261-271. doi:10.1084/jem.20101688
43. Clausen, B., Burkhardt, C., Reith, W. et al. Conditional gene targeting in macrophages and granulocytes using LysMcre mice. Transgenic Res 8, 265–277 (1999). https://doi.org/10.1023/A:1008942828960
44. Collaborative Group on Hormonal Factors in Breast Cancer. "Breast cancer and breastfeeding: collaborative reanalysis of individual data from 47 epidemiological studies in 30 countries, including 50302 women with breast cancer and 96973 women without the disease." Lancet (London, England) vol. 360,9328 (2002): 187-95. doi:10.1016/S0140-6736(02)09454-0
45. Colmone A, Amorim M, Pontier AL, Wang S, Jablonski E, Sipkins DA. Leukemic cells create bone marrow niches that disrupt the behavior of normal hematopoietic progenitor cells. Science. 2008;322(5909):1861-1865. doi:10.1126/science.1164390
46. Cordeiro Gomes A, Hara T, Lim VY, et al. Hematopoietic Stem Cell Niches Produce Lineage-Instructive Signals to Control Multipotent Progenitor Differentiation. Immunity. 2016;45(6):1219-1231. doi:10.1016/j.immuni.2016.11.004
47. Costa A, Kieffer Y, Scholer-Dahirel A, et al. Fibroblast Heterogeneity and Immunosuppressive Environment in Human Breast Cancer. Cancer Cell. 2018;33(3):463-479.e10. doi:10.1016/j.ccell.2018.01.011

48. Coughlin SS. Epidemiology of Breast Cancer in Women. Adv Exp Med Biol. 2019;1152:9-29. doi: 10.1007/978-3-030-20301-6_2. PMID: 31456177.
49. Cullen SJ, Fatemie S, Ladiges W. Breast tumor cells primed by endoplasmic reticulum stress remodel macrophage phenotype.Am J Cancer Res. 2013;3(2):196-210. Published 2013 Apr 3.
50. Curiel TJ, Coukos G, Zou L, et al. Specific recruitment of regulatory T cells in ovarian carcinoma fosters immune privilege and predicts reduced survival. Nat Med. 2004;10(9):942-949. doi:10.1038/nm1093
51. Curtis C, Shah SP, Chin SF, et al. The genomic and transcriptomic architecture of 2,000 breast tumours reveals novel subgroups. Nature. 2012;486(7403):346-352. Published 2012 Apr 18. doi:10.1038/nature10983
52. Dahl R, Walsh JC, Lancki D, et al. Regulation of macrophage and neutrophil cell fates by the PU.1:C/EBPalpha ratio and granulocyte colony-stimulating factor. Nat Immunol. 2003;4(10):1029-1036. doi:10.1038/ni973
53. Day CP, Merlino G, Van Dyke T. Preclinical mouse cancer models: a maze of opportunities and challenges. Cell. 2015;163(1):39-53. doi:10.1016/j.cell.2015.08.068
54. De Palma M, Naldini L. Transduction of a gene expression cassette using advanced generation lentiviral vectors. Methods Enzymol. 2002;346:514-529. doi:10.1016/s0076-6879(02)46074-0
55. DeNardo DG, Ruffell B. Macrophages as regulators of tumour immunity and immunotherapy. Nat Rev Immunol. 2019;19(6):369-382. doi:10.1038/s41577-019-0127-6
56. Deutsch PJ, Hoeffler JP, Jameson JL, Habener JF. Cyclic AMP and phorbol ester-stimulated transcription mediated by similar DNA elements that bind distinct proteins. Proc Natl Acad Sci U S A. 1988;85(21):7922-7926. doi:10.1073/pnas.85.21.7922
57. Di Nicola M, Carlo-Stella C, Magni M, et al. Human bone marrow stromal cells suppress T-lymphocyte proliferation induced by cellular or nonspecific mitogenic stimuli. Blood. 2002;99(10):3838-3843. doi:10.1182/blood.v99.10.3838
58. Diaz-Montero CM, Salem ML, Nishimura MI, Garrett-Mayer E, Cole DJ, Montero AJ. Increased circulating myeloid-derived suppressor cells correlate with clinical cancer stage, metastatic tumor burden, and doxorubicin-cyclophosphamide chemotherapy. Cancer Immunol Immunother. 2009;58(1):49-59. doi:10.1007/s00262-008-0523-4
59. Ding L, Morrison SJ. Haematopoietic stem cells and early lymphoid progenitors occupy distinct bone marrow niches [published correction appears in Nature. 2014 Oct 9;514(7521):262].Nature. 2013;495(7440):231-235. doi:10.1038/nature11885
60. Di Marcantonio D, Martinez E, Kanefsky JS, et al. ATF3 coordinates serine and nucleotide metabolism to drive cell cycle progression in acute myeloid leukemia. Mol Cell. 2021;81(13):2752-2764.e6. doi:10.1016/j.molcel.2021.05.008
61. Doulatov S, Notta F, Laurenti E, Dick JE. Hematopoiesis: a human perspective. Cell Stem Cell. 2012;10(2):120-136. doi:10.1016/j.stem.2012.01.006
62. Eferl R, Wagner EF. AP-1: a double-edged sword in tumorigenesis. Nat Rev Cancer. 2003;3(11):859-868. doi:10.1038/nrc1209
63. Ehninger A, Trumpp A. The bone marrow stem cell niche grows up: mesenchymal stem cells and macrophages move in. J Exp Med. 2011;208(3):421-428. doi:10.1084/jem.20110132
64. Elston CW, Ellis IO. Pathological prognostic factors in breast cancer. I. The value of histological grade in breast cancer: experience from a large study with long-term

follow-up.Histopathology. 1991;19(5):403-410. doi:10.1111/j.1365-2559.1991.tb00229.x
65. Endogenous Hormones and Breast Cancer Collaborative Group et al. “Sex hormones and risk of breast cancer in premenopausal women: a collaborative reanalysis of individual participant data from seven prospective studies.” The Lancet. Oncologyvol. 14,10 (2013): 1009-19. doi:10.1016/S1470-2045(13)70301-2
66. Engblom C, Pfirschke C, Zilionis R, et al. Osteoblasts remotely supply lung tumors with cancer-promoting SiglecFhigh neutrophils.Science. 2017;358(6367):eaal5081. doi:10.1126/science.aal5081
67. Farhood B, Najafi M, Mortezaee K. CD8+ cytotoxic T lymphocytes in cancer immunotherapy: A review. J Cell Physiol. 2019;234(6):8509-8521. doi:10.1002/jcp.27782
68. Fisher GH, Orsulic S, Holland E, et al. Development of a flexible and specific gene delivery system for production of murine tumor models. Oncogene. 1999;18(38):5253-5260. doi:10.1038/sj.onc.1203087
69. Friedman AD. Transcriptional control of granulocyte and monocyte development. Oncogene. 2007;26(47):6816-6828. doi:10.1038/sj.onc.1210764
70. Gabrilovich DI, Nagaraj S. Myeloid-derived suppressor cells as regulators of the immune system. Nat Rev Immunol. 2009;9(3):162-174. doi:10.1038/nri2506
71. Gabrilovich, D. I., Ostrand-Rosenberg, S., & Bronte, V. (2012). Coordinated regulation of myeloid cells by tumours. Nature reviews. Immunology, 12(4), 253–268. https://doi.org/10.1038/nri3175
72. Garrett TP, McKern NM, Lou M, et al. The crystal structure of a truncated ErbB2 ectodomain reveals an active conformation, poised to interact with other ErbB receptors. Mol Cell. 2003;11(2):495-505. doi:10.1016/s1097-2765(03)00048-0
73. Ge Y, Ahn D, Stricklett PK, et al. Collecting duct-specific knockout of endothelin-1 alters vasopressin regulation of urine osmolality. Am J Physiol Renal Physiol. 2005;288(5):F912-F920. doi:10.1152/ajprenal.00432.2004
74. Geissmann F, Jung S, Littman DR. Blood monocytes consist of two principal subsets with distinct migratory properties. Immunity. 2003;19(1):71-82. doi:10.1016/s1074-7613(03)00174-2
75. Gengenbacher N, Singhal M, Augustin HG. Preclinical mouse solid tumour models: status quo, challenges and perspectives. Nat Rev Cancer. 2017;17(12):751-765. doi:10.1038/nrc.2017.92
76. Gilchrist M, Henderson WR Jr, Clark AE, et al. Activating transcription factor 3 is a negative regulator of allergic pulmonary inflammation. J Exp Med. 2008;205(10):2349-2357. doi:10.1084/jem.20072254
77. Gilchrist M, Thorsson V, Li B, et al. Systems biology approaches identify ATF3 as a negative regulator of Toll-like receptor 4 [published correction appears in Nature. 2008 Feb 21;451(7181):1022. Roach, Jared C [added]].Nature. 2006;441(7090):173-178. doi:10.1038/nature04768
78. Gough PJ, Gordon S, Greaves DR. The use of human CD68 transcriptional regulatory sequences to direct high-level expression of class A scavenger receptor in macrophages in vitro and in vivo. Immunology. 2001;103(3):351-361. doi:10.1046/j.1365-2567.2001.01256.x
79. Greenbaum AM, Link DC. Mechanisms of G-CSF-mediated hematopoietic stem and progenitor mobilization. Leukemia. 2011;25(2):211-217. doi:10.1038/leu.2010.248
80. Hai T, Wolfgang CD, Marsee DK, Allen AE, Sivaprasad U. ATF3 and stress responses. Gene Expr. 1999;7(4-6):321-335.

81. Hai T. The ATF transcription factors in cellular adaptive responses. In Gene Expression and Regulation, a Current Scientific Frontiers Book. (Ma, J., ed.). 2006
82. Hamm A, Prenen H, Van Delm W, et al. Tumour-educated circulating monocytes are powerful candidate biomarkers for diagnosis and disease follow-up of colorectal cancer. Gut. 2016;65(6):990-1000. doi:10.1136/gutjnl-2014-308988
83. Hanahan D, Weinberg RA. The hallmarks of cancer. Cell. 2000;100(1):57-70. doi:10.1016/s0092-8674(00)81683-9
84. Harbeck N, Penault-Llorca F, Cortes J, et al. Breast cancer. Nat Rev Dis Primers. 2019;5(1):66. Published 2019 Sep 23. doi:10.1038/s41572-019-0111-2
85. Hashimoto Y, Zhang C, Kawauchi J, et al. An alternatively spliced isoform of transcriptional repressor ATF3 and its induction by stress stimuli. Nucleic Acids Res. 2002;30(11):2398-2406. doi:10.1093/nar/30.11.2398
86. Haverkamp JM, Crist SA, Elzey BD, Cimen C, Ratliff TL. In vivo suppressive function of myeloid-derived suppressor cells is limited to the inflammatory site. Eur J Immunol. 2011;41(3):749-759. doi:10.1002/eji.201041069
87. Hawila E, Razon H, Wildbaum G, et al. CCR5 Directs the Mobilization of CD11b+Gr1+Ly6Clow Polymorphonuclear Myeloid Cells from the Bone Marrow to the Blood to Support Tumor Development. Cell Rep. 2017;21(8):2212-2222. doi:10.1016/j.celrep.2017.10.104
88. Hayashi T, Fujita K, Nojima S, et al. Peripheral blood monocyte count reflecting tumor-infiltrating macrophages is a predictive factor of adverse pathology in radical prostatectomy specimens. Prostate. 2017;77(14):1383-1388. doi:10.1002/pros.23398
89. Heissig B, Hattori K, Dias S, et al. Recruitment of stem and progenitor cells from the bone marrow niche requires MMP-9 mediated release of kit-ligand. Cell. 2002;109(5):625-637. doi:10.1016/s0092-8674(02)00754-7
90. Hérault A, Binnewies M, Leong S, et al. Myeloid progenitor cluster formation drives emergency and leukaemic myelopoiesis. Nature. 2017;544(7648):53-58. doi:10.1038/nature21693
91. Hirai H, Zhang P, Dayaram T, et al. C/EBPbeta is required for 'emergency' granulopoiesis. Nat Immunol. 2006;7(7):732-739. doi:10.1038/ni1354
92. Hirai H, Yokota A, Tamura A, Sato A, Maekawa T. Non-steady-state hematopoiesis regulated by the C/EBPβ transcription factor. Cancer Sci. 2015;106(7):797-802. doi:10.1111/cas.12690
93. Hoover-Plow J, Gong Y. Challenges for heart disease stem cell therapy. Vasc Health Risk Manag. 2012;8:99-113. doi: 10.2147/VHRM.S25665. Epub 2012 Feb 17. PMID: 22399855; PMCID: PMC3295632.
94. Jiang HY, Wek SA, McGrath BC, et al. Activating transcription factor 3 is integral to the eukaryotic initiation factor 2 kinase stress response. Mol Cell Biol. 2004;24(3):1365-1377. doi:10.1128/MCB.24.3.1365-1377.2004
95. Kanayama M, Xu S, Danzaki K, et al. Skewing of the population balance of lymphoid and myeloid cells by secreted and intracellular osteopontin. Nat Immunol. 2017;18(9):973-984. doi:10.1038/ni.3791
96. Kaplanov I, Carmi Y, Kornetsky R, et al. Blocking IL-1β reverses the immunosuppression in mouse breast cancer and synergizes with anti-PD-1 for tumor abrogation. Proc Natl Acad Sci U S A. 2019;116(4):1361-1369. doi:10.1073/pnas.1812266115
97. Keith B, Johnson RS, Simon MC. HIF1α and HIF2α: sibling rivalry in hypoxic tumour growth and progression. Nat Rev Cancer. 2011;12(1):9-22. Published 2011 Dec 15. doi:10.1038/nrc3183

98. Kersten, Kelly et al. “Genetically engineered mouse models in oncology research and cancer medicine.” EMBO molecular medicinevol. 9,2 (2017): 137-153. doi:10.15252/emmm.201606857
99. Kfoury Y, Scadden DT. Mesenchymal cell contributions to the stem cell niche. Cell Stem Cell. 2015;16(3):239-253. doi:10.1016/j.stem.2015.02.019
100. Kim H, Kim M, Im SK, Fang S. Mouse Cre-LoxP system: general principles to determine tissue-specific roles of target genes. Lab Anim Res. 2018;34(4):147-159. doi:10.5625/lar.2018.34.4.147
101. Kim JE, Nakashima K, de Crombrugghe B. Transgenic mice expressing a ligand-inducible cre recombinase in osteoblasts and odontoblasts: a new tool to examine physiology and disease of postnatal bone and tooth. Am J Pathol. 2004;165(6):1875-1882. doi:10.1016/S0002-9440(10)63240-3
102. Kiss M, Van Gassen S, Movahedi K, Saeys Y, Laoui D. Myeloid cell heterogeneity in cancer: not a single cell alike. Cell Immunol. 2018;330:188-201. doi:10.1016/j.cellimm.2018.02.008
103. Kiss M, Caro AA, Raes G, Laoui D. Systemic Reprogramming of Monocytes in Cancer. Front Oncol. 2020;10:1399. Published 2020 Sep 17. doi:10.3389/fonc.2020.01399
104. Koike Y, Kanai T, Saeki K, et al. MyD88-dependent interleukin-10 production from regulatory CD11b^{+}Gr-1(high) cells suppresses development of acute cerulein pancreatitis in mice. Immunol Lett. 2012;148(2):172-177. doi:10.1016/j.imlet.2012.08.008
105. Kondo M, Weissman IL, Akashi K. Identification of clonogenic common lymphoid progenitors in mouse bone marrow. Cell. 1997;91(5):661-672. doi:10.1016/s0092-8674(00)80453-5
106. Kurihara T, Warr G, Loy J, Bravo R. Defects in macrophage recruitment and host defense in mice lacking the CCR2 chemokine receptor. J Exp Med. 1997;186(10):1757-1762. doi:10.1084/jem.186.10.1757
107. Kuziel WA, Morgan SJ, Dawson TC, et al. Severe reduction in leukocyte adhesion and monocyte extravasation in mice deficient in CC chemokine receptor 2. Proc Natl Acad Sci U S A. 1997;94(22):12053-12058. doi:10.1073/pnas.94.22.12053
108. Kwon, JW., Kwon, HK., Shin, HJ. et al. Activating transcription factor 3 represses inflammatory responses by binding to the p65 subunit of NF-κB. Sci Rep 5, 14470 (2015). https://doi.org/10.1038/srep14470
109. LaBreche HG, Nevins JR, Huang E. Integrating factor analysis and a transgenic mouse model to reveal a peripheral blood predictor of breast tumors. BMC Med Genomics. 2011;4:61. Published 2011 Jul 22. doi:10.1186/1755-8794-4-61
110. Labzin LI, Schmidt SV, Masters SL, et al. ATF3 Is a Key Regulator of Macrophage IFN Responses. J Immunol. 2015;195(9):4446-4455. doi:10.4049/jimmunol.1500204
111. Lahmar Q, Keirsse J, Laoui D, Movahedi K, Van Overmeire E, Van Ginderachter JA. Tissue-resident versus monocyte-derived macrophages in the tumor microenvironment. Biochim Biophys Acta. 2016;1865(1):23-34. doi:10.1016/j.bbcan.2015.06.009
112. Lambertsen RH, Weiss L. A model of intramedullary hematopoietic microenvironments based on stereologic study of the distribution of endocloned marrow colonies. Blood. 1984;63(2):287-297.
113. Laoui D, Van Overmeire E, Di Conza G, et al. Tumor hypoxia does not drive differentiation of tumor-associated macrophages but rather fine-tunes the M2-like

macrophage population. Cancer Res. 2014;74(1):24-30. doi:10.1158/0008-5472.CAN-13-1196

114. Lara-Astiaso D, Weiner A, Lorenzo-Vivas E, et al. Immunogenetics. Chromatin state dynamics during blood formation. Science. 2014;345(6199):943-949. doi:10.1126/science.1256271

115. Laslo P, Spooner CJ, Warmflash A, et al. Multilineage transcriptional priming and determination of alternate hematopoietic cell fates. Cell. 2006;126(4):755-766. doi:10.1016/j.cell.2006.06.052

116. Le Magnen, Clémentine et al. "Optimizing mouse models for precision cancer prevention." Nature reviews. Cancer vol. 16,3 (2016): 187-96. doi:10.1038/nrc.2016.1

117. Leek RD, Talks KL, Pezzella F, et al. Relation of hypoxia-inducible factor-2 alpha (HIF-2 alpha) expression in tumor-infiltrative macrophages to tumor angiogenesis and the oxidative thymidine phosphorylase pathway in Human breast cancer. Cancer Res. 2002;62(5):1326-1329.

118. Lehmann BD, Bauer JA, Chen X, et al. Identification of human triple-negative breast cancer subtypes and preclinical models for selection of targeted therapies. J Clin Invest. 2011;121(7):2750-2767. doi:10.1172/JCI45014

119. Levental KR, Yu H, Kass L, et al. Matrix crosslinking forces tumor progression by enhancing integrin signaling. Cell. 2009;139(5):891-906. doi:10.1016/j.cell.2009.10.027

120. Lévesque JP, Hendy J, Takamatsu Y, Williams B, Winkler IG, Simmons PJ. Mobilization by either cyclophosphamide or granulocyte colony-stimulating factor transforms the bone marrow into a highly proteolytic environment. Exp Hematol. 2002;30(5):440-449. doi:10.1016/s0301-472x(02)00788-9

121. Lévesque JP, Winkler IG, Larsen SR, Rasko JE. Mobilization of bone marrow-derived progenitors. Handb Exp Pharmacol. 2007;(180):3-36. doi:10.1007/978-3-540-68976-8_1

122. Lewis C, Murdoch C. Macrophage responses to hypoxia: implications for tumor progression and anti-cancer therapies. Am J Pathol. 2005;167(3):627-635. doi:10.1016/S0002-9440(10)62038-X

123. Lewis JS, Landers RJ, Underwood JC, Harris AL, Lewis CE. Expression of vascular endothelial growth factor by macrophages is up-regulated in poorly vascularized areas of breast carcinomas. J Pathol. 2000;192(2):150-158. doi:10.1002/1096-9896(2000)9999:9999<::AID-PATH687>3.0.CO;2-G

124. Li H, Han Y, Guo Q, Zhang M, Cao X. Cancer-expanded myeloid-derived suppressor cells induce anergy of NK cells through membrane-bound TGF-beta 1. J Immunol. 2009;182(1):240-249. doi:10.4049/jimmunol.182.1.240

125. Liang G, Wolfgang CD, Chen BP, Chen TH, Hai T. ATF3 gene. Genomic organization, promoter, and regulation. J Biol Chem. 1996;271(3):1695-1701. doi:10.1074/jbc.271.3.1695

126. Linde N, Casanova-Acebes M, Sosa MS, et al. Macrophages orchestrate breast cancer early dissemination and metastasis. Nat Commun. 2018;9(1):21. Published 2018 Jan 2. doi:10.1038/s41467-017-02481-5

127. Liu Y, Chen Y, Deng X, Zhou J. ATF3 Prevents Stress-Induced Hematopoietic Stem Cell Exhaustion. Front Cell Dev Biol. 2020;8:585771. Published 2020 Oct 27. doi:10.3389/fcell.2020.585771

128. Lord BI, Testa NG, Hendry JH. The relative spatial distributions of CFUs and CFUc in the normal mouse femur. Blood. 1975;46(1):65-72.

129. Lotti F, Menguzzato E, Rossi C, et al. Transcriptional targeting of lentiviral vectors by long terminal repeat enhancer replacement. J Virol. 2002;76(8):3996-4007. doi:10.1128/jvi.76.8.3996-4007.2002
130. Lucchini F, Sacco MG, Hu N, et al. Early and multifocal tumors in breast, salivary, harderian and epididymal tissues developed in MMTY-Neu transgenic mice. Cancer Lett. 1992;64(3):203-209. doi:10.1016/0304-3835(92)90044-v
131. Mahadevan NR, Anufreichik V, Rodvold JJ, Chiu KT, Sepulveda H, Zanetti M. Cell-extrinsic effects of tumor ER stress imprint myeloid dendritic cells and impair $CD8^+$ T cell priming. PLoS One. 2012;7(12):e51845. doi:10.1371/journal.pone.0051845
132. Mahadevan NR, Rodvold J, Sepulveda H, Rossi S, Drew AF, Zanetti M. Transmission of endoplasmic reticulum stress and pro-inflammation from tumor cells to myeloid cells.Proc Natl Acad Sci U S A. 2011;108(16):6561-6566. doi:10.1073/pnas.1008942108
133. Mahmoud SM, Paish EC, Powe DG, et al. Tumor-infiltrating CD8+ lymphocytes predict clinical outcome in breast cancer. J Clin Oncol. 2011;29(15):1949-1955. doi:10.1200/JCO.2010.30.5037
134. Majorini MT, Cancila V, Rigoni A, et al. Infiltrating Mast Cell-Mediated Stimulation of Estrogen Receptor Activity in Breast Cancer Cells Promotes the Luminal Phenotype. Cancer Res. 2020;80(11):2311-2324. doi:10.1158/0008-5472.CAN-19-3596
135. Majumdar MK, Thiede MA, Haynesworth SE, Bruder SP, Gerson SL. Human marrow-derived mesenchymal stem cells (MSCs) express hematopoietic cytokines and support long-term hematopoiesis when differentiated toward stromal and osteogenic lineages. J Hematother Stem Cell Res. 2000;9(6):841-848. doi:10.1089/152581600750062264
136. Mantovani A, Sozzani S, Locati M, Allavena P, Sica A. Macrophage polarization: tumor-associated macrophages as a paradigm for polarized M2 mononuclear phagocytes. Trends Immunol. 2002;23(11):549-555. doi:10.1016/s1471-4906(02)02302-5
137. Mao Y, Poschke I, Kiessling R. Tumour-induced immune suppression: role of inflammatory mediators released by myelomonocytic cells. J Intern Med. 2014;276(2):154-170. doi:10.1111/joim.12229
138. Marastoni S, Ligresti G, Lorenzon E, Colombatti A, Mongiat M. Extracellular matrix: a matter of life and death. Connect Tissue Res. 2008;49(3):203-206. doi:10.1080/03008200802143190
139. Martinez FO, Gordon S, Locati M, Mantovani A. Transcriptional profiling of the human monocyte-to-macrophage differentiation and polarization: new molecules and patterns of gene expression. J Immunol. 2006;177(10):7303-7311. doi:10.4049/jimmunol.177.10.7303
140. Martinez FO, Gordon S. The M1 and M2 paradigm of macrophage activation: time for reassessment. F1000Prime Rep. 2014;6:13. Published 2014 Mar 3. doi:10.12703/P6-13
141. Maruyama K, Fukasaka M, Vandenbon A, et al. The transcription factor Jdp2 controls bone homeostasis and antibacterial immunity by regulating osteoclast and neutrophil differentiation. Immunity. 2012;37(6):1024-1036. doi:10.1016/j.immuni.2012.08.022
142. Mavaddat N, Pharoah PD, Michailidou K, et al. Prediction of breast cancer risk based on profiling with common genetic variants. J Natl Cancer Inst. 2015;107(5):djv036. Published 2015 Apr 8. doi:10.1093/jnci/djv036

143. Meinke G, Bohm A, Hauber J, Pisabarro MT, Buchholz F. Cre Recombinase and Other Tyrosine Recombinases. Chem Rev. 2016;116(20):12785-12820. doi:10.1021/acs.chemrev.6b00077
144. Melani C, Chiodoni C, Forni G, Colombo MP. Myeloid cell expansion elicited by the progression of spontaneous mammary carcinomas in c-erbB-2 transgenic BALB/c mice suppresses immune reactivity. Blood. 2003;102(6):2138-2145. doi:10.1182/blood-2003-01-0190
145. Melani C, Sangaletti S, Barazzetta FM, Werb Z, Colombo MP. Amino-biphosphonate-mediated MMP-9 inhibition breaks the tumor-bone marrow axis responsible for myeloid-derived suppressor cell expansion and macrophage infiltration in tumor stroma. Cancer Res. 2007;67(23):11438-11446. doi:10.1158/0008-5472.CAN-07-1882
146. Méndez-Ferrer S, Battista M, Frenette PS. Cooperation of beta(2)- and beta(3)-adrenergic receptors in hematopoietic progenitor cell mobilization. Ann N Y Acad Sci. 2010;1192:139-144. doi:10.1111/j.1749-6632.2010.05390.x
147. Méndez-Ferrer S, Michurina TV, Ferraro F, et al. Mesenchymal and haematopoietic stem cells form a unique bone marrow niche.Nature. 2010;466(7308):829-834. doi:10.1038/nature09262
148. Messmer MN, Netherby CS, Banik D, Abrams SI. Tumor-induced myeloid dysfunction and its implications for cancer immunotherapy. Cancer Immunol Immunother. 2015;64(1):1-13. doi:10.1007/s00262-014-1639-3
149. Mitroulis I, Kalafati L, Bornhäuser M, Hajishengallis G, Chavakis T. Regulation of the Bone Marrow Niche by Inflammation. Front Immunol. 2020;11:1540. Published 2020 Jul 21. doi:10.3389/fimmu.2020.01540
150. Miyawaki K, Arinobu Y, Iwasaki H, et al. CD41 marks the initial myelo-erythroid lineage specification in adult mouse hematopoiesis: redefinition of murine common myeloid progenitor. Stem Cells. 2015;33(3):976-987. doi:10.1002/stem.1906
151. Molinero L, Li Y, Chang CW, et al. Tumor immune microenvironment and genomic evolution in a patient with metastatic triple negative breast cancer and a complete response to atezolizumab. J Immunother Cancer. 2019;7(1):274. Published 2019 Oct 23. doi:10.1186/s40425-019-0740-8
152. Morikawa S, Mabuchi Y, Kubota Y, et al. Prospective identification, isolation, and systemic transplantation of multipotent mesenchymal stem cells in murine bone marrow. J Exp Med. 2009;206(11):2483-2496. doi:10.1084/jem.20091046
153. Movahedi K, Guilliams M, Van den Bossche J, et al. Identification of discrete tumor-induced myeloid-derived suppressor cell subpopulations with distinct T cell-suppressive activity. Blood. 2008;111(8):4233-4244. doi:10.1182/blood-2007-07-099226
154. Movahedi K, Laoui D, Gysemans C, et al. Different tumor microenvironments contain functionally distinct subsets of macrophages derived from Ly6C(high) monocytes. Cancer Res. 2010;70(14):5728-5739. doi:10.1158/0008-5472.CAN-09-4672
155. Muller W J et al. “Single-step induction of mammary adenocarcinoma in transgenic mice bearing the activated c-neu oncogene.” Cell vol. 54,1 (1988): 105-15. doi:10.1016/0092-8674(88)90184-5
156. Murdoch C, Tazzyman S, Webster S, Lewis CE. Expression of Tie-2 by human monocytes and their responses to angiopoietin-2. J Immunol. 2007;178(11):7405-7411. doi:10.4049/jimmunol.178.11.7405

157. Mussai F, De Santo C, Abu-Dayyeh I, et al. Acute myeloid leukemia creates an arginase-dependent immunosuppressive microenvironment. Blood. 2013;122(5):749-758. doi:10.1182/blood-2013-01-480129
158. Nagareddy PR, Kraakman M, Masters SL, et al. Adipose tissue macrophages promote myelopoiesis and monocytosis in obesity. Cell Metab. 2014;19(5):821-835. doi:10.1016/j.cmet.2014.03.029
159. Nagy A. Cre recombinase: the universal reagent for genome tailoring. Genesis. 2000;26(2):99-109.
160. Nakorn TN, Miyamoto T, Weissman IL. Characterization of mouse clonogenic megakaryocyte progenitors. Proc Natl Acad Sci U S A. 2003;100(1):205-210. doi:10.1073/pnas.262655099
161. Naveiras O, Nardi V, Wenzel PL, Hauschka PV, Fahey F, Daley GQ. Bone-marrow adipocytes as negative regulators of the haematopoietic microenvironment. Nature. 2009;460(7252):259-263. doi:10.1038/nature08099
162. Neve RM, Lane HA, Hynes NE. The role of overexpressed HER2 in transformation. Ann Oncol. 2001;12 Suppl 1:S9-S13. doi:10.1093/annonc/12.suppl_1.s9
163. Niehans GA, Singleton TP, Dykoski D, Kiang DT. Stability of HER-2/neu expression over time and at multiple metastatic sites. J Natl Cancer Inst. 1993;85(15):1230-1235. doi:10.1093/jnci/85.15.1230
164. Omatsu Y, Sugiyama T, Kohara H, et al. The essential functions of adipo-osteogenic progenitors as the hematopoietic stem and progenitor cell niche. Immunity. 2010;33(3):387-399. doi:10.1016/j.immuni.2010.08.017
165. Paik S, Hazan R, Fisher ER, et al. Pathologic findings from the National Surgical Adjuvant Breast and Bowel Project: prognostic significance of erbB-2 protein overexpression in primary breast cancer. J Clin Oncol. 1990;8(1):103-112. doi:10.1200/JCO.1990.8.1.103
166. Palframan RT, Jung S, Cheng G, et al. Inflammatory chemokine transport and presentation in HEV: a remote control mechanism for monocyte recruitment to lymph nodes in inflamed tissues. J Exp Med. 2001;194(9):1361-1373. doi:10.1084/jem.194.9.1361
167. Pan PY, Ma G, Weber KJ, et al. Immune stimulatory receptor CD40 is required for T-cell suppression and T regulatory cell activation mediated by myeloid-derived suppressor cells in cancer. Cancer Res. 2010;70(1):99-108. doi:10.1158/0008-5472.CAN-09-1882
168. Papaioannou VE, Behringer RR. Early embryonic lethality in genetically engineered mice: diagnosis and phenotypic analysis. Vet Pathol. 2012;49(1):64-70. doi:10.1177/0300985810395725
169. Parrish-Novak J, Dillon SR, Nelson A, et al. Interleukin 21 and its receptor are involved in NK cell expansion and regulation of lymphocyte function. Nature. 2000;408(6808):57-63. doi:10.1038/35040504
170. Pauletti G, Godolphin W, Press MF, Slamon DJ. Detection and quantitation of HER-2/neu gene amplification in human breast cancer archival material using fluorescence in situ hybridization. Oncogene. 1996;13(1):63-72.
171. Peinado H, Alečković M, Lavotshkin S, et al. Melanoma exosomes educate bone marrow progenitor cells toward a pro-metastatic phenotype through MET [published correction appears in Nat Med. 2016 Dec 6;22(12):1502].Nat Med. 2012;18(6):883-891. doi:10.1038/nm.2753

172. Peled A, Kollet O, Ponomaryov T, et al. The chemokine SDF-1 activates the integrins LFA-1, VLA-4, and VLA-5 on immature human CD34(+) cells: role in transendothelial/stromal migration and engraftment of NOD/SCID mice. Blood. 2000;95(11):3289-3296.
173. Perou CM, Sørlie T, Eisen MB, et al. Molecular portraits of human breast tumours. Nature. 2000;406(6797):747-752. doi:10.1038/35021093
174. Pickup MW, Mouw JK, Weaver VM. The extracellular matrix modulates the hallmarks of cancer. EMBO Rep. 2014;15(12):1243-1253. doi:10.15252/embr.201439246
175. Pietras EM, Mirantes-Barbeito C, Fong S, et al. Chronic interleukin-1 exposure drives haematopoietic stem cells towards precocious myeloid differentiation at the expense of self-renewal. Nat Cell Biol. 2016;18(6):607-618. doi:10.1038/ncb3346
176. Pittenger MF, Mackay AM, Beck SC, et al. Multilineage potential of adult human mesenchymal stem cells. Science. 1999;284(5411):143-147. doi:10.1126/science.284.5411.143
177. Prockop DJ. Marrow stromal cells as stem cells for nonhematopoietic tissues. Science. 1997;276(5309):71-74. doi:10.1126/science.276.5309.71
178. Qian BZ, Li J, Zhang H, et al. CCL2 recruits inflammatory monocytes to facilitate breast-tumour metastasis. Nature. 2011;475(7355):222-225. Published 2011 Jun 8. doi:10.1038/nature10138
179. Quaglino E, Mastini C, Forni G, Cavallo F. ErbB2 transgenic mice: a tool for investigation of the immune prevention and treatment of mammary carcinomas. Curr Protoc Immunol. 2008;Chapter 20:. doi:10.1002/0471142735.im2009s82
180. Quatromoni JG, Eruslanov E. Tumor-associated macrophages: function, phenotype, and link to prognosis in human lung cancer. Am J Transl Res. 2012;4(4):376-389.
181. Raes G, Noël W, Beschin A, Brys L, de Baetselier P, Hassanzadeh GH. FIZZ1 and Ym as tools to discriminate between differentially activated macrophages. Dev Immunol. 2002;9(3):151-159. doi:10.1080/1044667031000137629
182. Ramos RN, Rodriguez C, Hubert M, et al. CD163+ tumor-associated macrophage accumulation in breast cancer patients reflects both local differentiation signals and systemic skewing of monocytes. Clin Transl Immunology. 2020;9(2):e1108. Published 2020 Feb 13. doi:10.1002/cti2.1108
183. Reynaud D, Pietras E, Barry-Holson K, et al. IL-6 controls leukemic multipotent progenitor cell fate and contributes to chronic myelogenous leukemia development. Cancer Cell. 2011;20(5):661-673. doi:10.1016/j.ccr.2011.10.012
184. Ridker PM, MacFadyen JG, Thuren T, et al. Effect of interleukin-1β inhibition with canakinumab on incident lung cancer in patients with atherosclerosis: exploratory results from a randomised, double-blind, placebo-controlled trial. Lancet. 2017;390(10105):1833-1842. doi:10.1016/S0140-6736(17)32247-X
185. Rodriguez PC, Quiceno DG, Zabaleta J, et al. Arginase I production in the tumor microenvironment by mature myeloid cells inhibits T-cell receptor expression and antigen-specific T-cell responses. Cancer Res. 2004;64(16):5839-5849. doi:10.1158/0008-5472.CAN-04-0465
186. Rohini M, Haritha Menon A, Selvamurugan N. Role of activating transcription factor 3 and its interacting proteins under physiological and pathological conditions. Int J Biol Macromol. 2018;120(Pt A):310-317. doi:10.1016/j.ijbiomac.2018.08.107

187. Rose S, Misharin A, Perlman H. A novel Ly6C/Ly6G-based strategy to analyze the mouse splenic myeloid compartment. Cytometry A. 2012;81(4):343-350. doi:10.1002/cyto.a.22012
188. Rosenberger CM, Clark AE, Treuting PM, Johnson CD, Aderem A. ATF3 regulates MCMV infection in mice by modulating IFN-gamma expression in natural killer cells. Proc Natl Acad Sci U S A. 2008;105(7):2544-2549. doi:10.1073/pnas.0712182105
189. Ruffell B, Chang-Strachan D, Chan V, et al. Macrophage IL-10 blocks CD8+ T cell-dependent responses to chemotherapy by suppressing IL-12 expression in intratumoral dendritic cells. Cancer Cell. 2014;26(5):623-637. doi:10.1016/j.ccell.2014.09.006
190. Rusakiewicz S, Semeraro M, Sarabi M, et al. Immune infiltrates are prognostic factors in localized gastrointestinal stromal tumors. Cancer Res. 2013;73(12):3499-3510. doi:10.1158/0008-5472.CAN-13-0371
191. Sacchetti B, Funari A, Michienzi S, et al. Self-renewing osteoprogenitors in bone marrow sinusoids can organize a hematopoietic microenvironment [published correction appears in Cell. 2008 May 30;133(5):928]. Cell. 2007;131(2):324-336. doi:10.1016/j.cell.2007.08.025
192. Sangaletti S, Stoppacciaro A, Guiducci C, Torrisi MR, Colombo MP. Leukocyte, rather than tumor-produced SPARC, determines stroma and collagen type IV deposition in mammary carcinoma. J Exp Med. 2003;198(10):1475-1485. doi:10.1084/jem.20030202
193. Sangaletti S, Tripodo C, Cappetti B, et al. SPARC oppositely regulates inflammation and fibrosis in bleomycin-induced lung damage [published correction appears in Am J Pathol. 2012 Mar;180(3):1324]. Am J Pathol. 2011;179(6):3000-3010. doi:10.1016/j.ajpath.2011.08.027
194. Sangaletti S, Tripodo C, Sandri S, et al. Osteopontin shapes immunosuppression in the metastatic niche. Cancer Res. 2014;74(17):4706-4719. doi:10.1158/0008-5472.CAN-13-3334
195. Sangaletti S, Tripodo C, Vitali C, et al. Defective stromal remodeling and neutrophil extracellular traps in lymphoid tissues favor the transition from autoimmunity to lymphoma. Cancer Discov. 2014;4(1):110-129. doi:10.1158/2159-8290.CD-13-0276
196. Sangaletti S, Tripodo C, Santangelo A, et al. Mesenchymal Transition of High-Grade Breast Carcinomas Depends on Extracellular Matrix Control of Myeloid Suppressor Cell Activity. Cell Rep. 2016;17(1):233-248. doi:10.1016/j.celrep.2016.08.075
197. Sangaletti S, Talarico G, Chiodoni C, et al. SPARC Is a New Myeloid-Derived Suppressor Cell Marker Licensing Suppressive Activities. Front Immunol. 2019;10:1369. Published 2019 Jun 20. doi:10.3389/fimmu.2019.01369
198. Sauer B. Inducible gene targeting in mice using the Cre/lox system. Methods. 1998;14(4):381-392. doi:10.1006/meth.1998.0593
199. Schaaf MB, Garg AD, Agostinis P. Defining the role of the tumor vasculature in antitumor immunity and immunotherapy. Cell Death Dis. 2018;9(2):115. Published 2018 Jan 25. doi:10.1038/s41419-017-0061-0
200. Scharf P, Broering MF, Oliveira da Rocha GH, Farsky SHP. Cellular and Molecular Mechanisms of Environmental Pollutants on Hematopoiesis.Int J Mol Sci. 2020;21(19):6996. Published 2020 Sep 23. doi:10.3390/ijms21196996

201. Schmitz ML, Shaban MS, Albert BV, Gökçen A, Kracht M. The Crosstalk of Endoplasmic Reticulum (ER) Stress Pathways with NF-κB: Complex Mechanisms Relevant for Cancer, Inflammation and Infection. Biomedicines. 2018;6(2):58. Published 2018 May 16. doi:10.3390/biomedicines6020058
202. Schuettpelz LG, Borgerding JN, Christopher MJ, et al. G-CSF regulates hematopoietic stem cell activity, in part, through activation of Toll-like receptor signaling. Leukemia. 2014;28(9):1851-1860. doi:10.1038/leu.2014.68
203. Schürch CM, Riether C, Ochsenbein AF. Cytotoxic CD8+ T cells stimulate hematopoietic progenitors by promoting cytokine release from bone marrow mesenchymal stromal cells. Cell Stem Cell. 2014;14(4):460-472. doi:10.1016/j.stem.2014.01.002
204. Scott LM, Priestley GV, Papayannopoulou T. Deletion of alpha4 integrins from adult hematopoietic cells reveals roles in homeostasis, regeneration, and homing. Mol Cell Biol. 2003;23(24):9349-9360. doi:10.1128/MCB.23.24.9349-9360.2003
205. Serbina NV, Pamer EG. Monocyte emigration from bone marrow during bacterial infection requires signals mediated by chemokine receptor CCR2. Nat Immunol. 2006;7(3):311-317. doi:10.1038/ni1309
206. Sica A, Guarneri V, Gennari A. Myelopoiesis, metabolism and therapy: a crucial crossroads in cancer progression. Cell Stress. 2019;3(9):284-294. Published 2019 Jul 1. doi:10.15698/cst2019.09.197
207. Sica A, Schioppa T, Mantovani A, Allavena P. Tumour-associated macrophages are a distinct M2 polarised population promoting tumour progression: potential targets of anti-cancer therapy. Eur J Cancer. 2006;42(6):717-727. doi:10.1016/j.ejca.2006.01.003
208. Simpson PT, Gale T, Fulford LG, Reis-Filho JS, Lakhani SR. The diagnosis and management of pre-invasive breast disease: pathology of atypical lobular hyperplasia and lobular carcinoma in situ. Breast Cancer Res. 2003;5(5):258-262. doi:10.1186/bcr624
209. Slamon DJ, Clark GM, Wong SG, Levin WJ, Ullrich A, McGuire WL. Human breast cancer: correlation of relapse and survival with amplification of the HER-2/neu oncogene.Science. 1987;235(4785):177-182. doi:10.1126/science.3798106
210. Song N, Scholtemeijer M, Shah K. Mesenchymal Stem Cell Immunomodulation: Mechanisms and Therapeutic Potential. Trends Pharmacol Sci. 2020 Sep;41(9):653-664. doi: 10.1016/j.tips.2020.06.009.
211. Sousa S, Brion R, Lintunen M, et al. Human breast cancer cells educate macrophages toward the M2 activation status. Breast Cancer Res. 2015;17(1):101. Published 2015 Aug 5. doi:10.1186/s13058-015-0621-0
212. Spranger S, Gajewski TF. Impact of oncogenic pathways on evasion of antitumour immune responses. Nat Rev Cancer. 2018;18(3):139-147. doi:10.1038/nrc.2017.117
213. Sternberg N, Austin S, Hamilton D, Yarmolinsky M. Analysis of bacteriophage P1 immunity by using lambda-P1 recombinants constructed in vitro. Proc Natl Acad Sci U S A. 1978;75(11):5594-5598. doi:10.1073/pnas.75.11.5594
214. Sternberg N, Hamilton D. Bacteriophage P1 site-specific recombination. I. Recombination between loxP sites. J Mol Biol. 1981;150(4):467-486. doi:10.1016/0022-2836(81)90375-2
215. Strauss L, Sangaletti S, Consonni FM, et al. RORC1 Regulates Tumor-Promoting "Emergency" Granulo-Monocytopoiesis. Cancer Cell. 2015;28(2):253-269. doi:10.1016/j.ccell.2015.07.006

216. Strobl H, Scheinecker C, Csmarits B, Majdic O, Knapp W. Flow cytometric analysis of intracellular CD68 molecule expression in normal and malignant haemopoiesis. Br J Haematol. 1995;90(4):774-782. doi:10.1111/j.1365-2141.1995.tb05195.x
217. Swartz MA, Iida N, Roberts EW, et al. Tumor microenvironment complexity: emerging roles in cancer therapy. Cancer Res. 2012;72(10):2473-2480. doi:10.1158/0008-5472.CAN-12-0122
218. Taichman RS, Emerson SG. The role of osteoblasts in the hematopoietic microenvironment. Stem Cells. 1998;16(1):7-15. doi:10.1002/stem.160007
219. Taichman RS. Blood and bone: two tissues whose fates are intertwined to create the hematopoietic stem-cell niche. Blood. 2005;105(7):2631-2639. doi:10.1182/blood-2004-06-2480
220. Takizawa H, Boettcher S, Manz MG. Demand-adapted regulation of early hematopoiesis in infection and inflammation. Blood. 2012;119(13):2991-3002. doi:10.1182/blood-2011-12-380113
221. Tamoutounour S, Guilliams M, Montanana Sanchis F, et al. Origins and functional specialization of macrophages and of conventional and monocyte-derived dendritic cells in mouse skin. Immunity. 2013;39(5):925-938. doi:10.1016/j.immuni.2013.10.004
222. Tamura T, Kurotaki D, Koizumi S. Regulation of myelopoiesis by the transcription factor IRF8. Int J Hematol. 2015;101(4):342-351. doi:10.1007/s12185-015-1761-9
223. Tay J, Levesque JP, Winkler IG. Cellular players of hematopoietic stem cell mobilization in the bone marrow niche. Int J Hematol. 2017;105(2):129-140. doi:10.1007/s12185-016-2162-4
224. Terashima A, Okamoto K, Nakashima T, Akira S, Ikuta K, Takayanagi H. Sepsis-Induced Osteoblast Ablation Causes Immunodeficiency. Immunity. 2016;44(6):1434-1443. doi:10.1016/j.immuni.2016.05.012
225. Terry RL, Miller SD. Molecular control of monocyte development. Cell Immunol. 2014;291(1-2):16-21. doi:10.1016/j.cellimm.2014.02.008
226. Thomas DA, Massagué J. TGF-beta directly targets cytotoxic T cell functions during tumor evasion of immune surveillance. Cancer Cell. 2005;8(5):369-380. doi:10.1016/j.ccr.2005.10.012
227. Thompson MR, Xu D, Williams BR. ATF3 transcription factor and its emerging roles in immunity and cancer. J Mol Med (Berl). 2009;87(11):1053-1060. doi:10.1007/s00109-009-0520-x
228. Tikhonova AN, Dolgalev I, Hu H, et al. The bone marrow microenvironment at single-cell resolution [published correction appears in Nature. 2019 Aug;572(7767):E6]. Nature. 2019;569(7755):222-228. doi:10.1038/s41586-019-1104-8
229. Tower H, Ruppert M, Britt K. The Immune Microenvironment of Breast Cancer Progression. Cancers (Basel). 2019;11(9):1375. Published 2019 Sep 16. doi:10.3390/cancers11091375
230. Tripodo C, Sangaletti S, Guarnotta C, et al. Stromal SPARC contributes to the detrimental fibrotic changes associated with myeloproliferation whereas its deficiency favors myeloid cell expansion. Blood. 2012;120(17):3541-3554. doi:10.1182/blood-2011-12-398537
231. Tripodo C, Burocchi A, Piccaluga PP, et al. Persistent Immune Stimulation Exacerbates Genetically Driven Myeloproliferative Disorders via Stromal

Remodeling. Cancer Res. 2017;77(13):3685-3699. doi:10.1158/0008-5472.CAN-17-1098

232. Trumpp A, Essers M, Wilson A. Awakening dormant haematopoietic stem cells. Nat Rev Immunol. 2010;10(3):201-209. doi:10.1038/nri2726

233. Tzeng YS, Li H, Kang YL, Chen WC, Cheng WC, Lai DM. Loss of Cxcl12/Sdf-1 in adult mice decreases the quiescent state of hematopoietic stem/progenitor cells and alters the pattern of hematopoietic regeneration after myelosuppression. Blood. 2011;117(2):429-439. doi:10.1182/blood-2010-01-266833

234. Ueda Y, Cain DW, Kuraoka M, Kondo M, Kelsoe G. IL-1R type I-dependent hemopoietic stem cell proliferation is necessary for inflammatory granulopoiesis and reactive neutrophilia. J Immunol. 2009;182(10):6477-6484. doi:10.4049/jimmunol.0803961

235. Ueda Y, Kondo M, Kelsoe G. Inflammation and the reciprocal production of granulocytes and lymphocytes in bone marrow. J Exp Med. 2005;201(11):1771-1780. doi:10.1084/jem.20041419

236. Ulyanova T, Scott LM, Priestley GV, et al. VCAM-1 expression in adult hematopoietic and nonhematopoietic cells is controlled by tissue-inductive signals and reflects their developmental origin. Blood. 2005;106(1):86-94. doi:10.1182/blood-2004-09-3417

237. Van Dam H, Wilhelm D, Herr I, Steffen A, Herrlich P, Angel P. ATF-2 is preferentially activated by stress-activated protein kinases to mediate c-jun induction in response to genotoxic agents. EMBO J. 1995;14(8):1798-1811.

238. Visnjic D, Kalajzic Z, Rowe DW, Katavic V, Lorenzo J, Aguila HL. Hematopoiesis is severely altered in mice with an induced osteoblast deficiency. Blood. 2004;103(9):3258-3264. doi:10.1182/blood-2003-11-4011

239. Wendt C, Margolin S. Identifying breast cancer susceptibility genes - a review of the genetic background in familial breast cancer. Acta Oncol. 2019 Feb;58(2):135-146. doi: 10.1080/0284186X.2018.1529428. Epub 2019 Jan 3. PMID: 30606073.

240. Whitmore MM, Iparraguirre A, Kubelka L, Weninger W, Hai T, Williams BR. Negative regulation of TLR-signaling pathways by activating transcription factor-3. J Immunol. 2007;179(6):3622-3630. doi:10.4049/jimmunol.179.6.3622

241. Wieduwilt MJ, Moasser MM. The epidermal growth factor receptor family: biology driving targeted therapeutics. Cell Mol Life Sci. 2008;65(10):1566-1584. doi:10.1007/s00018-008-7440-8

242. Wilson A, Trumpp A. Bone-marrow haematopoietic-stem-cell niches. Nat Rev Immunol. 2006;6(2):93-106. doi:10.1038/nri1779

243. Wolfgang CD, Chen BP, Martindale JL, Holbrook NJ, Hai T. gadd153/Chop10, a potential target gene of the transcriptional repressor ATF3. Mol Cell Biol. 1997;17(11):6700-6707. doi:10.1128/MCB.17.11.6700

244. Wolfgang CD, Liang G, Okamoto Y, Allen AE, Hai T. Transcriptional autorepression of the stress-inducible gene ATF3. J Biol Chem. 2000;275(22):16865-16870. doi:10.1074/jbc.M909637199

245. Wolford CC, McConoughey SJ, Jalgaonkar SP, et al. Transcription factor ATF3 links host adaptive response to breast cancer metastasis. J Clin Invest. 2013;123(7):2893-2906. doi:10.1172/JCI64410

246. Wu TC, Xu K, Martinek J, et al. IL1 Receptor Antagonist Controls Transcriptional Signature of Inflammation in Patients with Metastatic Breast Cancer. Cancer Res. 2018;78(18):5243-5258. doi:10.1158/0008-5472.CAN-18-0413

247. Xie Y, Yin T, Wiegraebe W, et al. Detection of functional haematopoietic stem cell niche using real-time imaging [published correction appears in Nature. 2010 Aug 26;466(7310):1134]. Nature. 2009;457(7225):97-101. doi:10.1038/nature07639
248. Yakar S, Liu JL, Stannard B, et al. Normal growth and development in the absence of hepatic insulin-like growth factor I.Proc Natl Acad Sci U S A. 1999;96(13):7324-7329. doi:10.1073/pnas.96.13.7324
249. Yamamoto R, Morita Y, Ooehara J, et al. Clonal analysis unveils self-renewing lineage-restricted progenitors generated directly from hematopoietic stem cells. Cell. 2013;154(5):1112-1126. doi:10.1016/j.cell.2013.08.007
250. Yáñez A, Coetzee SG, Olsson A, et al. Granulocyte-Monocyte Progenitors and Monocyte-Dendritic Cell Progenitors Independently Produce Functionally Distinct Monocytes. Immunity. 2017;47(5):890-902.e4. doi:10.1016/j.immuni.2017.10.021
251. Yang J, Zhang L, Yu C, Yang XF, Wang H. Monocyte and macrophage differentiation: circulation inflammatory monocyte as biomarker for inflammatory diseases. Biomark Res. 2014;2(1):1. Published 2014 Jan 7. doi:10.1186/2050-7771-2-1
252. Yarden Y, Sliwkowski MX. Untangling the ErbB signalling network. Nat Rev Mol Cell Biol. 2001;2(2):127-137. doi:10.1038/35052073
253. Yin X, Dewille JW, Hai T. A potential dichotomous role of ATF3, an adaptive-response gene, in cancer development. Oncogene. 2008;27(15):2118-2127. doi:10.1038/sj.onc.1210861
254. Youn JI, Nagaraj S, Collazo M, Gabrilovich DI. Subsets of myeloid-derived suppressor cells in tumor-bearing mice. J Immunol. 2008;181(8):5791-5802. doi:10.4049/jimmunol.181.8.5791
255. Zambetti NA, Ping Z, Chen S, et al. Mesenchymal Inflammation Drives Genotoxic Stress in Hematopoietic Stem Cells and Predicts Disease Evolution in Human Pre-leukemia. Cell Stem Cell. 2016;19(5):613-627. doi:10.1016/j.stem.2016.08.021
256. Zhang QW, Liu L, Gong CY, et al. Prognostic significance of tumor-associated macrophages in solid tumor: a meta-analysis of the literature. PLoS One. 2012;7(12):e50946. doi:10.1371/journal.pone.0050946
257. Zhang W, Jiang M, Chen J, et al. SOCS3 Suppression Promoted the Recruitment of CD11b+Gr-1-F4/80-MHCII- Early-Stage Myeloid-Derived Suppressor Cells and Accelerated Interleukin-6-Related Tumor Invasion via Affecting Myeloid Differentiation in Breast Cancer. Front Immunol. 2018;9:1699. Published 2018 Jul 23. doi:10.3389/fimmu.2018.01699
258. Zhao JL, Ma C, O'Connell RM, et al. Conversion of danger signals into cytokine signals by hematopoietic stem and progenitor cells for regulation of stress-induced hematopoiesis. Cell Stem Cell. 2014;14(4):445-459. doi:10.1016/j.stem.2014.01.007
259. Zhu J, Emerson SG. Hematopoietic cytokines, transcription factors and lineage commitment.Oncogene. 2002;21(21):3295-3313. doi:10.1038/sj.onc.1205318
260. Zilionis R, Engblom C, Pfirschke C, et al. Single-Cell Transcriptomics of Human and Mouse Lung Cancers Reveals Conserved Myeloid Populations across Individuals and Species. Immunity. 2019;50(5):1317-1334.e10. doi:10.1016/j.immuni.2019.03.009
261. Zitvogel L, Pitt JM, Daillère R, Smyth MJ, Kroemer G. Mouse models in oncoimmunology. Nat Rev Cancer. 2016;16(12):759-773. doi:10.1038/nrc.2016.91